Overhead sign structures – gantry

Structural response to truck induced wind loads by measurements and analysis

TU Delft

Rijkswaterstaat
Ministry of Infrastructure and Water Management

CIE5060-09 Master thesis

Student: C.D Fikkers (4232763)

May 31, 2018

Overhead sign structures - gantry

Structural response to truck induced wind loads by measurements and analysis

By

C.D. Fikkers

in partial fulfilment of the requirements for the degree of

Master of Science
in Civil Engineering

Structural Engineering – Steel, hybrid and composite structures

at the Delft University of Technology,

May 31, 2018

Thesis committee:

	Prof. dr. M. Veljkovic	TU Delft
	Dr.ir R. Abspoel	TU Delft
	Dr.ir A. Jarquin Laguna	TU Delft
(daily supervisor)	MSEng O. Joostensz	Rijkswaterstaat

Cover photograph: https://beeldbank.rws.nl, Rijkswaterstaat

TU Delft

Rijkswaterstaat
Ministry of Infrastructure and Water Management

Preface

This research is the final step in order to graduate for the study: Civil Engineering – Structural Engineering at the Delft University of Technology. The research is partly carried out outside the university environment at Rijkswaterstaat which is part of the Ministry of Infrastructure and Water Management. This made it possible to also experience some of the practical sides of civil engineering.

Before starting with this thesis I had never observed sign support structures when I was driving at the highway, now I never miss one. My broad interest made me curious when I heard about the problem of vehicle induced wind loads and sign support structures at Rijkswaterstaat. Ostar and Arjan helped me with all the questions I had about these structures, I would like to thank them for their great contribution to this work. I would also like to thank Prof. dr. M. Veljkovic and Dr.ir R. Abspoel for learning me everything about steel structures during my study and guiding me during my graduation work together with Dr.ir A. Jarquin Laguna, who I would like to thank for giving me very helpful advices on the dynamic computations. I want to thank Yvonne for helping me with the measurements and sharing thoughts and I want to thank Fabian for giving me advice on how to model the dynamic structural response of the sign gantry.

The amount of civil engineering works is enormous. My study made me look at them in a different way, this changed my daily life experience and therefore I would like to thank the university.

Utrecht, May 2018

Coen Fikkers

Table of contents

Abstract

The standard sign gantries at the highways in the Netherlands have different geometrical and structural characteristics than sign gantries in other countries. The sign gantries have in total four oblique columns instead of two straight columns and have a triangular shaped spatial truss beam. The design loads that are currently taken into account include the effects of the self weight, natural wind and settlements. This research focuses on the structural response to vehicle induced wind loads.

The vehicle induced wind loads cause a vibration of the truss beam mainly in its first horizontal mode. The vibration of the beam can be modelled by discretizing a simply supported Euler-Bernoulli beam with rotational springs at the supports that take into account the rotational stiffness of the columns. From literature the vehicle induced wind load is characterized as a pulse load, which is applied to the discrete beam model. The mass, stiffness and damping matrices are used to compute the structural response numerically in the time domain using MATLAB. This numerical calculation model is verified and fitted to the full scale measurements. The measurements were performed with multiple video cameras that were focussed on specific details of the structure and the vehicles that pass the structure. It was found that it is possible to approximate the amplitude of vibration in time using a single pulse load for trailer trucks and trucks.

The stresses in the structure are calculated by applying a deformation that was caused by vehicle induced wind loads to a calculation model with bar elements in MatrixFrame. These stresses are compared with the cut off limit for fatigue detail classes. Based on the preliminary measurements and the calculation model it can be concluded that no fatigue damage is caused by vehicle induced wind loads for the newer series of structures (2012). The older series (2005) could encounter fatigue damage, but it depends on the span length of the beam.

1 Introduction

This chapter gives an introduction to the problem and describes the content and structure of this report.

1.1 Sign gantries

Every day vehicles use the national highways to move from A to B, route information is given via several sign types which are mounted on support structures. The route information provides an efficient vehicle flow at all types of roads. Informing the road users is an important aspect for a good and safe traffic flow, other aspects are for example types of crossings and design of the road construction. Several ways of providing information to the road user are currently used: fixed signs, or variable signs (mechanically and electronically). Route information boards on motorways are mostly located over the carriageway as speed limit signs are placed in the verge of the road. Several types of sign support structures exist, e.g. a single clamped column in the verge of the road, cantilevered overhead structures, overhead gantries, and signs are also mounted on viaducts. This study focuses on overhead sign gantries used at Dutch national highways. Nowadays information is given more and more on electronic navigation devices in vehicles. With this technology and self-driven cars in development the signs might be unnecessary in the future. However, currently the information panels play an important role in the infrastructure system and will be important for the upcoming years.

Traffic sign gantries exist in many different types of structural forms. The main function of the structure is to support signboards or other traffic related information directly above the carriageway. The structures are mostly made up of steel and aluminium but also timber sign gantries are used. In the Netherlands the type of structure that is mostly used consists of a triangular shaped spatial truss supported by the so called “A-frames” (two oblique columns), see figure 1.1. The truss is made up of circular hollow sections with an end plate at both sides. The end plate is bolted to the columns which are made of rectangular hollow sections. The columns are anchored in a concrete foundation block.

Figure 1.1 A typical sign gantry in the Netherlands with signboards and electronic signs

It is interesting to notice that this structure can be made in many different structural forms when it is compared with other countries. Figures 1.2 to 1.5 give an overview of structures for several countries. It is difficult to say which of these structures has the best design, since every country maintains their own design guidelines to which the structure has to fulfil. In Belgium the beam and the columns are made of rectangular hollow sections, in Switzerland a Vierendeel frame is used as a beam. In Germany and the United Kingdom large rectangular hollow sections are used and often a catwalk is present on the structure for maintenance work on the signs. The typical columns used in the Netherlands are not used in other countries, the advantage of this is less fatigue problems at the foundation but the foundation block has to be larger.

Figure 1.2 Sign support structure in Belgium (Google street view, 2017)

Figure 1.3 Sign support structure in Switzerland (Google street view, 2017)

Figure 1.4 Sign support structure in Germany (Rijkswaterstaat, 2017)

Figure 1.5 Sign support structure in the United Kingdom (geograph.org.uk, 2017)

1.2 Loads and design

The structure experiences loads from self-weight, atmospheric wind, vehicle induced wind, temperature changes, settlements and collisions. The latter is mostly prevented by a guard rail at the columns. In the Netherlands the design of the structure is standardized, this leads to consistent expectations of the road user's perception of traffic related information. Moreover, the structure can be used anywhere since it is also calculated by national design rules set by the government (Rijkswaterstaat, 2017). The current design codes cover all of the mentioned loading types except for vehicle-induced wind loads and impact loads. No prematurely failures on large sign structures, such as overhead sign gantries, have been experienced yet. However, smaller sign structures along the road showed damage which was presumably caused by vehicle-induced wind loads. Besides that, small vibrations due to vehicle induced wind loads were clearly visible in sign gantries. The observed bending vibrations were in the first mode shape in horizontal direction.

1.3 Energy content

An interesting question is whether truck induced wind flows can be used to generate electricity with a wind energy harvesting device suitable for concentrated transient wind flows. Traffic sign gantries might be suitable as support structures as they provide space above the highway. Minor research has been performed on this topic and no suitable devices exist to convert the energy of the truck induced wind flow to electricity. The amount of energy that is contained in the vibration in the structure is observed and compared with the results from literature.

1.4 Objective and scope of the research

The aim of this research is to assess truck induced wind loads for an estimation of the fatigue load on typical overhead sign structures along the Dutch national Highway. Besides, the amount of energy that is stored in the structural vibration from vehicle induced wind loads is estimated to compare it with literature on energy harvesting of vehicle induced wind flows.

The main research question:

> Should vehicle induced wind loads be incorporated in the design of sign gantries in the Netherlands?

This question results in various sub-questions:

- How can the vehicle induced wind load be represented as a static or dynamic load and what will be the magnitude or shape of the pulse load?
- How can the structural response to vehicle induced wind loads be modelled and can it be validated?
- Could vehicle induced wind loads affect the lifespan of the structure in terms of (extra) fatigue load cycles next to fatigue loads from atmospheric wind loads?
- If vehicle induced wind loads should be taken into account in the design what would be an appropriated design rule?

In the beginning of this research full scale measurements of the structure were planned, due to time delay these measurements have not been performed yet. However, preliminary measurements are performed based on a simple and low cost measurement method using video cameras. Therefore the research is only limited to the structural response to vehicle induced wind loads and not to a combination with atmospheric wind loading. Only horizontal displacements of the beam are observed. Sign gantries with a variable message sign are not in the scope of this research.

1.5 Thesis outline

A general study on the atmospheric wind load and the structural properties of sign support structures is given in chapter 2. This general study is performed to compare the magnitude of the atmospheric wind load with vehicle induced wind loads in the next chapter. In chapter 3 the vehicle induced wind load is assessed by a literature study. In this chapter static equivalent design rules for vehicle induced wind loads are discussed based on results from literature and also the load is characterized as a pulse load. In chapter 4 this pulse load is used to compute the response of the structure on an analytical way with a single degree of freedom (SDOF) model and a numerical discrete Euler-Bernoulli beam model. This calculation model is validated with full scale measurements in chapter 5. After the calculation model was validated a parametric study is performed in chapter 6, this study consists of the determination of the maximum theoretic amplitude of vibration due to vehicle induced wind loads and a fatigue study. Chapter 7 describes the results of harvesting energy from vehicle induced wind loads based on literature. These results are compared with the energy contained in the structural vibration based on the calculation model. In chapter 8 the results are discussed and a conclusion is made.

(this page is intentionally left blank)

2 The design of the current structure

This chapter describes the current design rules for sign gantries in the Netherlands. Unclear or questionable parts of the design rules are compared with literature research. Also a discussion is made which mechanical scheme can be used to model the structure.

2.1 General information about sign gantries

Sign structures are currently designed according to the Eurocode and extra design rules set by Rijkswaterstaat which is part of the Ministry of Infrastructure and Water Management in the Netherlands. The design of the sign gantries is standardized in such a way that all structures can be used anywhere in the Netherlands without recalculation. This means that sign gantries which are located in an area with relative low wind speeds are over-designed. The technical design life of the structure should be at least 50 years and it should be maintenance free for 25 years, after this period the structure needs a new coating to prevent corrosion. The structure including all mountings should be minimal 5.15 m above the carriageway and the standard length of the structure is limited to 60 m with a maximum panel surface area of 219 m^2 (lower for smaller spans)(Rijkswaterstaat, Componentspecificatie Verkeerskundige Draagconstructies (VDC), 2012). If larger spans or special configurations are required, then these are calculated individually for its use.

2.2 Atmospheric wind loading

Atmospheric wind loads are calculated according to NEN-EN 1991-1-4 art. 5.3:

$$F_w = c_s c_d \cdot c_f \cdot q_p(z_e) \cdot A_{ref} \tag{2.1}$$

With $c_s c_d$ is the structural factor taking into account non-simultaneously occurrence of the maximum pressure on the surface of the structure and vibrations due to turbulence
c_f is the force coefficient of the element, also known as the drag coefficient
$q_p(z_e)$ is the extreme pressure at reference height z_e
A_{ref} is the surface area of the element

Factor $c_s c_d$

The factor $c_s c_d$ has to be calculated according to NEN-EN 1991-1-4 chapter 6. The procedure of this calculation is a complex and time consuming process. The sign support structures are currently calculated with a value of 1.0 for simplification of the design process. This factor was studied with a FEM of different types of structures by a company (PT Structural, 2016) commissioned by Rijkswaterstaat. In general it was found that this factor has a value lower than 1.0 for the typical sign support structures, the factor has a minimum of 0.85 which is given in NEN-EN 1991-1-4. By using a standard value of 1.0 the design is on the safe side.

Factor c_f

This factor is also known as the drag coefficient and can be calculated by dividing a measured force by known parameters such as the wind speed (v), air density (ρ) and the reference area (A_{ref}). c_f is prescribed as 1.8 for signboards and hoardings according to the Eurocode.

According to the current (2017) design rules from Rijkswaterstaat the wind load is calculated for the wind direction perpendicular to signs/structure combined with the wind direction parallel to the signs/structure. The governing wind load direction of 45° does not have to be calculated to simplify the design process. This governing load configuration is now covered by the combined parallel and perpendicular loads (PT Structural, 2016). The force on the signboards are in this case calculated with a coefficient of 1.8 for a perpendicular wind flow and with a coefficient of 0.15 for a parallel wind flow, the frontal area of the signboards should be used in both cases.

The force coefficient, or drag coefficient, was studied by Letchford (2001) with wind tunnel studies on scaled rectangular panels with different sizes and at various elevations. A design formula for the force

coefficient was set from this research, equation 2.2. This equation leads to lower values of c_f for signboards than is prescribed by the Eurocode.

$$c_f = 1.45 + 0.5\left(0.7 + \log_{10}\left(b/c\right)\right)\left(0.5 - c/h\right) \tag{2.2}$$

With *b* is the width of the panel
c is the height of the panel
h is the height from the ground to the top of the panel

The force coefficient is calculated using this formula for common sizes and heights of signboards in the Netherlands, table 2.1 shows an overview. Based on these values it can be concluded that a force coefficient of 1.8 is conservative, the force coefficient is generally between 1.45 and 1.5. For exceptional cases the force coefficient could be higher than 1.5. A range of applicable aspect ratios were given for formula 2.2: 0.2 < b/c < 5 and 0.2 < c/h < 1.0, within this range the error is ±0.1. The observed signboards are within these ranges.

Table 2.1 Values of the force coefficient for commonly used signboard sizes in the Netherlands according to the formula of Letchford (2001)

Width signboard [m] (b)	Height signboard [m] (c)	Height with respect to ground level [m] (h)	Force coefficient [-]
5	3.9	9.1	1.48
9	3.9	9.1	1.49
6	5.1	10.3	1.45
12	5.1	10.3	1.45
8	4	10	1.50
20 (exceptional)	4	10	1.52

As the Eurocode only provides one value for the force coefficient of signboards and hoardings the above mentioned study shows the force coefficient depends on the height of the signboard and its aspect ratio. A literature study was performed by Giannoulis, Stathopoulos, Briassoulis & Mistriotis (2012), this study gives the state of art of the force coefficient on rectangular boards. A comparison is made for the study of Letchford (2001), a study on full scale experiments, ASCE 7-10 (2010) and EN-1991-4 (2005). The studies and design codes show discrepancies and similarities because the ASCE 7-10 (2010) is based on the study of Letchford (2001) and the origin of the force coefficient of 1.8 from the Eurocode is not given. There was no agreement between the full scale experiments and the scaled experiments from Letchford (2001). Giannoulis et al. (2012) concluded from their comparison study that further research is needed to obtain and understand possible resemblance of the observed studies. However, in calculations on sign structures based on the old Dutch design code (TGB 1972) and additional wind tunnel studies a force coefficient of 1.5 was used for a wind flow perpendicular to the signboards (Rijkswaterstaat, 1981). For a wind direction of 45° a value of 1.5 (perpendicular component) and 0.15 (parallel component) were used, also with an eccentricity with respect to the panel centre. This value of the force coefficient is similar as the values obtained from the study of Letchford (2001).

Based on this review and the review of wind tunnel experiments by Leendertz (2016) a force coefficient of 1.8, seems to be too conservative. A force coefficient of 1.6 is more realistic and it covers all possible signboard configurations from the study of Letchford (2001) and the wind tunnel study from Rijkswaterstaat.

The force coefficient on structural elements, i.e. the chords, braces and columns are calculated according to NEN-EN 1991-1-4. These values depend on several parameters and are not simplified as the force coefficient for signboards and hoardings.

Design pressure and fatigue

The Dutch national annex to NEN-EN 1991-1-4 provides a table for the design pressure for different reference heights and wind area zones. These pressures are based on the local wind speed, roughness length and terrain category.

Fatigue cycles and relative stresses due to wind loads are giving in annex B3 of NEN-EN 1991-1-4. Rijkswaterstaat has set a similar method of this into a design table for the number of stress cycles and its corresponding relative stresses. In this design table also stresses higher than the maximum stress are taken into account, see table 2.2.

Table 2.2 Amount of cycles per wind load with a reference period of 50 years from table 5-1 from ROK 1.4 (Rijkswaterstaat, 2017)

H (m)	25	25	25	25
f (Hz)	0,5	1	2	≥ 4
n	$\Delta S/S_k$ (%)	$\Delta S/S_k$ (%)	$\Delta S/S_k$ (%)	$\Delta S/S_k$ (%)
1	150	132	110	100
9	137	120	101	93
90	110	98	84	78
900	82	75	67	64
9000	55	53	50	49
90000	36	36	36	36
900000	26	26	26	26
9000000	17	17	17	17
90000000	9	9	9	9

With *H* is the height of the wind force at the structure
f is the governing eigenfrequency of the structure or the structural element
n is the amount of cycles that should be taken into account with a corresponding stress range of $\Delta S/S_k$ in %, where S_k is the extreme static wind load

2.3 Properties of the structure for full scale measurements

In the future Rijkswaterstaat will perform full scale measurements in order to verify the current design loads on sign gantries and to obtain more knowledge on the loads on signboards from passing traffic underneath. The forces in the structure will be determined using strain gauges in several components in the structure. Prior to this experiment, which is not part of this research, an analysis based on the current design rules and literature is made. After the experiment, the results are compared with the prediction based on the literature study and design codes. The strain measurements in the structure are compared with a FE model to obtain the forces acting on the structure. These forces are compared with the local wind speed measurements at the structure. These calculations should verify the force coefficients used for the wind load calculation. If the truck induced load is significantly large it can be taken into account into the current design specifications from Rijkswaterstaat. In this research preliminary measurements are performed on the structural behaviour due to vehicle induced wind loads. The sign structure that is used for these measurements is shown in figure 2.1. This structure is further analysed in this report.

Figure 2.1 Sign gantry planned for full scale measurements

Construction drawings of this structure can be found in Appendix A, table 2.3 shows a summary of specifications. The construction drawings show a different signboard configuration compared to the actual situation. Based on site visits a sketch of the signboard configuration is made, the locations of the signboards are estimated from the location of the connections and the geometry of the truss girder, this sketch is also added in Appendix A.

Table 2.3 Specifications of the structure and cross section of the truss

Location	Rotterdam A20 (kilometre marker 36.600)
Span length	52 m
Height (gantry)	8.9 m (top of the column)
Steel grade	S235
Chords	CHS ø168.3x20 mm
Braces	CHS ø76.1x6.3 mm
Columns	RHS 350x350x12.5 mm
Number of signboards	5
Total signboard area	30.6+30.6+3.6+35.1+19.5=119.4 m^2

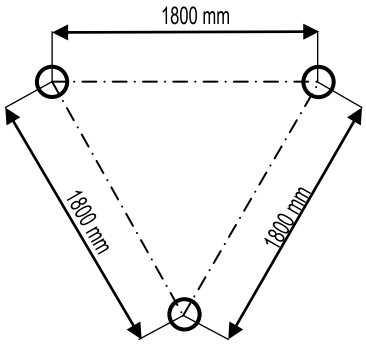

Simplifications in modelling the structure

The truss can be modelled as a simply support beam if it is analysed for horizontal oriented forces and displacements because the rotational stiffness of the column ("A-frame") is relatively low and the horizontal stiffness is relatively high (Rijkswaterstaat, Berkening standaard - portaal tot 30 m, 1981). This assumption is checked with the mechanical scheme shown in figure 2.2, if the stiffness of the rotational springs is equal to zero then the mechanical scheme represents a simply supported beam.

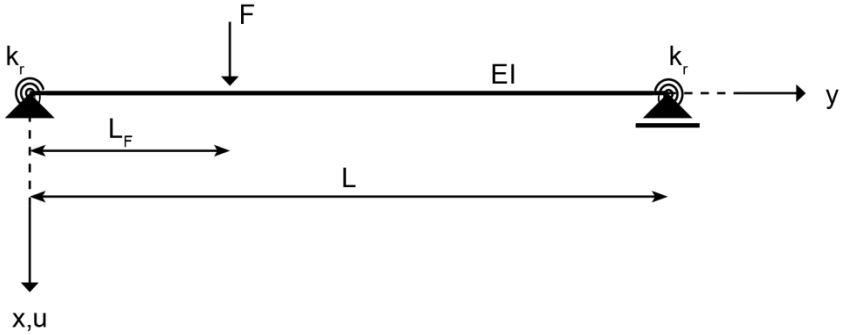

Figure 2.2 Mechanical scheme for calculation of the horizontal deflection of the beam with rotational springs at the supports. In general the x-axis is parallel to the traffic flow.

The truss beam of the structure is modelled as an Euler Bernoulli beam with an equivalent stiffness based on Steiner's rule. The height/length ratio (horizontal) of the beam is equal to 0.034, in general the Euler Bernoulli beam theory is applicable for slender beams with a ratio smaller than 1/10. The second moment of area is calculated only for the chords and to take into account shear deformation in the truss it is multiplied with a factor 0.85. A Young's modulus of 210000 MPa is used.

To compare the two mechanical schemes on how the structure can be modelled, the rotational stiffness of the column (A-frame) is estimated. The column is modelled in SCIA Engineer using plate elements based on the theory of Kirchhoff and the rotational stiffness of the column is estimated. A torsion moment is applied to the top and the rotation is computed (see figure 2.3 and Appendix B). This results in an equivalent rotational stiffness of the top of the column, equal to $1.241 \cdot 10^7$ Nm/rad. The deformation of a simply supported beam is compared to the deformation of simply supported beam with rotational springs at the supports. The displacement at mid span of a simply supported beam including rotational springs at the supports due to the rotational resistance of the column is 8.0% lower than the displacement without rotational stiffness at the supports with a concentrated load at mid

span. For calculating the displacements this assumption of a simply supported beam is conservative, but for the calculation of the forces this approach might be unsuitable.

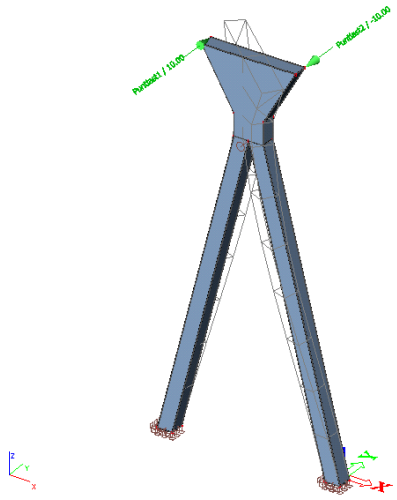

Figure 2.3 Estimation of the rotational stiffness of the column using SCIA Engineer

Besides the torsion stiffness of the “A-frame”, the horizontal stiffness is also calculated (see figure 2.4 and Appendix B). Two forces were applied in one direction to compute the horizontal displacement. This results in the equivalent spring stiffness of the column at the top equal to $2.22 \cdot 10^7$ N/m. Two columns have an equivalent stiffness of $4.44 \cdot 10^7$ N/m. The beam has an equivalent stiffness of $9.2 \cdot 10^5$ N/m at mid span. The equivalent stiffness of this system of two springs in series is equal to $9.0 \cdot 10^5$ N/m, so the error by neglecting the horizontal deformation of the column is only 2%.

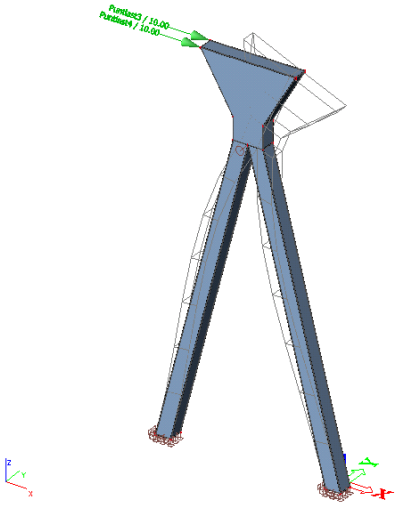

Figure 2.4 Estimation of the horizontal stiffness of the column using SCIA Engineer

Static deformations from natural wind loading

Preliminary results for deformations or forces in the structure can be used as a reference for the results obtained from vehicle induced wind loads. The wind load according to NEN-EN 1991-1-4 is applied to the structure to calculate the deformation. A reference height of 10 m is used (wind area II, unbuilt), 1.6 for c_f and the calculation of the factor $c_s c_d$ resulted in 0.91. Only the load on the signboards is taken into account and the displacement is calculated on an analytical way for a simply supported beam with and without rotational springs at both ends. The maximum static displacement according to the design rules about atmospheric wind loads is equal to 115 mm excluding rotational springs and 106 mm including rotational springs, this calculation can be found in Appendix B.

2.4 Discussion and conclusion

Based on the review of several studies on the force coefficient (c_f) on signboards, the factor of 1.8 that is currently used and prescribed by NEN-EN 1991-1-4 is conservative. From these studies it appears that a force coefficient of 1.6 is more realistic and less conservative.

The truss beam can be modelled as a simply supported beam, but then the displacements are over estimated. If rotational stiffness of the supports (the A-frames) is taken into account via rotational springs at both ends, the difference between a model without rotational springs at both ends is not negligible. However, the rotational stiffness is estimated using SCIA Engineer and the stiffness might be lower due to losses in bolted connections which are not taken into account in this model. In this research both boundary conditions for the supports are used and compared for calculation models.

Currently the used $c_s c_d$ factor for this structure is equal to 1.0 and calculations show that this value is also conservative and generally lower than 1.0 for frequently occurring configurations of the structure. However, the calculation procedure consists of many assumptions for modelling the structure and for some cases the value of $c_s c_d$ is close to 1.0. Therefore a general value of 1.0 seems to be conservative but is a good simplification for the design of all different types sign gantries.

The static deformation of the structure due to atmospheric wind loading can be compared with the dynamic response of the structure due to vehicle induced wind loads. This is described in next chapters of this research.

3 Truck-induced wind loading

This chapter describes the phenomena of truck-induced wind loading. Based on a literature study the truck-induced wind load (pulse) is estimated for a signboard used on sign gantries. This pulse is applied to the structure in the next chapter.

3.1 Introduction

As it was mentioned in the introduction no premature failures on large sign gantries in the Netherlands have occurred yet, but small road sign panels showed early failure due to truck induced wind loads. Also from field observations vibrations in a sign gantry were clearly visible. The Eurocode does not provide information to calculate loads from passing vehicles, except for trains. Several researches exist focussing on vehicle induced wind loads, full scale experiments were carried out on measuring the pressure on small road signs placed above and next to the road (Lichtneger & Ruck, 2014). In the AASHTO standardisation (American Association of State Highway and Transportation Officials) vehicle induced wind loads are covered, but studies by (Hosch & Fouad, 2010) show that the design rule is very conservative. Truck induced wind loads are also covered in the British and Irish design codes under the name 'vehicle buffeting'. An overview on vehicle induced wind design rules is given in the next paragraph. The vehicle induced wind load has several parameters that influence the magnitude and/or the area on which it is acting:

- Aerodynamic shape of the vehicle and frontal surface area
- Speed of the vehicle
- Distance between the vehicle and the object
- Force coefficient and size of the structural element
- Group of vehicles

The moving vehicle displaces the air in front of it, hence a vehicle with a larger frontal area will have to displace more air and experiences a higher drag force than a vehicle with a smaller frontal area. The displaced air has to flow around the vehicle, so the air flow is not uniform in velocity, closer to the vehicle the velocity will be higher than further away from the vehicle. If an object is located in this flow field it will experience a load and thus the distance between the object and the vehicle is also an important parameter. The aerodynamic shape of the vehicle does not influence how much air has to be displaced but it does influence how smooth the air is displaced around the vehicle. The speed of the vehicle influences the velocity of the displaced air and therefore has a great influence on the load since the pressure is related quadratic to the speed in Bernoulli's flow principle.

Objects at roads are always placed taking into account the structure gauge, so as was mentioned in chapter 2 the minimum height of an object or structure is 5.15 m. Passenger cars are generally not higher than 2 m and have a more aerodynamic shape than trucks. The height of trucks is limited to 4 m and therefore signs and signboards could be located close to the vehicle, consequently the vehicle induced wind load on the structure will be governed by trucks, that is why it is mostly called truck induced wind loading.

Since the vehicle induced wind flow is turbulent and not uniform, when large objects are observed, it cannot be easily calculated with hand calculations. In the next sections the vehicle induced wind load is first assessed from design rules and after that it is assessed based on full scale measurements.

3.2 Overview design rules

The design rules from literature are applied to the existing sign gantry mentioned in section 2.3. The vehicle induced load is applied to a signboard of 5 m wide and 3.9 m high. The vehicle induced wind load is compared with the characteristic static design load for atmospheric wind. This load is calculated according to the stated method in chapter 2 of this document. The reference height of the signboard is equal to 10 m, this leads to an extreme pressure of 0.85 kN/m^2 (area without buildings). Using a force coefficient of 1.6 and a $c_s c_d$ value of 0.91 this results in a characteristic force of 24 kN on the signboard.

In the discussed design rules the following parameters were used (not all design rules require input parameters): the distance between the signboard and the road surface is 5.2 m according to the construction drawings; the height of the vehicle is 4 m and the speed of the vehicle is 80 km/h (i.e. 22.2 m/s). The design rules that are observed give equivalent static design pressures in horizontal and/or vertical direction. Vertical loads are applied to mounted objects with a large surface area in the XY-plane (with Z the vertical axis), vertical loads are not of interest for signboards.

The following design rules are compared and give an equivalent static design pressure:

- Design load according to Irish and British design rules (Transport Infrastructure Ireland, 2014)

$$P_d = 600h^{-0.25} - 400 \tag{3.1}$$

With: P_d is the static design pressure for fatigue applied in vertical downward direction and horizontal against traffic direction in N/m^2
h is the distance from the top of the high sided vehicle to the underside of any horizontal or vertical surface in m

The parameter in this design rule is the distance between the vehicle and the structure. The pressure is uniformly distributed over the panel area. Also information is given on the amount of load cycles on different types of roads and lanes. The amount of cycles is given by: $1.6 \cdot 10^7 \cdot L \cdot F_i$, with L is the design life in years and F_i the lane allocation factor varying from 0 to 0.7. No background information on the study for this design rule was given.

This leads to a force of 3.4 kN on the signboard, which is 14% of the maximum characteristic atmospheric wind load.

- Design load according to AASHTO (Hosch & Fouad, 2010) for pressure in vertical direction

$$P_{TG} = 18.8 C_d I_F \left(\frac{V}{65} \right)^2 \tag{3.2}$$

With: P_{TG} is the static design fatigue pressure due to a truck gust in psf (1 psf = 47.88 N/m^2)
C_d is the drag coefficient equal to 1.6
I_F importance factor equal to 0.85
V is the truck speed in mph (50 mph=80km/h)

This formula gives the design pressure in vertical direction because the vertical component is adopted as the governing load direction for fatigue instead of the horizontal direction which is governed by atmospheric loads (Hosch & Fouad, 2010). Many sign structures in the United States have a catwalk construction which results in a surface area susceptible for vertical loads. The sign gantries in the Netherlands do not have a catwalk construction, so vertical loads are not of interest for a structure with only signboards, a sign support structure with a variable message sign (VMS) can be susceptible to the vertical component of vehicle induced loads because it has a larger surface area in vertical direction. This design rule is applied, and especially set, for sign support structures in the US with a VMS. The parameters in this design rule are the speed of the vehicle and the force coefficient of the structural element. The pressure should be applied to heights ≤ 6 m and for heights > 6 m the pressure should be linearly reduced to 0 at a height of 10 m, this leads to an eccentricity with respect to the panel's neutral axis, if applied horizontally. The pressure should be applied to a width of 3.66 m, which is the lane width. For the comparison with other design loads this load is applied horizontally on a 1:1 ratio, see figure 3.1.

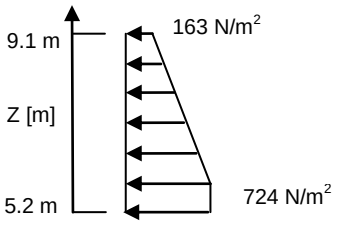

Figure 3.1 Pressure over the height of the signboard

This leads to a force of 7.2 kN on the signboard, which is 30% of the maximum characteristic atmospheric wind load.

- Design load according to the specifications for temporary and mobile signal structures (Rijkswaterstaat D. V., 2012)

  A static pressure of 0.48 kN/m^2 should be applied to the structure in horizontal and vertical direction. The amount of load cycles should be taken from table 2 from NEN-EN 13001-1 table 2 U9: $4 \cdot 10^6 < C < 8 \cdot 10^6$.

  No parameters in this design rule are used. The pressure of 0.48 kN/m^2 is equal to a pressure that results from a wind flow of 100 km/h. This design rules seems to be very conservative since the load has to be applied to the whole structure in vertical and horizontal direction. Also no information is given on the distance between the moving vehicle and the structure.

  This leads to a force of 9.4 kN on the signboard, which is 39% of the maximum atmospheric wind load.

- Alternative design pressure to the AASHTO (Hosch & Fouad, 2010)

  Hosch & Fouad (2010) made an alternative design load for vehicle induced wind loads next to the AASHTO requirements as this seems to be very conservative. Their alternative static design pressure is a function of speed and natural frequency of the structure in the form of a design graph. The design rule is also set for the vertical oriented pressures. This load is applied horizontally to compare it with other design rules. Their design load is based on full scale pressure measurements taken from a bridge spanning a highway. These pressures resulted in a triangular shaped pulse function shown in figure 3.2. This pulse function is applied to a damped SDOF system to compute its dynamic amplification. This resulted in a frequency and speed based design graph for vertical truck-induced pressures, see figure 3.3. The pressure has to be applied in a similar manner as in the AASHTO specification (first design rule).

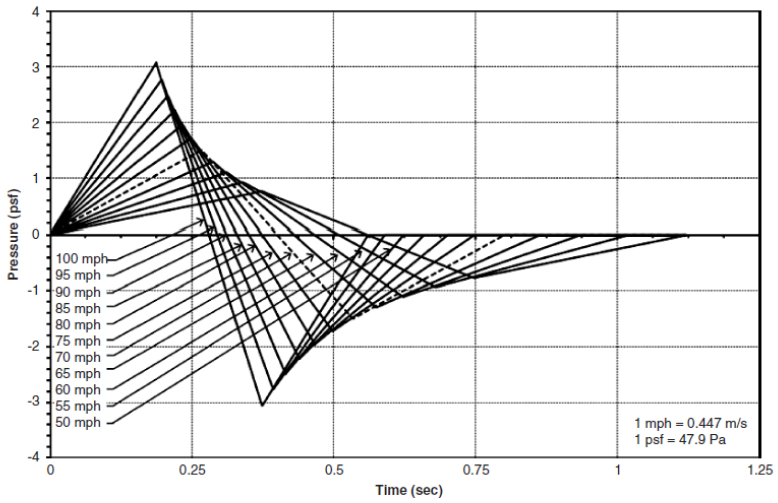

Figure 3.2 Vertical truck-induced wind gust pulse for one truck from Hosch & Fouad (2010)

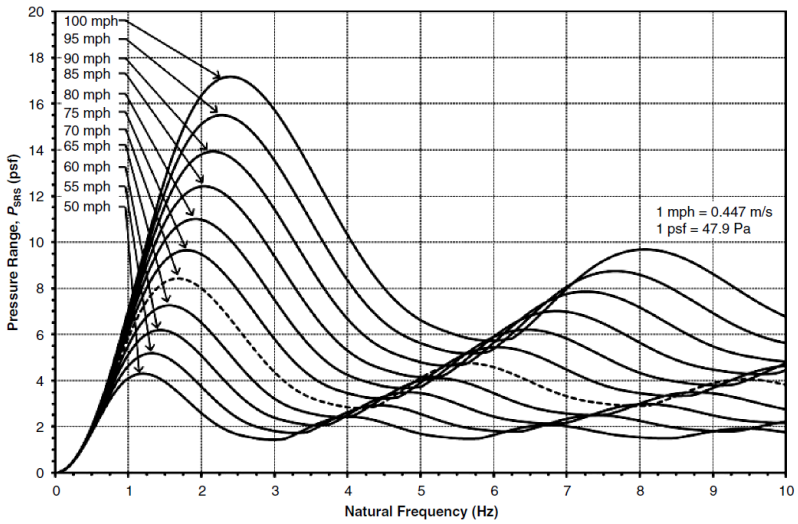

Figure 3.3 Vertical truck-induced design pressure from Hosch & Fouad (2010)

The maximum pressure for a truck driving 50 mph is used (=240 N/m^2)

This design rule leads to a force of 2.3 kN on the signboard if the vertical pressure is applied in horizontal direction on a 1:1 ratio for a truck travelling at 50 mph (=80 km/h). This is 10% of the maximum atmospheric wind load.

- A similar study of Hosch & Fouad (2010) is performed by Hong, Zu, & King (2016). They also set up a design formula based on the natural frequency of the structure and the speed of the vehicle, also with the use of a design graph. To simplify the design rule a formula is set where the natural frequency of the structure is taken which results in the highest pressure. The pressure has to be applied in the same way as the first design rule that was discussed. This resulted in the following design rules with distinction between horizontal and vertical pressures:

$$q_{DV} = 0.46V^2C_d$$
$$q_{DH} = 0.65V^2C_d \quad (3.3)$$

q_{DV} is the equivalent static truck induced pressure in vertical direction in N/m^2
q_{DH} is the equivalent static truck induced pressure in horizontal direction N/m^2
V is the speed of the truck in m/s
C_d is the drag coefficient equal to 1.6

This leads to a force of 5.1 kN on the signboard, which is 21% of the maximum atmospheric wind load.

In this study difference is made between the horizontal and vertical pressure. Noticeable is that the horizontal pressure is higher than the vertical pressure. This means that the assumption of applying the vertical pressure in horizontal direction in the before mentioned design rules is on the low side.

From these design rules on truck induced wind loads it seems that there is no similarity of the design load and that organisations tend to set up a conservative design rule. Most of the 5 design rules depend on several parameters (i.e. speed, distance between object and vehicle, natural frequency and drag coefficient of the object), where the speed of the vehicle seems an important parameter. However, the speed limit for trucks is 80 km/h in Europe, this is in contrast to the design rules from the US and Canada where the speed limits are higher. The British design rule requires only the distance between the vehicle and the object as input parameter. An overview of the results from the design rules is given in table 3.1.

Table 3.1 Overview of design rules on truck-induced wind loads to a signboard with a surface area of 19.5 m^2, for trucks with a height of 4 m, a speed of 80 km/h and the distance between the road and the signboard of 5.2 m.

Design rule	Force (static loads)	Relative to max. static atmospheric wind load	Amount of cycles
P = 0.48 kN/m^2 (Rijkswaterstaat, 2012) for temporary structures	9.4 kN	39%	NEN13001-1 table 2 U9: $4 \cdot 10^6 < C < 8 \cdot 10^6$
Design load according to Irish and British design rules(Transport Infrastructure Ireland, 2014)	3.4 kN	14%	$1.6 \cdot 10^7 \cdot L \cdot F_i$ = $5.6 \cdot 10^8$ (very high)
AASHTO for VMS support structures (Hosch & Fouad, 2010)	7.2 kN	30%	Not mentioned
Design graph based on truck speed and eigenfrequency of the structure for VMS support structures (Hosch & Fouad , 2010)	2.3 kN	10%	Not mentioned
Design graph based on truck speed and eigenfrequency of the structure (Hong, Zu & King , 2016)	5.1 kN	21%	Not mentioned

Compared to the static force from natural wind loads the static truck induced wind loads seem to be large and should not be neglected. In the next section the truck induced wind load is observed as a dynamic pulse load.

3.3 Elaboration full scale measurements from literature

Two studies on truck induced wind loads are used in this section. A review of other studies was given by Ginal (2003) and the most recent and extensive study with full scale measurements is from Lichtneger & Ruck (2014).

Lichtneger & Ruck (2014) performed full scale pressure measurements on small panels placed above and to the sides of the road with multiple pressure sensors over the panel area. Several types of vehicles were used to obtain the vehicle induced pressure on panels this resulted in many data for further elaboration. The data were used to make an empirical design rule for the force on a specific panel and also specific load curves for different vehicle types, panel configuration and passing distances are measured. The research from Ginal (2003) gives a general pulse load for a typical truck pass. This section assesses these results for a prediction of the dynamic behaviour of a sign support structure. The truck pulses are used to compute the structural response in chapter 4.

Pulse based on Lichtneger & Ruck (2014)

The test set-up of these measurements is shown in figure 3.4. The panel configuration C is of interest for the situation of overhead sign support structures.

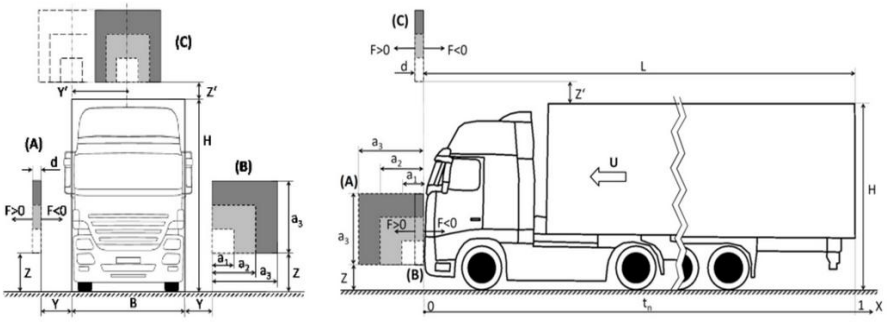

Figure 3.4 Test set-up full scale measurements by Lichtneger & Ruck (2014)

In all test cases similar results were obtained in the pressure time relation (pulse), the results show first an overpressure followed by a large under pressure and end with an overpressure on the panel, but the last part is different for the type of vehicle. The magnitude of the peaks depend on the type of vehicle – aerodynamic shape – see figure 3.5 to figure 3.7 for the test results for a trailer truck, which is mostly used vehicle in long distance transport and has therefore the highest chance of occurrence. Figure 3.8 shows a figure from Lichtneger & Ruck (2014) where the pulse loads for different types of vehicles are shown. The results of specific test cases are presented in videos where the pressure over the panel area is shown in time. The results show that the pressure is highly concentrated in the bottom part of the panel for the suction peak. In these figures the time is normalized with the vehicle's speed and length. So at T=0 the front of the vehicle is located underneath the panel and at T=1 the end of the trailer is underneath the panel.

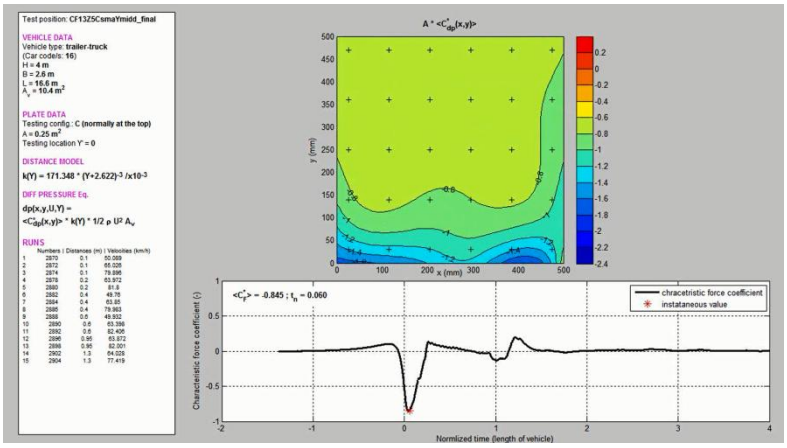

Figure 3.5 Pressure profile in time and pressure distribution on a panel of 0.5x0.5 m^2, screenshot of the pressure distribution at the suction peak (Lichtneger & Ruck, 2014)

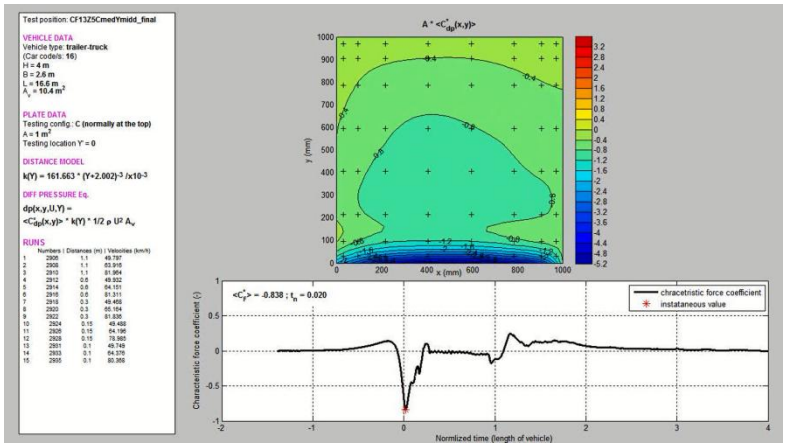

Figure 3.6 Pressure profile in time and pressure distribution on a panel of 1.0x1.0 m^2, screenshot of the pressure distribution at the suction peak (Lichtneger & Ruck, 2014)

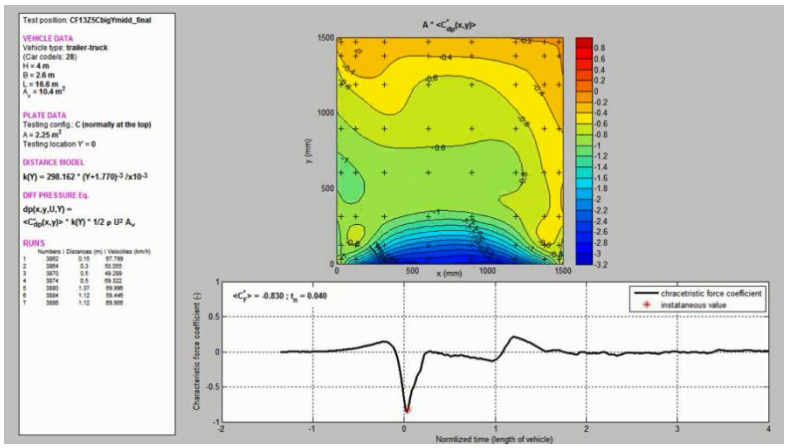

Figure 3.7 Pressure profile in time and pressure distribution on a panel of 1.5x1.5 m^2, screenshot of the pressure distribution at the suction peak (Lichtneger & Ruck, 2014)

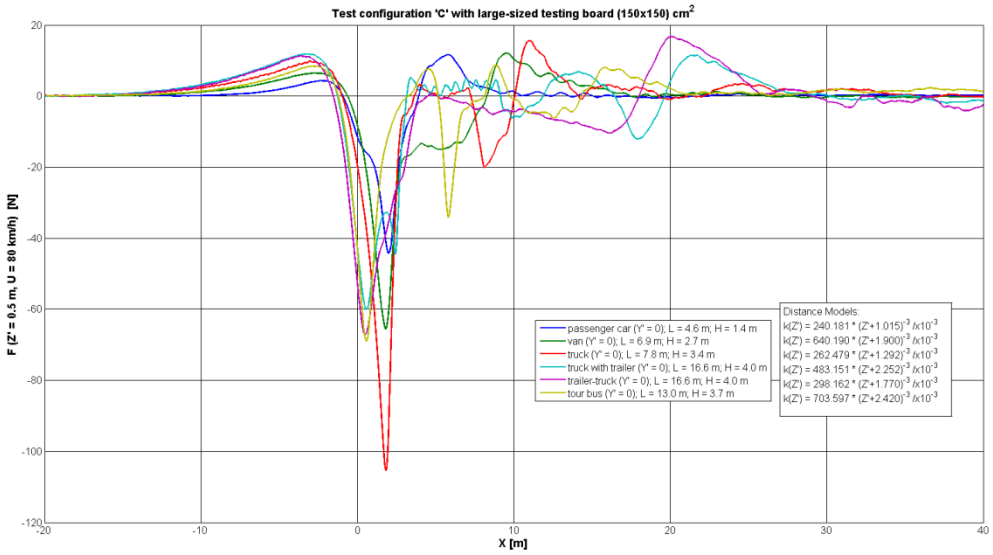

Figure 3.8 Pulses of vehicle induced wind loads for different type of vehicles on a signboard of 1.5x1.5 m^2 and 0.5 m above the vehicle. Figure from the full scale measurements from Lichtneger & Ruck (2014)

For every vehicle type and panel configuration a distance model k(Z') and a design graph with a force coefficient in time (c_F) were made. This distance model is made using test results with varying distance between the panel and the vehicle. The distance model is unique for every plate configuration and vehicle type, it can be used to compute the load F(T) on the plate for different distances between the vehicle and the object. The following design equation was set up by Lichtneger and Ruck (2014) where A_v is the frontal surface area of the vehicle

$$F(T) = \frac{\rho U^2}{2} A_V k(Z') c_F(T) \tag{3.4}$$

The forces on the used panels are calculated using design equation 3.4 and are presented in table 3.2. As expected the load becomes higher when the panel area increases. However, the surface area of these panels is very small compared to the signboards that are used on sign support structures. From only three test cases on small panels no precise extrapolation can be made for panels with a larger surface area such as directional signboards. Noticeable is that very small values are obtained from these measurements compared to the static design loads described in section 3.2.

Table 3.2 Force in Newton on the panel at lowest peak in time (negative value means a force against driving direction)

Test	Measured force (under pressure peak)
Signboard A = 0.25 m^2	- 8.4 N
Signboard A = 1.00 m^2	-13 N
Signboard A = 2.25 m^2	-30 N

In order to make an assessment of vehicle-induced wind loads on a sign gantry the results of the pressure distribution on panels with a surface area of 0.25; 1.00 and 2.25 m^2 are used to make a prediction of the load on a panel with a much larger surface area (e.g. 5x3.9 m^2). The panels used in the experiments of Lichtneger & Ruck (2014) have a smaller width than the truck that passes underneath. An assumption of the pressure distribution and magnitude on a large panel (e.g. 5x3.9 m^2) is made according to the observed measurements and data from figure 3.5 to figure 3.7. The results shown in these figures are further elaborated, the pressure is computed along the height of the centre of the panels for the under pressure peak of the pulse, this is shown in figure 3.10. On the vertical axis the pressure is shown and on the horizontal axis the height of the panel is shown (during the under pressure peak in pressure time relation). The red line represents the pressure along the mid vertical of the panel with size 1.5x1.5 m^2, this line is extrapolated with a logarithmic function (dashed line) to account for panels that have a larger height. This pressure profile over the height of the panel is used to compute the pulse load for a larger panel. The line is described by the following function:

$$P_{height} = 55 - \frac{100}{0.5\log(z + 65)} \tag{3.5}$$

With P_{height} is the pressure over the height in the middle of the panel in N/m^2
z is the vertical coordinate in m

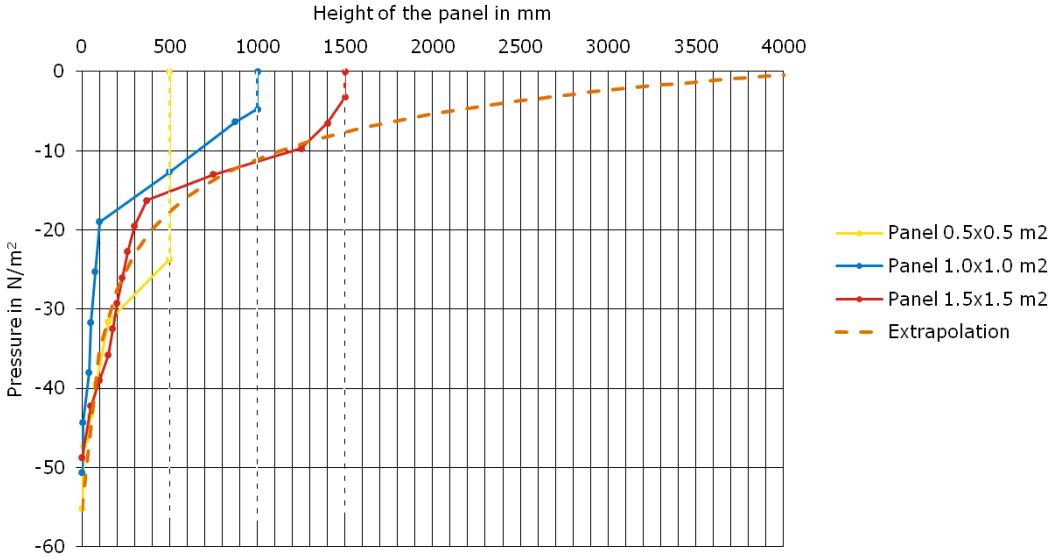

Figure 3.9 Pressure along the height in the middle of the panels with a surface area of: 0.25; 1.00 and 2.25 m^2. The pressure along the height of the largest panel is extrapolated this is approximated with equation 3.5.

Besides estimation for the pressure over the height, also estimation for the pressure distribution in horizontal direction should be made. No research has been performed on the horizontal pressure gradient of the truck induced load in the reviewed researches by Ginal (2003) and the panels used in the research of Lichtneger & Ruck (2014) are very small for extrapolating the pressure in width. From another research on object-vehicle interaction for energy harvesting purposes by Mattana et al. (2014), the truck induced pressure is observed using CFD for two different heights above the vehicle, see figure 3.10. From these results an empircal estimation of the relative horizontal pressure distribution can be made. The solid blue line is approximated by a cosine function for a vehicle width (W) of 2.6 m:

$$P_{horizontal} = \frac{-4.5\cos\left(0.8055\left(y - \frac{b}{2}\right)\right) - 11.5}{16} \tag{3.6}$$

With $P_{horizontal}$ is the pressure variation over the width in N/m^2
y is the horizontal coordinate in m
b is the half width of the signboard in m

Now the pressure over a signboard area can be computed by combining the two functions of pressure variation in width and height:

$$P_x(y,z) = P_{horizontal}(y) \cdot P_{height}(z) \tag{3.7}$$

The combination of the horizontal and vertical distribution results in a 2D pressure plot shown in figure 3.11.

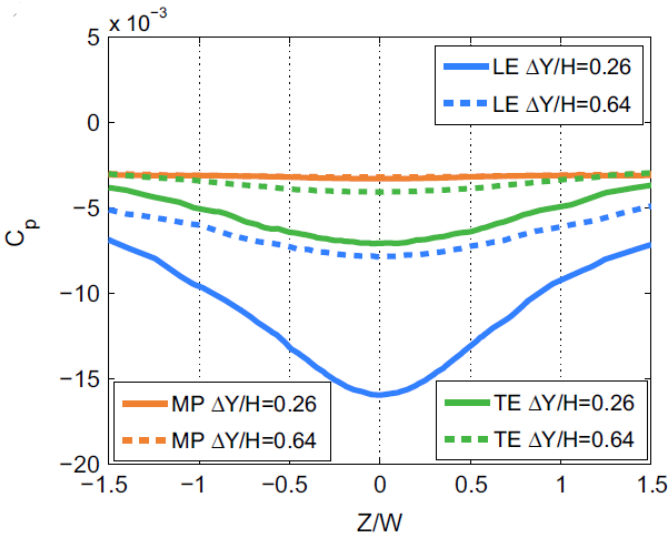

Figure 3.10 Pressure variations in horizontal direction at two different heights (Mattana et al., 2014). In this figure Z is the horizontal coordinate, W is the vehicle width, ΔY is the distance between the vehicle and the object, H is the vehicle height and C_p is a pressure coefficient. LE stands for leading edge, MP for mid-point and TE for trailing edge.

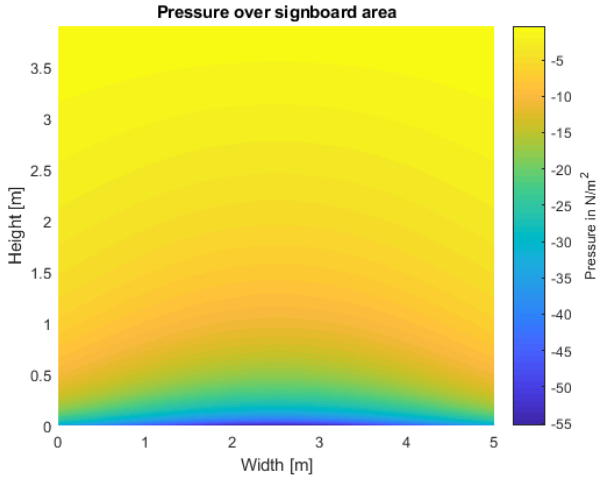

Figure 3.11 Pressure variation over the area of the signboard for the under pressure peak

If the pressure is integrated over the surface area of the signboard the load for the under pressure peak is obtained. In this case for a signboard of 5x3.9 m^2 it results in a load of -143 N.

Now that the load for the under pressure peak is known the load over time is also known from the pulses shown in figure 3.5 to figure 3.7, these pulses show the relative magnitude of the force in time. From this the pulse load on a signboard of 5 m wide and 3.9 high is calculated, this is shown in figure 3.12. This pulse load is only valid for a trailer-truck passing a signboard at a vertical distance between the vehicle and the object of 1.2 m at a speed of 80 km/h. The pulse is simplified and has sharp corners compared to results shown in figure 3.5 to figure 3.7.

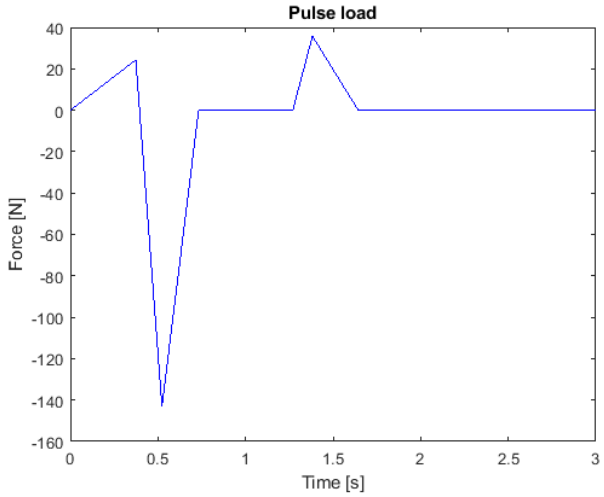

Figure 3.12 Pulse load on a signboard for a trailer truck based on the extrapolated results of Lichtneger & Ruck (2014). Length of the truck 16.6 m; height of the truck; 4 m; width of the truck 2.6 m; distance between truck and signboard 1.2 m. Signboard 5 m wide and 3.9 m high.

Pulse based on Ginal (2003)

Ginal (2003) has reviewed researches on truck induced wind loads. In this literature review several measurements are compared. The most useful research is from Cook, Bloomquist and Agosta about Truck-Induced Dynamic Wind Loads on Variable-Message Signs (1996), in this research truck induced wind pressures were measured from a bridge spanning a highway. Test vehicles with multiple runs were used to measure the pressure on different altitudes above the truck. At a height of 5.18 m above the highway pressures were measured between -44 and -69 N/m^2. The pressure gradient showed a decrease of 10% per feet (=0.3048 m) between 17 and 20 feet, but the results show a large scatter and the speed of the test vehicle was 105 km/h. The pressures at a height of 5.18 seem to correspond with the pressure profile obtained from the results of Lichtneger & Ruck (2014).

The available results from the research of Ginal (2003) are less extensive than the research of Lichtneger & Ruck (2014) and the parameters for the measurements are not described as accurately. Ginal (2003) used the results of a typical truck pulse of Cook et al. (1996) this is shown in figure 3.13. The pulse is greatly simplified as a triangular shaped pulse with a positive peak and a negative peak with the same amplitude. The original pulse is different from a typical pulse of Lichtneger & Ruck (2003), see figure 3.7. The pulse shown in figure 3.7 has a smaller positive pressure peak compared to the original pulse in figure 3.13 and at the end of the pulse there is no positive peak. The simplified pulse can easily be used for computing the structural response, but does not have a realistic shape. This pulse is further elaborated for different truck speeds by Hosch & Fouad (2010) (see figure 3.2). In this figure truck induced wind pulses are given for vertical oriented pressures. In a similar study of Hong, Zu, & King (2016) a factor of 1.4 is used for scaling the vertical pressures to horizontal pressures. Both studies of Hosch & Fouad and Hong, Zu & King used the pulse from Ginal. If the pulse from figure 3.2 for a truck speed of 50 mph (≈80 km/h) is multiplied with 1.4 a truck induced wind pulse is obtained for pressures in horizontal direction, this results in a peak pressure of 54 N/m^2, same magnitude for the negative peak.

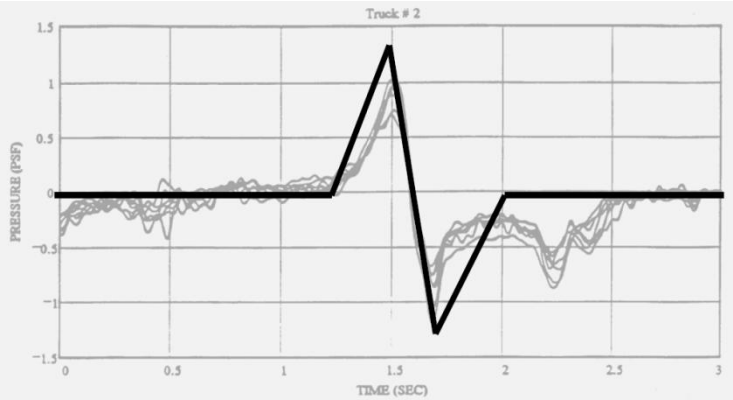

Figure 3.13 Typical truck pulse simplified by Ginal (2003)

If this pulse is also applied to a signboard of 5 m wide and 3.9 m high, then the pressure is applied to a width of 3.66 m, which is equal to the lane width, this is corresponds to the design rule from Hosch & Fouad (2010). The pressure decrement over the height of 10% per 0.3048 m is not used for calculating the pressure over the height as it was only measured for the first meter. The design rules of Hosch & Fouad (2010) uses a linearly decrement starting at a height of 6 m to zero at a height of 10 m (see figure 3.1.). This pressure variation over the height is used with a pressure of 54 N/m^2. This results in a peak pressure of 534 N in magnitude.

Figure 3.14 shows the two pulses in one graph. The pulse based on Ginal (2003) has a much higher momentum than the pulse based on Lichtneger & Ruck (2014). This large difference can arise from an error in extrapolation of pressures based on smaller signboards. Furthermore, the pulse from Ginal (2003) is based on many assumptions from other researches and the research of Lichtneger & Ruck (2014) is based on full scale measurements. The magnitude of the dynamic pulse loads is also much smaller than the static design loads discussed in section 3.2. This large difference probably comes from the dynamic amplification that is already taken into account in equivalent static design loads.

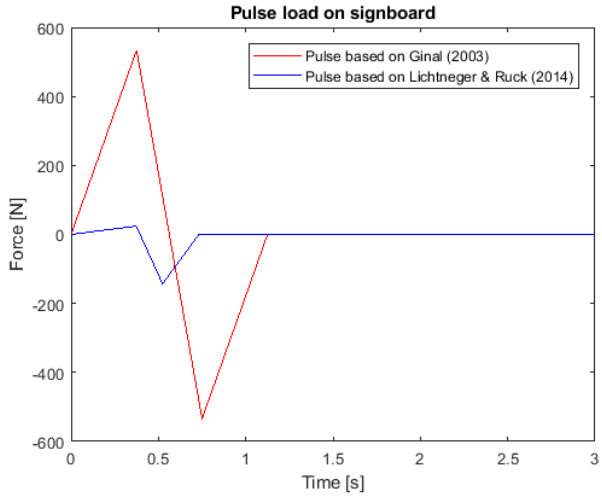

Figure 3.14 Comparison pulses based on data of Lichtneger & Ruck (2014) and results of Ginal (2003)

3.4 Discussion and conclusion

In this chapter design rules are discussed that give a static equivalent load for vehicle induced wind loads. The magnitudes of the loads were between 10% and 39% of the characteristic wind load on a specific signboard. The pulse of a truck induced wind load on a signboard with a width larger than the truck is not known from full scale measurements. Two different truck pulses on a specific signboard are obtained by using data of full scale measurements. The results of Lichtneger and Ruck (2014) on small signboards are extrapolated for the use on larger signboards. This resulted in a pulse load with small peak magnitudes compared to the pulse load obtained from the research of Ginal (2003), who

greatly simplified the pulse. The difference in magnitudes arises from the difference in pressure variation over the height of the signboard and also the pressure variation over the width of the signboard. The shape of the pulse from the research of Lichtneger & Ruck (2014) seems to be more realistic based on their extensive research with specific vehicle types. To obtain a realistic pulse of truck induced wind loads on a large signboard full scale measurements should be performed. This can be done in similar way as Lichtneger & Ruck (2014) or it can be done measuring displacements of an existing sign support structure and then calculate the pulse based on the vibrations in the structure since the shape of the pulse is known, but the magnitudes are not exactly known.

Since the magnitude and shape of the pulse load depends on many parameters it is not possible to obtain a general pulse load for vehicle induced wind loads. However, for design rules an upper limit of a pulse can be used to compute the structural response to truck induced wind loads. The variation of the distance between the signboards and the truck is small because the trucks have a standard height and the signboards have a minimum height above the road. A signboard with a width much larger than the truck and a height of 5 m or more gives the governing load on a signboard if the governing vehicle type is applied.

4 Structural response

In this chapter the structural response is calculated when the structure is subject to the truck induced wind loads discussed in chapter 3. First the dynamic response of the structure is analytically calculated based on a single degree of freedom (SDOF) model. Single truck events are compared with multiple truck events. After analysing the SDOF the beam is discretized and modelled as a n-degrees of freedom model where multiple truck events on different lanes are taken into account.

4.1 Simplified rigid body model

The truss beam is modelled as a SDOF rigid body with viscous damping. The pulse load resulting from one truck shown in figure 3.12 is applied to the dynamic model and the response is calculated using Duhamel's integral. The model is greatly simplified in this situation, the structural response to one pulse is analytically calculated for a truck passing under mid span of the truss. Figure 4.1 shows how the modelled system is simplified as a damped mass spring system. Field observations of this structure during a day with low wind speed (i.e. < 3 m/s) showed that the truss beam vibrates in its first mode shape due to vehicle induced wind loads, only horizontal vibrations were visible in this mode shape, this can be modelled using a SDOF. In this simplification trucks drive under the mid span of the structure which does not represent the exact load configuration, but it gives insight to the problem and can be used as verification of the extended model.

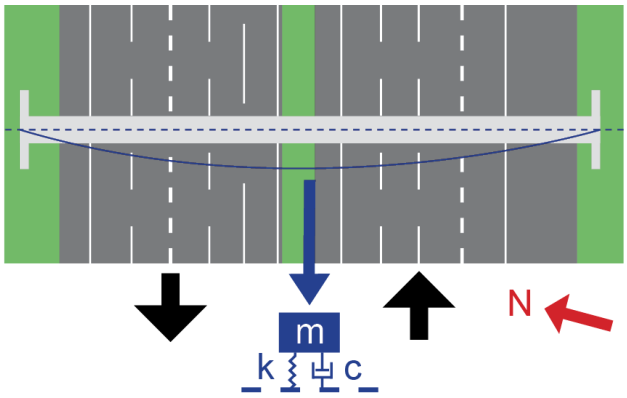

Figure 4.1 Simplification of the system into a damped mass spring system. Top view of the situation; in white the sign support structure, in grey the carriageways, in green the verge and the first mode shape in blue. The orientation to the north is shown in red

Mass

The mass of the beam is calculated and summarized in table 4.1. The mass of different components are taken from Rijkswaterstaat Dienst Infrastructuur (2012) and the mass of the steel sections is calculated based on the cross sectional area and the density of steel. For the chords CHS 168.3x20 are used and for the braces CHS 76.1x6.3 are used. To take into account possible variation in mass of the structural elements a thickness variation of ±0.3mm is used. The mass per cross sectional area of a signboard includes the stiffeners, and the mass of the background underneath the signboard (black part) has a mass per meter width. Interesting to notice is that the signboards have a relatively high mass compared to the truss structure. A minimum, nominal and maximum weight is tabulated.

Table 4.1 Mass of the beam and signboards

Beam

Element	Surface area/amount	Weight	Sum
Chords CHS ø168.3x20±0.3	3x 52m	$7850 \cdot 9.197 \cdot 10^{-3}$ kg/m $7850 \cdot 9.318 \cdot 10^{-3}$ kg/m $7850 \cdot 9.439 \cdot 10^{-3}$ kg/m	11262 kg (-0.3 mm) 11411 kg 11559 kg (+0.3 mm)
Braces CHS ø76.1x6.3±0.3	156x 1.901m	$7850 \cdot 1.321 \cdot 10^{-3}$ kg/m $7850 \cdot 1.381 \cdot 10^{-3}$ kg/m $7850 \cdot 1.441 \cdot 10^{-3}$ kg/m	3075 kg (-0.3 mm) 3213 kg 3355 kg (+0.3 mm)
Cables	52m	2.4 kg/m	125 kg

Signboards

Signboard no.	Surface area/amount	Weight	Sum
1	2 variable electronic signs, steel part 3.6x6m^2, background 6m wide	Variable electronic sign 120 kg, steel part 30 kg/m^2, background 37.5 kg/m	1057 kg (-5%) 1113 kg 1169 kg (+5%)
2	2 variable electronic signs, steel part 3.6x6m^2, background 6m wide	Variable electronic sign 120 kg, steel part 30 kg/m^2, background 37.5 kg/m	1057 kg (-5%) 1113 kg 1169 kg (+5%)
3	1 variable electronic sign and background	Variable electronic sign 120 kg, background 37.5 kg/m	247 kg (-5%) 260 kg 273 kg (+5%)
4	3 variable electronic signs, steel part 2.4x9m^2, background 9m wide	Variable electronic sign 120 kg, steel part 30 kg/m^2, background 37.5 kg/m	1279 kg (-5%) 1346 kg 1413 kg (+5%)
5	1 variable electronic sign, steel part 2.4x5m^2, background 5m wide	Variable electronic sign 120 kg, steel part 30 kg/m^2, background 37.5 kg/m	634 kg (-5%) 668 kg 701 kg (+5%)
		Sum	18736 kg (minimal) 19249 kg (nominal) 19764 kg (maximal)

These signboards are made of steel, currently all new signboards are made of aluminium. The total mass of the structure will be lower if aluminium signboards are used. The distributed mass for aluminium signboards is equal to 16 kg/m^2.

Stiffness

The equivalent stiffness of the beam at mid span is calculated according to

$$\delta = \frac{FL^3}{48EI} \tag{4.1}$$

$$k_{eq} = \frac{F}{\delta} = \frac{48EI}{L^3} \tag{4.2}$$

With δ is the horizontal displacement at mid span
F is the load at mid span
L is the span length of the beam
EI is the stiffness of the beam (Euler-Bernoulli)
k_{eq} is the equivalent spring stiffness of the beam at mid span

The Young's modules of steel is $2.1 \cdot 10^{11}$ N/m^2 and the length of the truss beam is 52 m. The second moment of area for the cross section of the truss beam is calculated according to Steiner's rule multiplied with 0.85 to take into account stiffness reduction due to shear deformations in the truss beam. This results in I= $1.29 \cdot 10^{-2}$ m^4 (see Appendix B).

The equivalent spring stiffness k_{eq} is then $9.2 \cdot 10^5$ N/m

Natural frequency
The eigenfrequency of the first mode for a bending beam can be calculated according to formula 4.3, the equivalent stiffness and mass is used. The equivalent mass is calculated as half the weight of the beam including all mounted units, i.e. 9625 kg.

$$f = \frac{1}{2\pi}\sqrt{\frac{k}{m}} \tag{4.3}$$

With m is the mass of the rigid body (half of the beam)
k_{eq} is the equivalent spring stiffness of the beam at mid span

This results in an eigenfrequency of 1.56 Hz (ω_0 = 9.78 rad/s) for the first mode shape of the beam in horizontal direction.

Damping
A viscous damper is applied to the model with a damping percentage of 0.5%, which is common for welded steel structures in general. Also measurements on steel sign support structures show similar values (Leendertz, 2016). The damped frequency (ω_1) for a low damping value is more or less equal to the natural frequency of the structure. From data of measurements on similar sign support structures (55 m long) a damping ratio was calculated of 0.41% (NLR, 1976). From other measurements on a sign support structure spanning 22 m in the USA a damping ratio of 0.361 % was found for the first horizontal mode shape of a bending beam (Fouad & Hosch, 2011).

Dynamic model
The equation of motion for a damped SDOF:

$$\ddot{u} + 2\zeta\omega_0\dot{u} + 2\omega_0^2 u = \frac{f(t)}{m} \tag{4.4}$$

With u is the horizontal displacement at mid span
ζ is the damping ratio
ω_0 is the natural undamped frequency
m is the mass of the rigid body
$f(t)$ is the load function in time t

The initial conditions, the displacement and velocity, are zero so the general solution of this second order ordinary differential equation consists only of the particular solution. The response to the pulse load can be represented in the form of convolution integral, equation 4.5.

$$u(t) = \frac{1}{m\omega_1}\int_0^t F_u(\tau)e^{-\zeta\omega_0(t-\tau)}\sin\left(\omega_1(t-\tau)\right)d\tau \tag{4.5}$$

With u is the horizontal displacement at mid span
ζ is the damping ratio
ω_0 is the natural undamped frequency
ω_1 is the damped frequency

m is the mass of the rigid body
F(τ) is the load function in time *τ*

The pulse load is divided into 7 parts shown in figure 4.2. The analytical solution to this problem is calculated using Maple software, the script can be found in Appendix C.

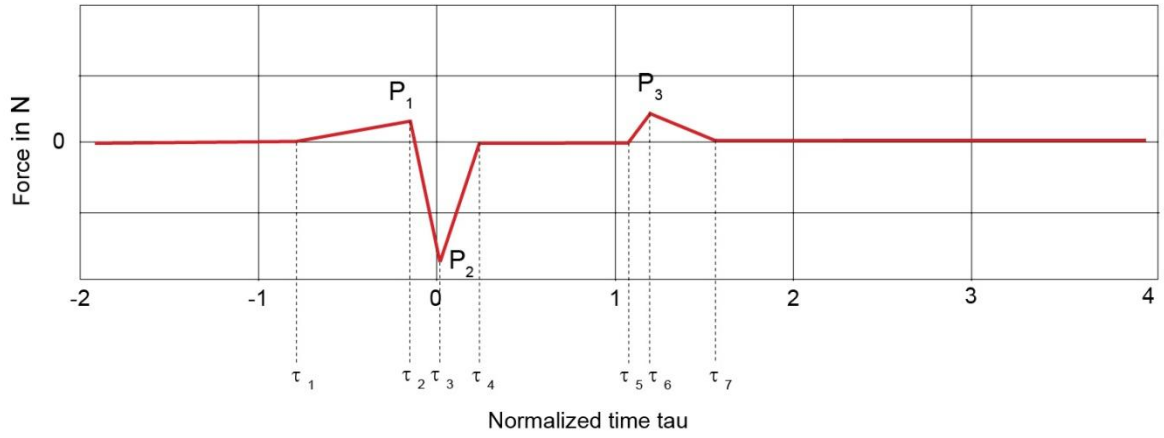

Figure 4.2 Pulse load divided into 7 parts

The load is defined as follows:

$F_1(\tau)$: $\tau_1 < t < \tau_2$
$F_2(\tau)$: $\tau_2 < t < \tau_3$
$F_3(\tau)$: $\tau_3 < t < \tau_4$
$F_4(\tau)$: $\tau_4 < t < \tau_5$
$F_5(\tau)$: $\tau_5 < t < \tau_6$
$F_6(\tau)$: $\tau_6 < t < \tau_7$
$F_7(\tau)$: $\tau_7 < t$

The response of the SDOF rigid body is calculated as follows (only the first two terms are shown here, see Appendix C for the other terms):

$$u_1(t) = \frac{1}{m\omega_1}\int_0^t F_1(\tau)e^{-\zeta\omega_0(t-\tau)}\sin\left(\omega_1(t-\tau)\right)d\tau \tag{4.6}$$

$$u_2(t) = \frac{1}{m\omega_1}\int_0^{\tau_1} F_1(\tau)e^{-\zeta\omega_0(t-\tau)}\sin\left(\omega_1(t-\tau)\right)d\tau + \frac{1}{m\omega_1}\int_{\tau_1}^t F_2(\tau)e^{-\zeta\omega_0(t-\tau)}\sin\left(\omega_1(t-\tau)\right)d\tau \tag{4.7}$$

For $u_{3,4,5,6,7}(t)$ (see Appendix C)

Results of the simplified dynamic model
The results of the simplified dynamic model are plotted in a diagram shown in figure 4.3. The maximum horizontal displacement of the structure is 0.36 mm for one truck pulse (i.e. two times the amplitude of the vibration). This seems to be a small value because this would not lead to significant deformations in the structure when it is compared with the design rules mentioned in table 3.1. A static displacement due to the lowest design load is equal to 3 mm (2.9 kN on sign of 5x3.9 m^2).

Also the results for two truck pulses with a time difference of two seconds in between is computed, this is shown in figure 4.4. From this diagram amplification is visible, if vehicles drive with a specific distance between each other the structure can resonate due to the periodic occurrence of the pulse loads, but the response can also be smaller when the pulse is in anti-phase with the current vibration in the structure.

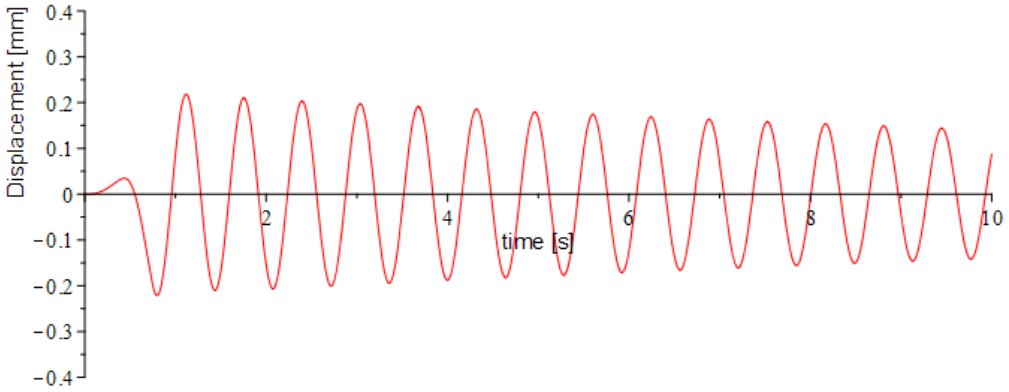

Figure 4.3 Analytical solution of the structural response of a SDOF to one truck pulse

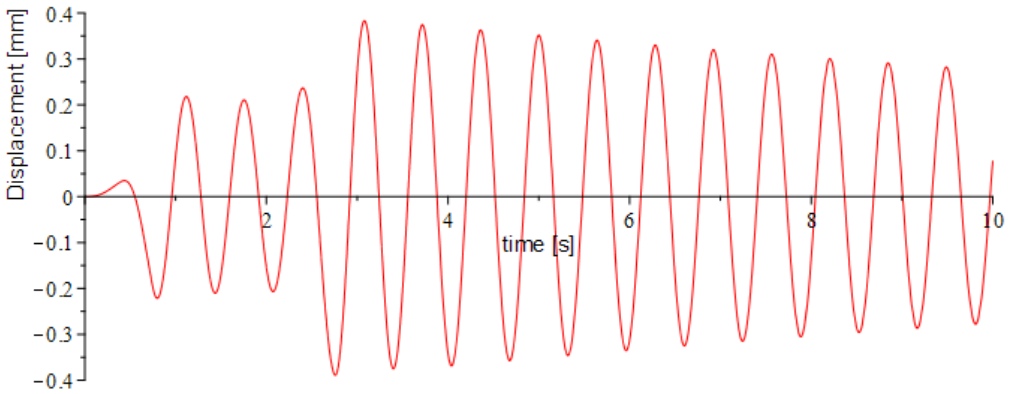

Figure 4.4 Analytical solution of the structural response of a SDOF to two truck pulses with a time difference of 2 seconds in between the pulses

From field observation the structural response to one truck passing was hardly visible, but when more trucks passed underneath the structure vibrations were clearly visible. From this observation it follows that the amount of trucks and the distance between the trucks play an important role on the structural behaviour of a sign gantry to truck induced wind loads. The structural response to a pulse load based on the work of Ginal (2003) is also computed and compared with the response of a pulse based on Lichtneger & Ruck (2014). The response to both pulses is plotted in figure 4.5. The displacements for the pulse based on Ginal (2003) are larger, because the pulse has a higher magnitude.

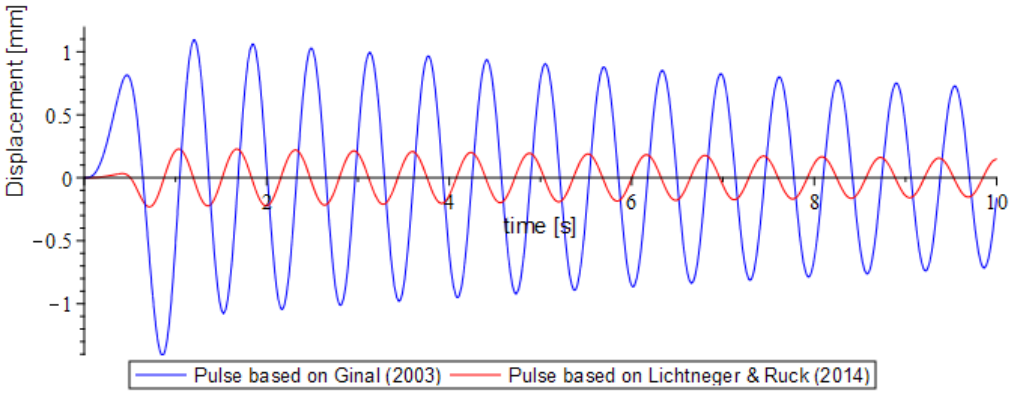

Figure 4.5 Analytical solution of the structural response of a SDOF to one truck pulse based on Lichtneger & Ruck (2014) and Ginal (2003)

4.2 Discrete Euler-Bernoulli beam model

To compute a more realistic structural response, the truss beam is discretized according to a similar method of finite difference in order to apply vehicle induced wind loads at several nodes (multiple lanes). The computation requires the mass, stiffness and damping matrix of the beam. The truss beam is modelled as a simply supported beam with and without rotational springs at both ends. The mass matrix is a diagonal matrix with on each entry the mass per segment, the total mass including the signboards is uniformly divided over the beam's length/nodes. The stiffness matrix is set up by lumping bending deformation in discrete springs for an Euler-Bernoulli beam. The damping matrix is a combination of the mass and stiffness matrix according to Rayleigh. The equation of motion of the system in general is as follows:

$$M\ddot{u} + C\dot{u} + Ku = F(t) \tag{4.8}$$

With u is the horizontal displacement vector
M is mass matrix
C is the damping matrix
K is the stiffness matrix
$F(t)$ is the force vector

As an example the beam is divided into 6 segments (i.e. 7 nodes), this results in a segment length '**a**' of 8.67 m. The derivation of the stiffness and mass matrices is shown:

Mass matrix

The mass matrix is a diagonal 5x5 matrix (the first and the last node are fixed so have zero displacement), if the density of the beam is constant then the mass matrix will look as following:

$$M = m\begin{pmatrix} 1 & & & & \\ & 1 & & & \\ & & 1 & & \\ & & & 1 & \\ & & & & 1 \end{pmatrix} \tag{4.9}$$

Where m is the total weight divided by 6 (number of segments)

Stiffness matrix

The beam is discretized for a simply supported case with and without rotational springs at both supports according to the example for a clamped free beam from Blauwendraad (2006). The beam is divided into 6 segments of length *'a'*, see figure 4.6. The beam is loaded by a distributed force '*f*'. In one segment the bending deformation is lumped into springs. From Euler-Bernoulli's beam theory the rotation of a simply supported beam loaded by two equal moments at both ends is equal to

$$\theta = \frac{M \cdot a}{2EI} \tag{4.10}$$

With M is the bending moment couple (see figure 4.7)
a is the element length
EI is the stiffness of the beam (Euler-Bernoulli)

this results in an equivalent bending spring stiffness of

$$k_{b,eq} = \frac{2EI}{a} \tag{4.11}$$

This gives the stiffness of a bending element, see figure 4.7.

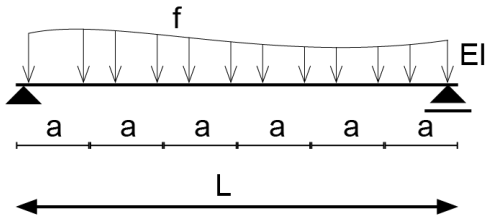

Figure 4.6 Beam divided into 6 segments of length ‘a’

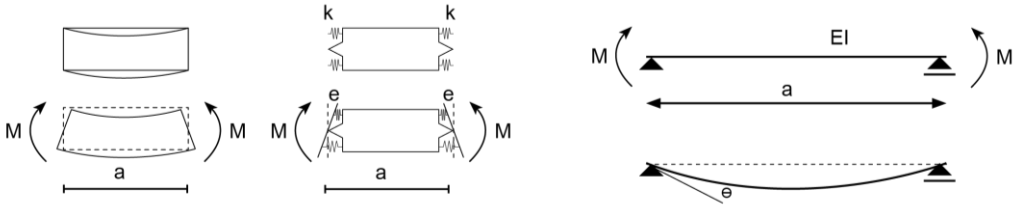

Figure 4.7 Stiffness of one segment

Now that the stiffness of a single element is known, the stiffness of a coupled segment can be obtained. The combined rotational stiffness of a coupled element is equal to (springs in series):

$$D = \frac{EI}{a} \tag{4.12}$$

The beam of 6 segments is now divided into 5 coupled elements, see figure 4.8. This resulted in 2 edge elements and 3 field elements.

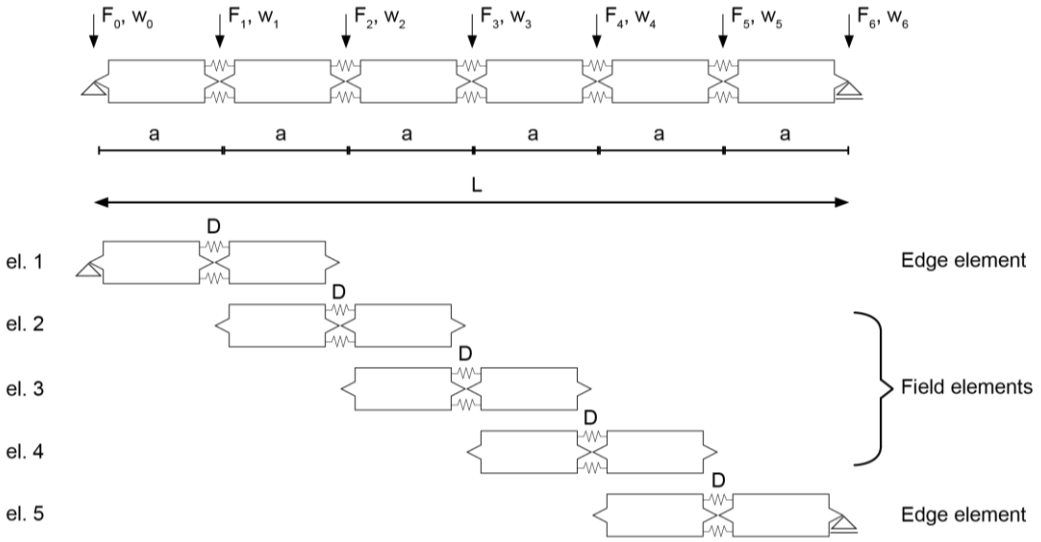

Figure 4.8 Division of the beam into 5 coupled segments, 2 edge elements and 3 field elements

From this the stiffness matrix of the single coupled elements can be computed, see figure 4.9. For the field element:

$$\left.\begin{aligned}\phi_{1,2} &= \frac{1}{a}(w_2 - w_1)\\ \phi_{2,3} &= \frac{1}{a}(w_3 - w_2)\end{aligned}\right\} \quad e = \phi_{1,2} - \phi_{2,3} \qquad e = \frac{1}{a}(-w_1 + 2w_2 - w_3)$$

$$M = De = \frac{D}{a}(-w_1 + 2w_2 - w_3)$$

$$F_1 = -\frac{M}{a} = \frac{D}{a^2}(-w_1 + 2w_2 - w_3)$$
$$F_2 = 2\frac{M}{a} = \frac{D}{a^2}(-2w_1 + 4w_2 - 2w_3)$$
$$F_3 = -\frac{M}{a} = \frac{D}{a^2}(-w_1 + 2w_2 - w_3)$$

The stiffness matrix of the field element is shown below. For an edge element without rotational stiffness the latter derivation is the same. However, w_0 is now equal to 0 and therefore the first row and column can be disregarded. If rotational stiffness at the supports is added to the problem, then the derivation of the stiffness matrix is similar, but the stiffness (D) is now equal to k_r. For a clamped boundary condition k_r is equal to EI/2a. The first row and column can also be disregarded because w_0 is equal to 0.

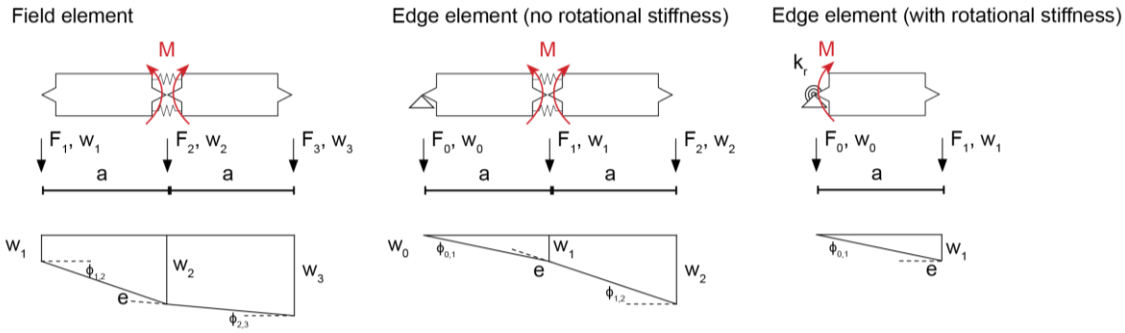

Figure 4.9 Determination of the stiffness matrices of the field and edge element with and without rotational stiffness

Field element:.

$$\begin{pmatrix}F_1\\F_2\\F_3\end{pmatrix} = \frac{EI}{a^3}\begin{pmatrix}1 & -2 & 1\\ -2 & 4 & -2\\ 1 & -2 & 1\end{pmatrix}\begin{pmatrix}w_1\\w_2\\w_3\end{pmatrix}$$

Edge element:

$$\begin{pmatrix}F_1\\F_2\end{pmatrix} = \frac{EI}{a^3}\begin{pmatrix}4 & -2\\ -2 & 1\end{pmatrix}\begin{pmatrix}w_1\\w_2\end{pmatrix}$$

Edge element (rotational spring):

$$\begin{pmatrix}F_0\\F_1\end{pmatrix} = \frac{k_r}{a^2}\begin{pmatrix}1 & -1\\ -1 & 1\end{pmatrix}\begin{pmatrix}w_0\\w_1\end{pmatrix}$$

If these matrices are added into one matrix the stiffness matrix of the discretized beam without rotational springs is obtained:

$$K = \frac{EI}{a^3}\begin{pmatrix}5 & -4 & 1 & 0 & 0\\ -4 & 6 & -4 & 1 & 0\\ 1 & -4 & 6 & -4 & 1\\ 0 & 1 & -4 & 6 & -4\\ 0 & 0 & 1 & -4 & 5\end{pmatrix} \tag{4.13}$$

When the beam is divided in more than 6 elements then the stiffness matrix will look similar, the first two and the last two rows will be the same. The 3th row [1 -4 6 -4 1] is repeated, this row is called the ‘beam molecule’.

If rotational springs are added to both supports of the beam, then the first and the last entry of the stiffness matrix will be different. Suppose a rotational spring k_r is added then the stiffness matrix is as follows:

$$K = \frac{EI}{a^3}\begin{pmatrix} 5+\frac{k_r a}{EI} & -4 & 1 & 0 & 0 \\ -4 & 6 & -4 & 1 & 0 \\ 1 & -4 & 6 & -4 & 1 \\ 0 & 1 & -4 & 6 & -4 \\ 0 & 0 & 1 & -4 & 5+\frac{k_r a}{EI} \end{pmatrix} \tag{4.14}$$

In case of a clamped beam k_r is equal to:

$$k_r = \frac{2EI}{a} \tag{4.15}$$

For a simply supported beam without rotational stiffness k_r is equal to zero and the stiffness matrix is equal to the 4.13.

Damping matrix

The damping matrix is constructed using the mass and stiffness matrix of the system this results in proportional damping and is also called Rayleigh damping. The mass and the stiffness matrices are multiplied with a coefficient and added up:

$$C = a_0 M + a_1 K \tag{4.16}$$

The constants a_0 and a_1 depend on the natural frequencies (ω) and damping ratios (ζ) of the first two modes.

$$a_0 = \frac{2\omega_1\omega_2\left(\zeta_1\omega_2 - \zeta_2\omega_1\right)}{\omega_2^2 - \omega_1^2} \tag{4.17}$$

$$a_1 = \frac{2\left(\zeta_2\omega_2 - \zeta_1\omega_1\right)}{\omega_2^2 - \omega_1^2} \tag{4.18}$$

The natural frequencies of the first two modes can be calculated, but the damping ratios have to be estimated based on similar structures. A damping ratio of 0.005 is chosen for the first mode and 0.01 for the second mode.

4.3 Results and validation

The structural response of the system is calculated using MATLAB. The equation of motion is a second order differential equation which can be written as a system of two coupled first order differential equations. This can be solved numerically in MATLAB using numerical integration.

In order to validate the discrete beam model, the stiffness matrix can be checked with analytical solutions for the static case. The mass matrix can be checked in combination with the stiffness matrix by calculating the undamped natural frequencies of the beam. When 52 segments are used and the total mass is uniformly distributed over the length, the error in first 5 natural frequencies and static displacement is less than 0.1%. The validation and the MATLAB-script can be found in Appendix D of this document.

The solution for a case with 10 segments is compared to the analytical solution of a SDOF, two consecutive truck pulses based on Lichtneger & Ruck are applied at mid span of the beam. Figure 4.10 shows that results are the same, the computational error can be neglected.

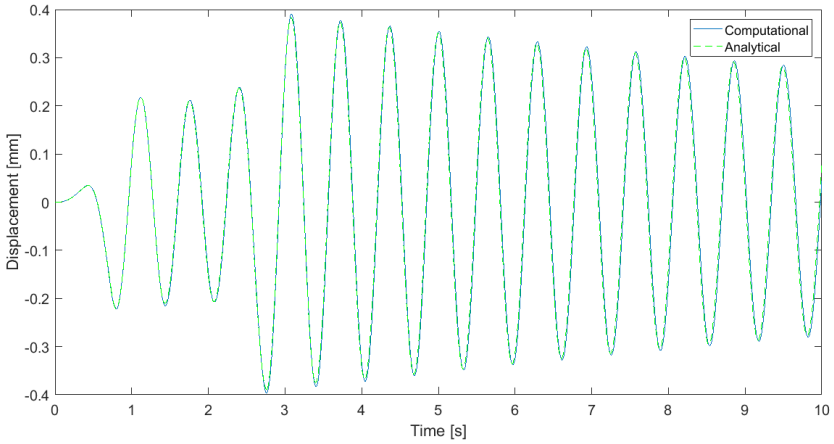

Figure 4.10 Analytical solution from Maple and computational solution from MATLAB for two truck pulses with time difference of 2s

A more realistic calculation is now performed for a situation where the beam is loaded by in total 5 trucks on two different lanes. For simplicity of the model also 10 segments are used, figure 4.11 shows the nodes in a top view of the structure . The truck pulses are based on the pulse obtained from the measurements of Lichtneger & Ruck (2014). The loads are applied to node 3 and node 8. These nodes correspond with ‘Lane 1’ and ‘Lane 2’ in the same figure. The response to these truck pulses is shown for the node at mid span.

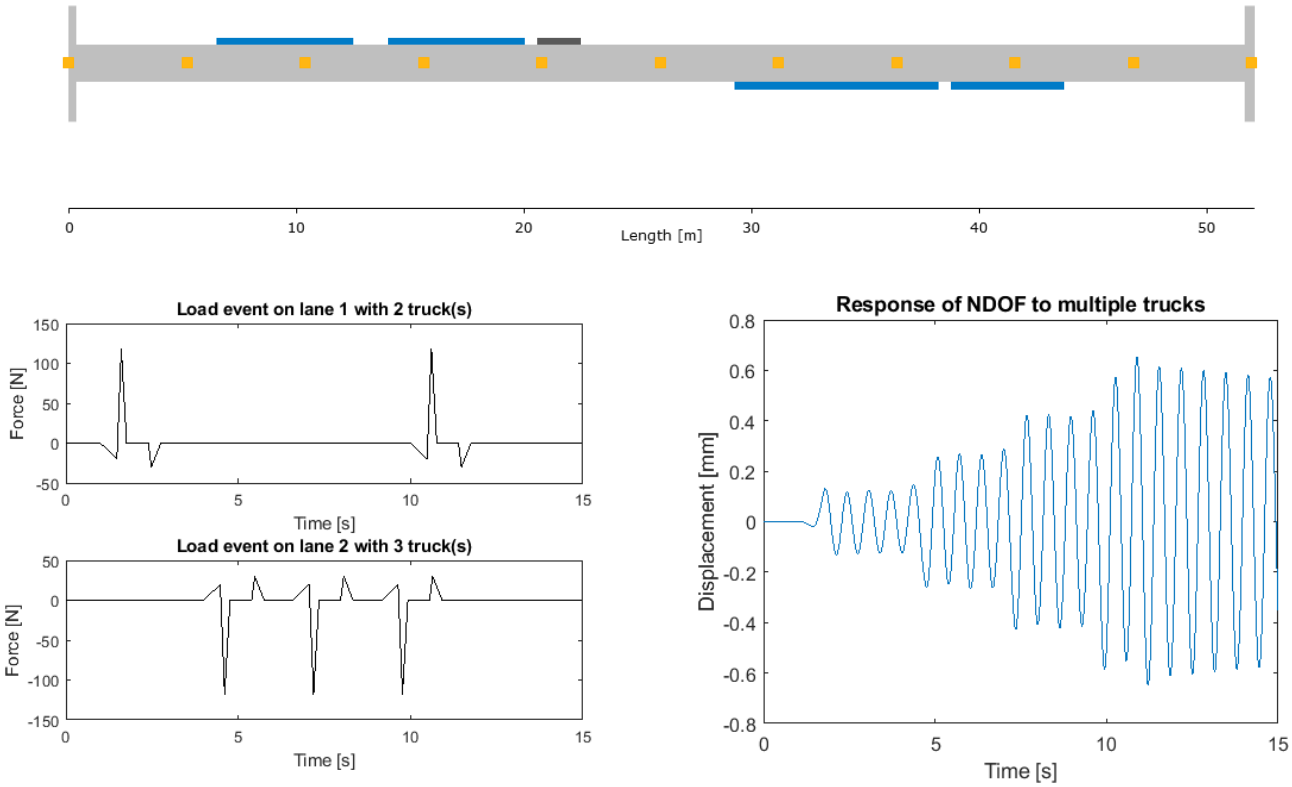

Figure 4.11 Computation of the structural response to 5 truck pulses at two lanes (node 3 and 8 in the top figure). The displacement of the 6th node is shown, this is the node at mid span of the beam.

4.4 Sensitivity of the dynamic model

Important parameters are the stiffness and the mass of the truss beam, these two parameters influence the natural frequency of the beam. The mass of the signboards is included to the total mass and uniformly distributed over the length of the beam. The stiffness of the beam is estimated based on the Euler Bernoulli beam theory, the mass of the beam is based on the cross sectional area of truss elements and for the mass of the signboards an equivalent mass per area is used. In table 4.1 the mass of the beam is calculated with nominal values and with assumed deviant values, the total mass of the beam is between 18736 kg (minimal), 19249 kg (nominal) and 19764 kg (maximal). The natural frequency of the beam is calculated for different masses and stiffness (±5%), the results are summarized in table 4.2. From this it is clear that the natural frequency can vary between 1.51 and 1.63 Hz based on a simply supported Euler Bernoulli beam, the natural frequency can vary between 1.58 Hz and 1.70 Hz for beam with rotational springs at both ends.

Table 4.2 Possible variance in the natural frequency of the beam based on deviating parameters

Mass (uniformly distributed over the length of the beam)	Stiffness	Natural frequency of the first mode (analytical simply supported)	Natural frequency of the first mode (computational N=52, rotational stiffness at both ends)
18736 (minimal)	$2.8422 \cdot 10^9$ Nm^2 (+5%)	1.632 Hz	1.703 Hz
19249 kg (nominal)	$2.7069 \cdot 10^9$ Nm^2	1.571 Hz	1.643 Hz
19764 kg (maximal)	$2.5716 \cdot 10^9$ Nm^2 (-5%)	1.509 Hz	1.584 Hz

Pulse and natural frequency

The oscillation period of one vibration is equal to 0.64 s and the length of the pulse is 1.644 s. Figure 4.12 shows that the time at which a truck passes the structure is very important and should be very accurate in order to have resonant effects. The passing truck could also lead to the opposite of resonance or something in between. Hence, the response of the beam is very sensitive to the time parameter of a passing truck.

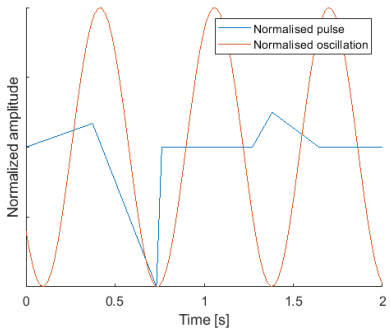

Figure 4.12 The shape and length of a truck pulse load compared to an oscillation in the natural frequency of the beam (i.e. 1.57 Hz)

4.5 Discussion and conclusion

To compute the dynamic response of a sign gantry spanning 9 lanes in two directions a SDOF rigid body model is not sufficient, therefore a discrete beam model was used. The computational model is validated with analytical solutions for simple problems (i.e. simply supported beams). The stiffness matrix is checked compared to static solutions and also in combination with the mass matrix to check the natural undamped frequency of the system. The beam was discretized with 26 segments and 52 segments. In both cases the discretization error was smaller than 0.6% therefore the computational model with 26 segments (size 2 m) is preferred since the computational time is reduced with a factor 20 compared to the computational model with 52 segments. The signboard configuration is different for each lane and therefore the pulse load from a vehicle should be different for each lane. But the pulse load from passing trucks is applied as concentrated forces on only one node, because the pressure variance is not exactly known from literature. In reality the load will be more distributed and different for other types of vehicles and location with respect to the signboard.

The two assumptions of the boundary conditions, hinged and rotational springs, are both computed and compared with a possible error in the mass and the stiffness. Overall this lead to a range in natural frequencies of the first horizontal mode shape between 1.51 Hz and 1.70 Hz.

Computational results showed that passing vehicles could amplify or reduce the amplitude of vibration and that the timing of a vehicle comes very precise for the response of the structure. The amplitude of vibration seems to be very low for the pulse based on the Lichtneger & Ruck (2014), larger amplitudes are calculated with the pulse based on Ginal (2003). The next chapter will show which pulse gives the most realistic response by comparing the computational response to full scale measurements.

5 Preliminary measurements

This chapter describes the test set-up of preliminary full scale measurements for determining the structural response to truck induced wind loads. The displacement of the structure is measured on a day with low wind speed (<3-5 m/s) with the use of video cameras. This simple measurement method is used instead of a more sophisticated method due to time delay and gives information about the amplitude and frequency of the vibrations due to truck induced wind loads. The measurements are used to validate and compare it with the calculation model.

5.1 Measurement report

Location

The structure is located at the highway A20 in Rotterdam near to the junction with the A16, see figure 5.1. The speed limit at this part of the highway is 100 km/h. The structure spans 52 m over in total 9 lanes, from where 5 are in westward direction and 4 are in eastward direction. The highway is surrounded by a sound barrier at the north side and by trees at the south side.

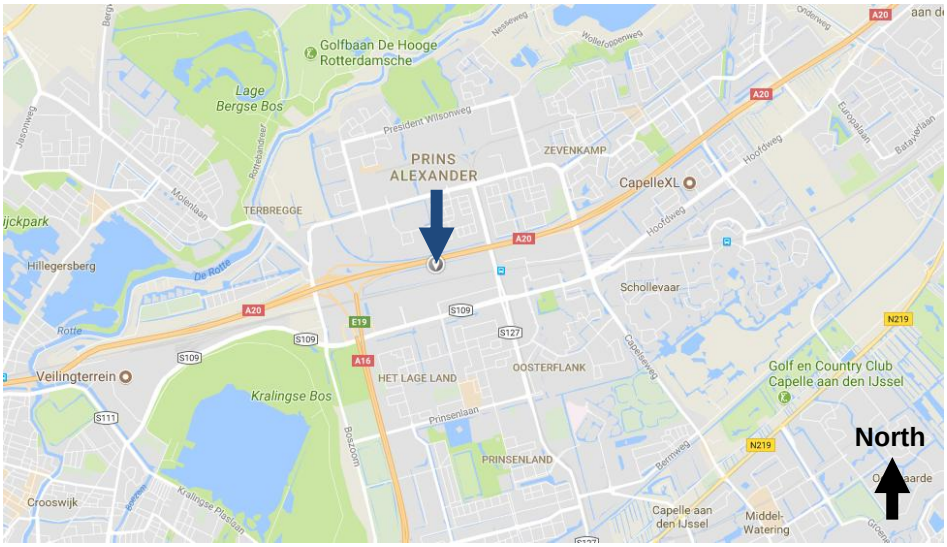

Figure 5.1 Location of the sign support structure (Google Maps, 2018)

Method

To perform measurements on the sign support structure without having access to the structure video cameras are used. Video cameras are located in the verge of the road, in this way traffic is not disturbed by road blocks for mounting equipment to the structure. Data of the structural behaviour is obtained which can be used for a preliminary assessment of the problem.

Parameters of interest are:

- Vehicle's height (specifically what type of truck)
- Lane at which the truck is driving
- Vehicle's speed
- Amplitude and frequency of vibration at a certain point in the beam
- Torsion vibrations of the beam

To capture the effects of these parameters, multiple cameras are required. One camera is used to capture the vehicle type and at which lane it is driving, this camera is located at a distance of approximately 50 m from the structure where it has an overview of the situation. Another camera is focussed on a specific detail of structure, the dimensions of this detail can be related to the displacement of the truss at this location. The data of this camera gives the amplitude of vibration and can be used to obtain the natural frequency. The last camera is focussed on the traffic to estimate the average speed and height of the vehicles when they pass the structure. An overview of the test set-up

is shown in figure 5.2 and table 5.1. The cameras are placed at the right hand side because this side is easy accessible, the other side has a narrow verge due to a sound barrier and is therefore less safe to perform measurements. All cameras are mounted on fixed points, 2 on tripods and 2 on the electronic installation cabinet.

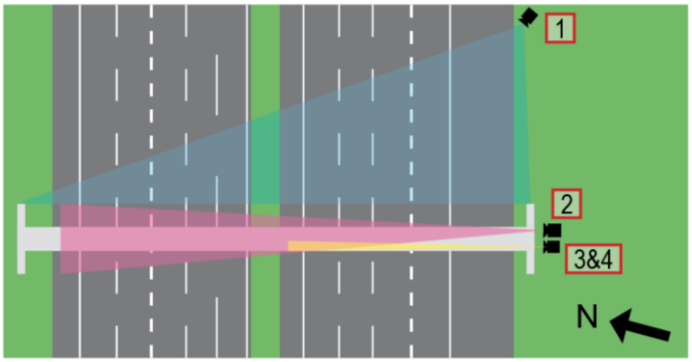

Figure 5.2 Set-up of the cameras for measurements. The camera with the blue area gives an overview of the situation, the camera with the pink area gives an overview of the vehicle's speed and the cameras with yellow area are focussed on two specific details

Table 5.1 Overview of the cameras

Camera	Parameters
1 and 2 (Overview)	Location of the vehicle and type of vehicle
2 (Overview perpendicular)	Speed and height of the vehicle
3 (Detail 1 lower part)	Amplitude and frequency of vibration
4 (Detail 2 upper part)	Amplitude and frequency of vibration

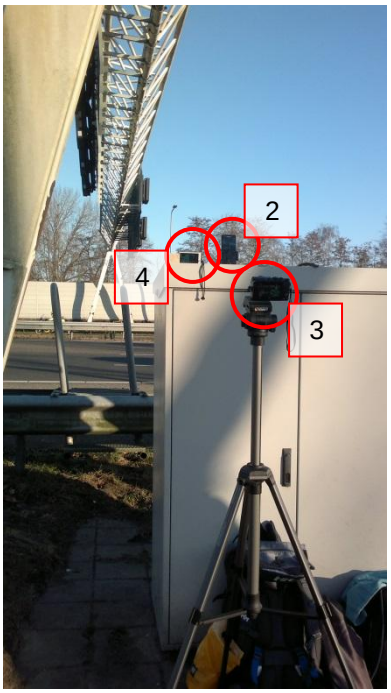

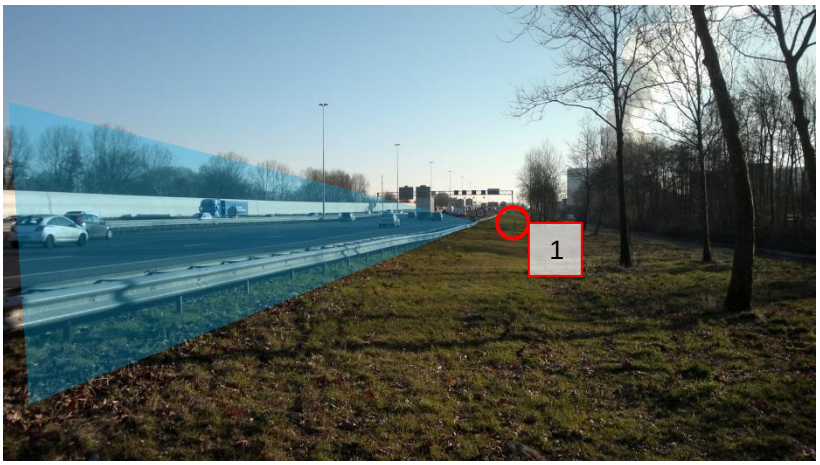

The specific detail is shown in figure 5.3. This detail has a small distance to the centre of the truss beam, therefore torsion effects in the displacements are minimised. The dimensions of the connection are known from shop drawings (see Appendix A), multiple details of this connection are used to relate observed vibrations to known amplitudes in mm, for example M16 bolts are used, the head of these bolts have a diameter of 24 mm.

In order to observe torsion effects in the truss and have a comparison point another detail was observed shown in figure 5.4. The lower part of the signboard has large distance between the centroidal axis of the truss beam. Therefore it will have the highest displacements if torsion of the truss beam occurs. The details are located at a length of approximately 22 m from the south side of the beam (figure 5.5).

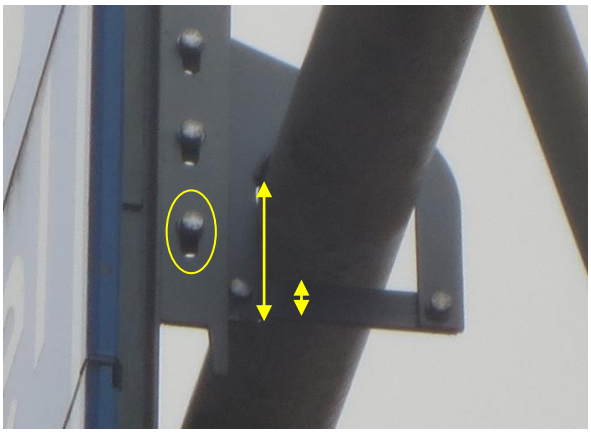

Figure 5.3 Specific detail of the structure for the focussed camera (upper part signboard)

Figure 5.4 Specific detail of the structure for the focussed camera (lower part signboard)

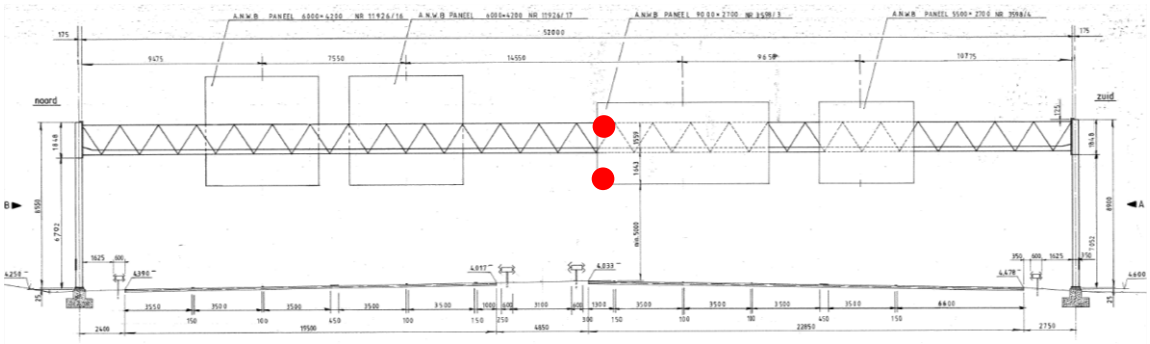

Figure 5.5 Location of the details marked in red (construction drawings do not represent the actual signboard configuration, see Appendix A for a sketch of the actual situation)

The video data is synchronized and edited in one video, see figure 5.6 for a screenshot of the video, also the view of the cameras can be seen in this figure. The speeds of the vehicles are estimated using the road surface markings, these lines have a standard length of 3 m and a length of 9 m in between. The vehicle height is also estimated using these lines, or by other known reference points and truck type. The displacements are estimated using the structural details as reference points.

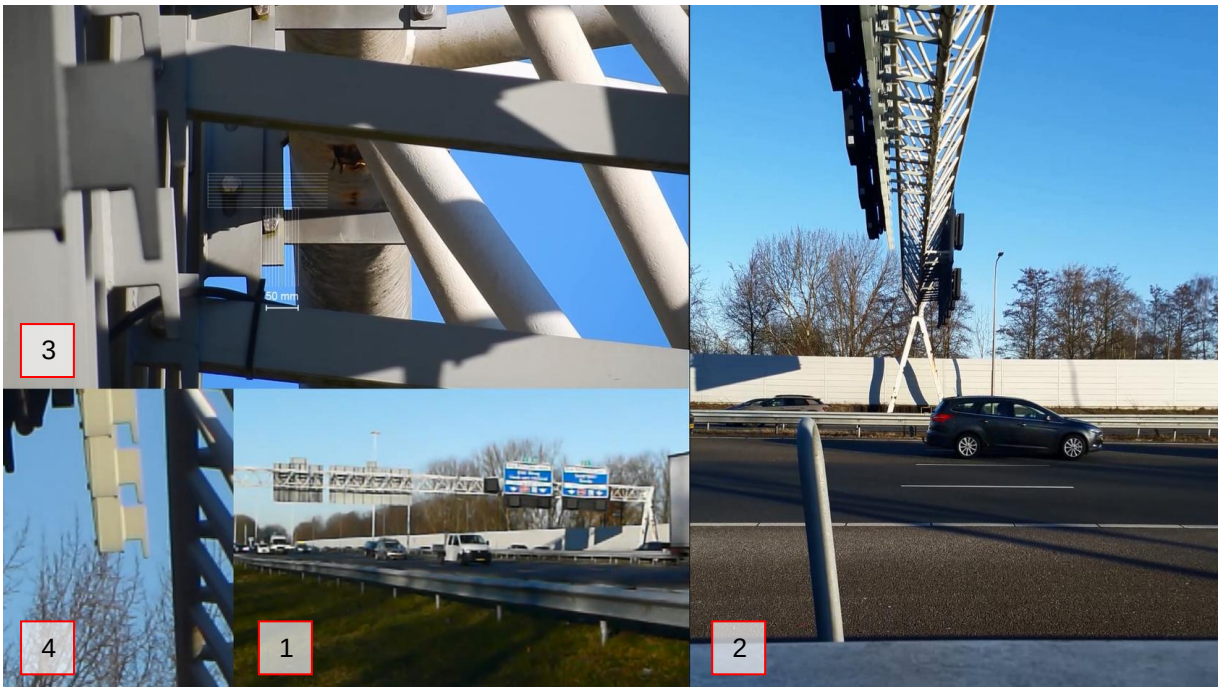

Figure 5.6 Numbered video images corresponding with the numbers in table 5.1 and figure 5.2

Weather information

The measurements were performed in the morning between 08:30 AM and 09:30 AM on the 27th of February 2018. A weather station in Rotterdam recorded hourly natural wind speeds and temperatures, this is summarized in table 5.2. Also weather information of a local non-official weather station is obtained, this is summarized in table 5.3. The first weather station is located at the airport in an open grass field which is more than 5 km away from the structure. The second weather station is located in a residential area 1 km away from the structure. Based on these wind data it is concluded that vibrations in the structure only occurred due to truck induced wind loads and possible small wind gusts.

Table 5.2 Local weather data in Rotterdam near the airport according to KNMI (KNMI, 2018)

Time	08:00 – 09:00 AM	09:00 – 10:00 AM
Averaged wind speed [m/s]	3.0	5.0
Wind direction [°]	50 (NE)	60 (NE)
Highest wind gust [m/s]	5.0	8.0
Temperature at 1.5 m [°C]	-3.9	-3.3

Table 5.3 Local data of a non-official weather station in Rotterdam-Alexander (Mijn eigen weer, 2018)

Time	Daily average
Wind speed [m/s]	3.9 (high) 1.1 (average)
Wind direction [-]	NE
Highest wind gust [m/s]	5.3
Temperature at 1.5 m [°C]	1.3 (high) -5.1 (low) -1.9 (average)
Wind speed at 08:30 AM was 2.8 m/s and at 09:30 AM 3.8 m/s	

Discussion

- The measurements were performed in the morning because the natural wind speed is lower. Local wind measurements proved that the wind speeds were small (<3.9 m/s).
- The 4 cameras were of a different type and filmed at different frame rates the synchronized video has a frame rate of 25 fps. The frame rate was too low to make a good estimation of the vehicle's speed, therefore a higher frame rate is preferred. There is also a small error in obtaining the time when a truck passes the structure due to the frame rate of the video camera.

- The camera focussed on a specific detail was zoomed in very close to the detail. When trucks passed the structure the camera also showed little vibrations, this is visible in the video and possibly causes an extra error in measuring the amplitude. A more stiff or heavy tripod would solve this problem. The vibration of the camera seems to arise from ground vibrations caused by passing trucks.

5.2 Test results

8 minutes of the film measurements were edited for further assessment. The truss beam vibrates in its first horizontal mode shape, the amount of vibrations are counted and divided by the elapsed time for every minute. If the vibrations were not clearly visible then the counting pace was held constant until the vibration was clearly visible again. This is tabulated in table 5.4.

Table 5.4 Estimated natural frequency of the truss beam in the first horizontal mode shape

Time frame [minute: second]	Estimated natural frequency [Hz]
0:00 – 0:59	1.60 (period with no vibration)
1:00 – 1:59	1.58
2:00 – 2:59	1.58
3:00 – 3:59	1.55 (period with no vibration)
4:00 – 4:59	1.53 (period with no vibration)
5:00 – 5:59	1.58 (period with no vibration)
6:00 – 6:59	1.58
7:00 – 7:59	1.58 (period with no vibration)

The averaged estimated frequency is equal to 1.57 Hz, but if only the clear time frames are used then the natural frequency is equal to 1.58 Hz. The calculated natural frequency of the truss in the same mode shape was equal to 1.56 Hz (SDOF), this is close to the value from the measurements. The difference can arise from small errors in the stiffness or the mass of the beam or in estimating the natural frequency from the video measurement. However, the error is that small that the assumed values for governing parameters are validated. From the discrete model natural frequencies of the first mode shape are between 1.51 Hz and 1.70 Hz, the natural frequency from the measurements lies also in this interval.

The displacement of the beam at the location of the observed detail during the measurements is estimated based on the dimensions of the signboard's connection. This connection which is called the 'ear' connects the signboard to the top chord of the truss beam. Based on this reference point a scale was edited in the video so that it was possible to read the displacements from the screen. The amplitude of vibration is further analysed by playing the video of the detail with a reference point on a large screen. The video was played frame by frame and during each vibration the maximum amplitude was measured from the screen with respect to the centre line of the scaled reference point in the video. This resulted in two data points in each oscillation period, 568 data points for 3 minutes. Then summing the absolute values of the amplitudes of one vibration and dividing it by two results in amplitude with respect to zero. This is done for the first 3 minutes and it resulted in a graph which shows the envelope of vibration's amplitude, figure 5.8. During the 8 minutes of video data the maximum displacement was in this time frame of 3 minutes, the maximum amplitude was equal to 5 mm. No torsion vibration was observed in the video images.

The type of truck and at which time it passes the structure is obtained from the video data as well. The time of passing trucks and trailer truck are noted, but the timing is not very accurate because the frame rate of the camera was too low. Trucks have a smaller height than trailer trucks but are allowed to drive faster and have a higher magnitude of the pulse load with respect to a trailer truck with the same distance to the object (figure 3.8), therefore only these types of vehicles are taken into account. Smaller vehicles are not taken into account because their influence on the structural vibrations is assumed to be negligible. Figure 5.7 and table 5.5 show the time and location of the trailer trucks and trucks.

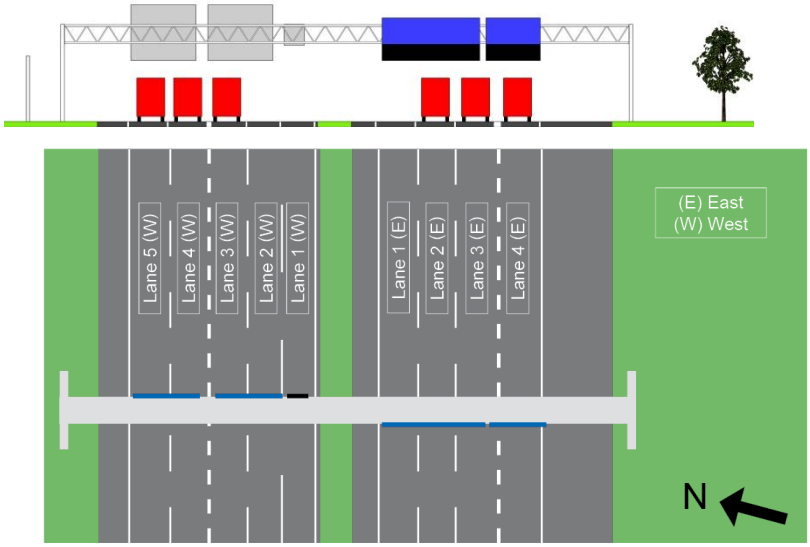

Figure 5.7 Overview and lane numbering

Table 5.5 Time of truck passing and lane location.

West					East			
Lane 5 [s]	Lane 4 [s]	Lane 3 [s]	Lane 2 [s]	Lane 1 [s]	Lane 1 [s]	Lane 2 [s]	Lane 3 [s]	Lane 4 [s]
0,87	46,24	17,89				66,19	7,60	110,36
38,54		44,69				90,29	33,19	137,94
47,69		78,00				91,96	40,80	
81,59		94,27				128,07	65,98	
88,18		110,96					79,33	
89,42		142,76					81,80	
108,37		153,79					98,04	
114,98		157,37					116,78	
121,35							123,72	
179,09							126,90	
							168,14	
							177,61	

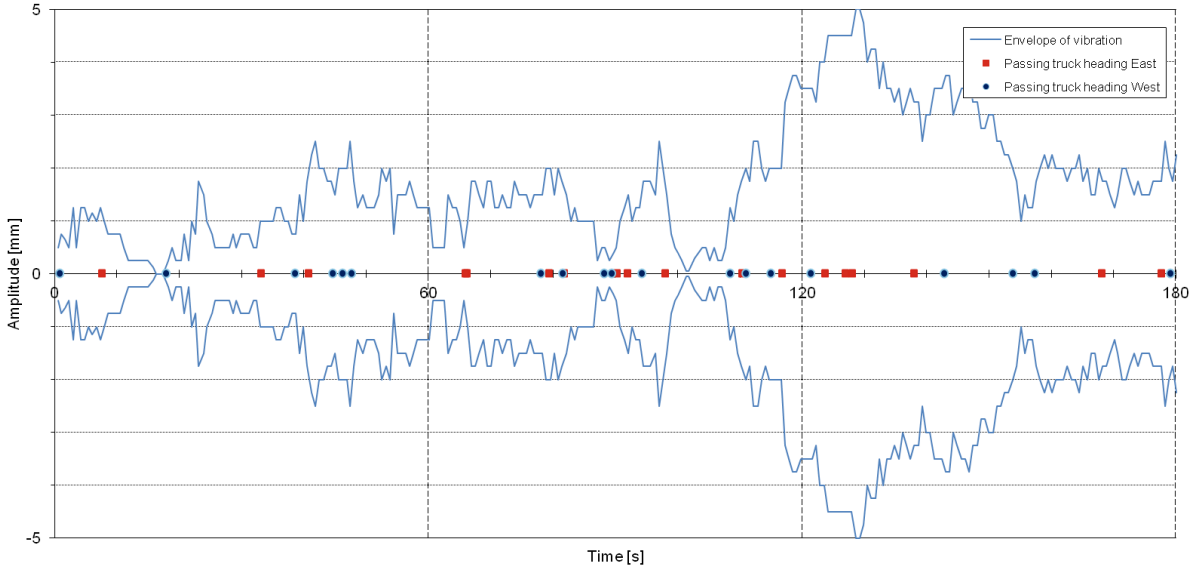

Figure 5.8 Envelope of the vibration's amplitude and the time of passing trucks

From figure 5.8 it is clear that passing vehicles bring the structure in motion and that the timing of the vehicle is an important parameter. The vehicle can amplify and reduce the amplitude of vibration. In the next section the structural response is modelled and compared with the measurements.

5.3 Comparison and validation with the calculation model

The results from the measurements are compared with the calculation model. For each truck or trailer truck the same pulse load is used. The pulse based on Lichtneger and Ruck (figure 3.12) is used, except that the last part of the pulse is neglected, because some trucks had a time distance that resulted in an overlapping pulse. From the literature research only single truck pulses are known and the magnitude and shape of the pulses from multiple trucks with a small time distance is not known. Besides, the pulse is based on a boxed trailer truck and last part of the pulse is different for each type of truck. Some trailers were empty or had a different shape than a boxed shaped trailer. The first part of the pulse is similar for all types of trucks (see figure 3.8 from chapter 3) and is the most influential part for the structural response, therefore the pulse is simplified and used for each type of truck. The result of the computation is shown in figure 5.9 and does not show resemblance with the measurements. The first thing that stands out is that the amplitude of the computation has a large difference from the measurements. From a closer look to the peaks and drops in the graph it seems that there is some resemblance between the measurements and the computation for the first 80 seconds.

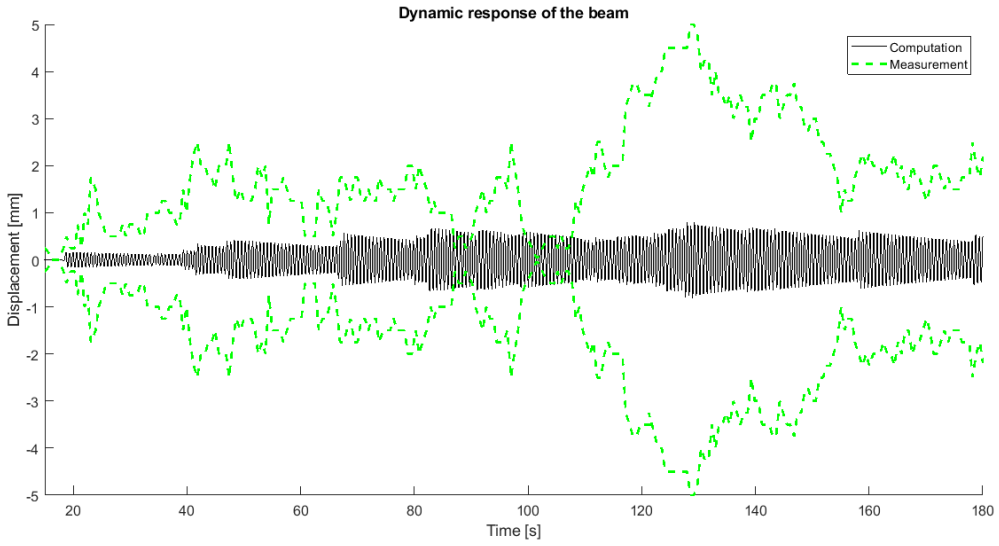

Figure 5.9 Results of the computation compared to the results from the measurements (beam: simply supported discretized with 53 nodes)

The natural frequency of the structure based on the video data was very close to the calculated natural frequency. Therefore the assumed stiffness, mass and boundary conditions (simply supported) were validated. From this point of view the difference between the amplitude could only arise from the magnitude of the pulse loads. A small difference between the natural frequency in the computation and reality results in a difference of peaks and drops. Also the times of truck passes have a certain error, because obtaining the time of a truck pass from the video data is not very accurate due to the low frame rate. To exactly model the observed situation the timing of the truck passes and frequency period should be perfect, because a truck that passes the structure for example at 18 s will influence the response of the structure when a new truck passes at 30 s. Based on a assumed error in the magnitude of the pulse load it is multiplied with a factor 4.2 to obtain matching results with the measurements. Also the passing time of some trucks are shifted with a maximum of ±0.20 s to obtain a fitted result of the computation to the measurements. For this computation the amount of nodes is decreased to 27 in order to save computational time, the error in natural frequency with 27 nodes is still smaller than 0.2% and the computational time is reduced with a factor 20. The result is shown in figure 5.10 and the computation shows a very accurate approximation of what is seen from the measurements.

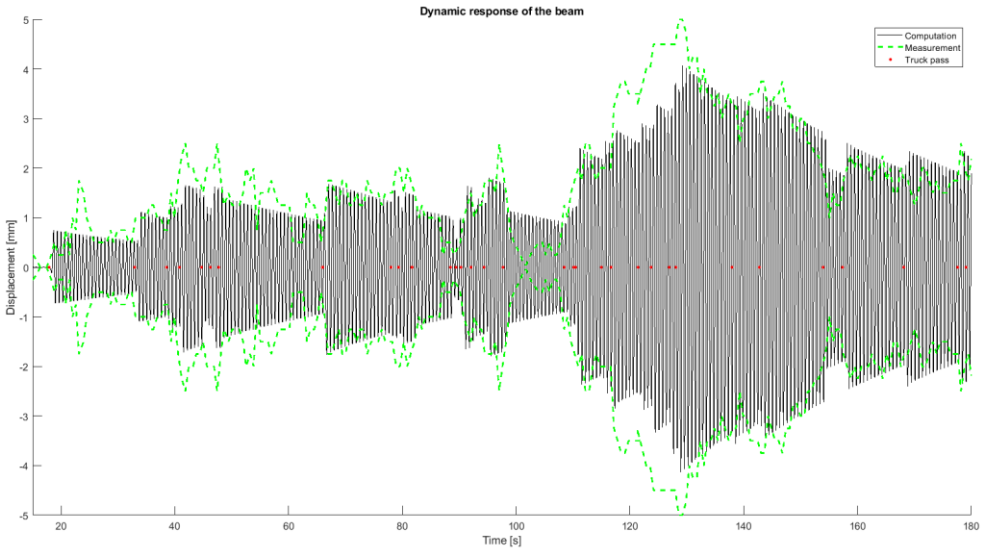

Figure 5.10 Response of the beam at the specific detail. Specific truck times shifted with 0.20 s and pulse multiplied with a factor 4.2 to obtain fitted results compared to the measurements (beam: simply supported discretized with 27 nodes)

Based on this comparison it is possible to tune the computational results to the measurements, by slightly shifting the time of a truck passing, this shift is partly within the measurement error of obtaining the time at which a truck passes the structure and the small error in the natural frequency of the structure. However, the error in magnitude of the pulse load should be explained based on possible wrong assumptions from estimating the pulse based on literature. The pulse load is based on the research of Lichtneger and Ruck (2012), they have performed full scale measurements on small panels with multiple vehicle types. These panels were much smaller than the signboards of the observed sign support structure, see figure 5.11. The results of their research were extrapolated to larger signs, presumably this extrapolation is not performed correctly. A higher maximum pressure would be likely to occur at larger signboards because the displaced air of the truck has to flow through a much smaller area, it cannot flow around the signboard due to the large width of the signboard. Also the assumed pressure variation over the height of the signboard is different than the pressure variation used in design rules for truck induced wind loading. In this design rule for an equivalent static load an almost linear pressure variation is used (figure 3.1). Using this same pressure variation over the height and a pressure of 54 N/m^2 results in a magnitude which is 4.2 times higher than the original pulse. This pulse is similar as the pulse of Ginal (2003), the only difference is that the magnitude of the first peak is lower and a pressure variation over the width is taken into account. The magnitude of the pulse should be checked with a similar experiment as Lichtneger and Ruck (2012) performed, but it could also be derived from a more accurate experiment on the structure using strain gauges and accelerometers that will be carried out in the near future. A test truck that drives underneath the structure at several locations without any interference of other large vehicle gives the response of a single truck passing. From the response of the structure the magnitude of the pulse can be derived in the same way as it is done it this research.

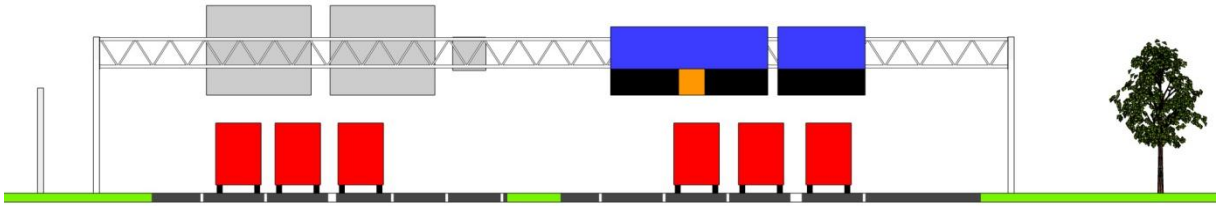

Figure 5.11 The largest panel size from the measurements of Lichtneger & Ruck (2014) is shown in orange and is compared with the size of the signboards.

Discussion of calculation model

The truss beam was modelled as a simply supported beam without rotational stiffness at the supports and the mass of the signboards was distributed uniformly over the length of the beam. These assumption lead to matching results with the measurements, but the results of a more refined calculation model are also checked.

The truss beam is modelled more accurately with a concentrated mass of the signboards at the corresponding nodes, an uniformly distributed mass of the self-weight of the truss and also the rotational stiffness of the supports is taken into account. The natural frequencies of the beam are respectively for 26 and 52 segments $f_{1;26}$ = 1.603 Hz and $f_{1;52}$ = 1.608 Hz. These natural frequencies are close to the natural frequency of the model with a hinged-hinged and an uniformly distributed mass over the length of the beam ($f_{1;26}$ = 1.569 Hz and $f_{1;52}$ = 1.570 Hz). These natural frequencies are both in accordance with the measurements (1.58 Hz). In the more accurate model the stiffness is higher because the rotational springs make the structure more stiff and the active mass in the vibration is higher because the mass of the signboards is not distributed over the full length of the beam but only distributed over the exact location (i.e. nodes). Table 5.6 shows 4 different modelling possibilities and the result of its natural frequency compared to the natural frequency of the measurements. The natural frequencies of the before discussed assumptions are closest to the natural frequency from the measurements. The assumption of a beam with rotational springs at both supports and a non-uniformly distributed mass of the signboards is the most realistic model and shows comparable results in the natural frequency with the measurements.

Table 5.6 Overview of natural frequencies for the first mode shape for different modelling assumptions

Assumption supports	Assumption mass	Natural frequency of the first mode shape
Hinged – hinged	Signboards uniformly distributed	1.57 Hz
Hinged – hinged	Signboards non-uniformly distributed	1.54 Hz
Rotational spring – rotational spring	Signboards uniformly distributed	1.64 Hz
Rotational spring – rotational spring	Signboards non-uniformly distributed	1.61 Hz
Natural frequency based on the measurements		1.58 Hz

In order to have the same response as the measurements the original pulse load has to be factored with 4.5 using a calculation model with rotational springs at both supports and a non-uniformly distributed mass of the signboards, see figure 5.12. The modified pulse is shown in figure 5.13 and is compared with the original pulse from the literature study. The structural response shows an almost similar result when the pulse based on Ginal (2003) is used.

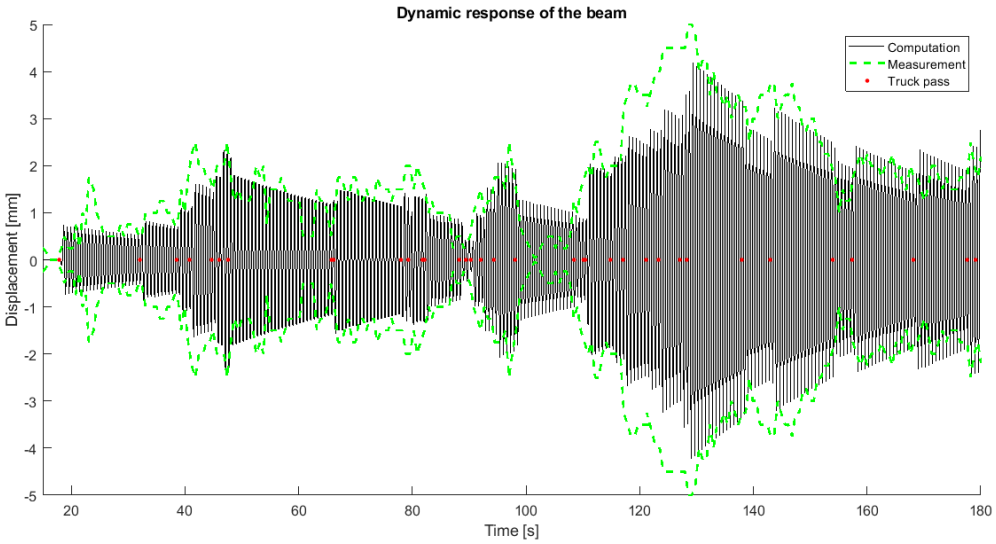

Figure 5.12 Response of the beam at the specific detail. Specific truck times shifted with ±0.2 s and load multiplied with a factor 4.5 to obtain fitted results compared to the measurements (beam: simply supported with rotational springs, mass of the signboards is non-uniformly distributed and the beam is discretized with 27 nodes)

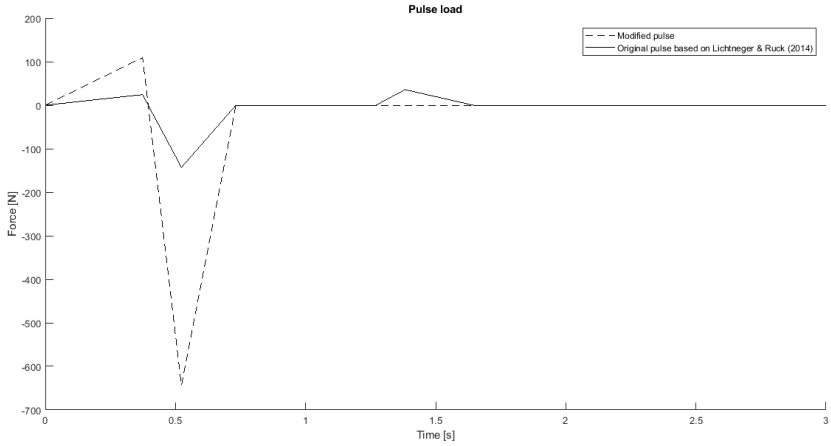

Figure 5.13 Modified general pulse based on fitting of the computation to the measurements and original pulse based on literature research

This modified pulse load is used in chapter 6 for a parametric study on the structural response to truck induced wind loads. All assumptions of the calculation model are summarized in table 5.7.

Table 5.7 Summary of all assumptions for the calculation model

Beam theory:	Euler Bernoulli. The stiffness of the truss is calculated using Steiner's rule for the chords and is reduced with a factor of 0.85 for taking into account shear deformation. The Young's modulus of steel is used.
Mechanical scheme	Simply supported with rotational springs at both ends. The rotational spring stiffness, from the columns, is estimated using SCIA Engineer
Discretization	26 elements for a beam of 52 m (one segment has a length of 2 m). Stiffness matrix based on method of finite difference and damping matrix based on Rayleigh method.
Mass of the truss	Uniformly distributed over the length of the beam
Mass of the signboards	Distributed over the nodes corresponding with the signboards location at the beam
Load	Single pulse load for different types of vehicles and signboard configuration. Only trucks and trailer trucks are taken into account.

5.4 Discussion and conclusion

The amplitude of the structural vibration is estimated using video images with a reference scale based on known dimensions of a specific detail. Despite that the error of this measurement method could be large it gave a good insight of the problem. However, more sophisticated experiments should be performed to compare and validate these measurements. It was possible to measure the natural frequency in satisfactory manner. Still the cameras should have a high frame rate in order to use the data for estimating the vehicle speed and time when it passes the structure. The use of video cameras is also required for measurements with strain gauges and accelerometers to obtain the location and time of the truck with respect to the structure. If it is possible it would improve the quality of the measurements if cameras are placed at both sides of the highway to observe the traffic location and time.

The calculation model approximated the envelope of vibration from the measurements after some minor adjustments in the timing of truck passes and a large scaling factor of the pulse load. The pressure distribution of the pulse load was derived from full scale measurements on small panels from literature, it can be concluded that these results are mot correctly extrapolated to larger signboards. The pulse load based on the research of Lichtneger and Ruck (2014) had to be factored with 4.5 to approximate the measurements with the calculation model. The pulse based on the research of Ginal (2003) approximated the measurements without a load factor. The pressure distribution over the height was estimated too small, a linear distribution from the bottom to the top of the signboard is required to model the problem. This pressure variation and pressure magnitude can only be verified by a similar measurement of Lichtneger & Ruck (2014) with large signboards. The shape of the pulse load is presumably independent of the size of the signboard this is in contrast to the pressure and its distribution. The final pulse that was used is a combination of both studies. With both pulse loads it was possible to use a single pulse load for different trucks, trailer trucks and signboards. There are too many parameters in order to estimate pulse loads for specific vehicles correctly and it would make the calculation model very complicated.

(this page is intentionally left blank)

6 Parametric study of the structural response

This chapter gives a parametric study of the structural response of sign gantries to vehicle induced wind loads. Sign gantries are standardized and can vary in length, stiffness and mass. These parameters influence the structural response to vehicle induced wind loads. With this study the response of standard sign gantries is observed. Also the fatigue stress ranges are calculated for the standard structures and for the structure that was used for the measurements.

6.1 Parameters

First the sign gantry used for measurements is observed and the response is computed for a truck time configuration that would lead to large displacement. This is a theoretic approach where all the trucks pass the structure at a very specific time in the natural frequency of the structure. The trucks pass the structure consecutively with a time interval that is an integer factor a of the oscillation period. This is in theory possible if platooning trucks pass the structure.

Also the responses of standard sign support structures are computed. Table 6.1 shows the parameters of different sign support structure that are used: length, maximum surface area of the signboards, dimensions of the truss and column types.

Table 6.1 Parameters of the standard sign support structures that are currently used (Rijkswaterstaat, 2017)

Length [m]	Maximum signboard area [m^2]	Width truss [mm]	Diameter chord [mm]	Thickness chord [mm]	Diameter brace [mm]	Thickness brace [mm]	Column width [mm]	Column thickness [mm]
15 - 25	109.5	1600	168.3	12.5	63.5	8	350	8
25.5 - 40	183	1800	168.3	16	63.5	8	350	10
40.5 - 50	219	1800	193.7	17.5	76.1	6.3	350	12.5
50.5 – 60	219	1800	193.7	20	76.1	8	350	16

The stiffness of the truss is calculated in the same way as was done in chapter 2, the results are shown in table 6.2. Also the rotational stiffness of the four different types of columns is estimated on a similar manner as is performed in chapter 2. All columns are made of square hollow sections of 350 mm in width and only the thickness varies. The rotational stiffness is calculated with the SCIA Engineer model described in Appendix B, for this situation only the thickness of the two oblique columns are changed and the height of the A-frame is kept constant at 8.9 m.

Table 6.2 Input parameters calculation model

Length [m]	Stiffness truss (EI) [Nm^2]	Rotational stiffness springs (k_r) [Nm/rad]	Average weight of the truss per meter [kg/m]
15 - 25	$1.408 \cdot 10^9$	$8.588 \cdot 10^6$	267
25.5 - 40	$2.226 \cdot 10^9$	$1.063 \cdot 10^7$	277
40.5 - 50	$2.822 \cdot 10^9$	$1.241 \cdot 10^7$	314
50.5 – 60	$3.178 \cdot 10^9$	$1.595 \cdot 10^7$	360

The weight of the signboards has to be added for each individual case, but since the signboard configuration depends on the road design it is not known. For the parameter study the same signboard is used for all structures. The weight is different if steel or aluminium signboards are used, the distributed weight for steel signboards is equal to 30 kg/m^2 and 16 kg/m^2 for aluminium signboards, both materials are currently used for signboards. Since the mass of the structure varies per sign gantry all natural frequencies are possible within a range. A damping value of 0.5% is assumed for all observed structures.

6.2 Structural response

In this section the structural responses are calculated according to the calculation model that was validated with the measurement in chapter 5 and the parameters from table 6.2.

Test structure (52 m)

The maximum displacement of this structure is computed by using a theoretical event for trucks passing at a following time distance of exact 5 times the oscillation period. For a natural frequency of 1.6025 Hz the time distance between the trucks is equal to 3.12 s. Figure 6.1 shows the response of the structure in mid span if 39 trucks drive in eastward direction at lane 2 with the same time interval of 3.12 s.

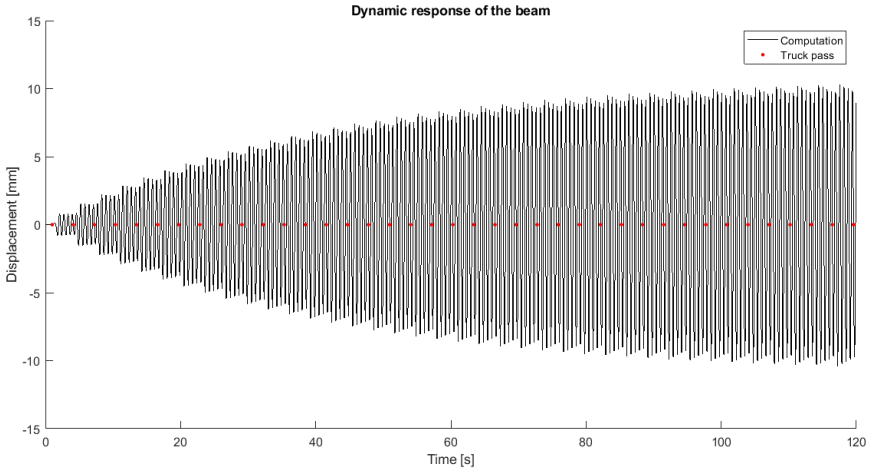

Figure 6.1 Response of the truss beam at mid span due to 39 trucks at lane 2 in eastward direction with at time distance of 3.12s

Due to the small damping of 0.5% and time difference between the trucks the oscillation of the beam reaches a certain equilibrium amplitude. In this situation the maximum theoretic amplitude is equal to 10 mm, twice as high as the displacement from the measurements. The damping is a very important factor in this approach of computing the maximum theoretical amplitude.

Standard structures

The responses of the standard sign gantries are calculated with one signboard of 5x3.9 m at mid span to only take into account the effects of one lane, the pulse loads are applied at this same location. The natural frequency, maximum theoretic amplitude and its corresponding equivalent static load are shown in table 6.3. Also a damping of 0.5% is used in this parametric study.

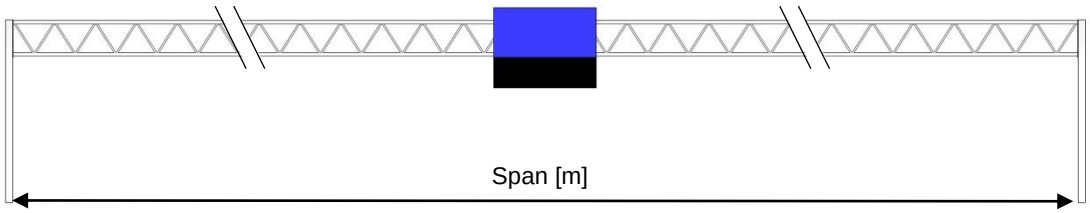

Figure 6.2 Configuration of the structure for the parametric study

Table 6.3 Results of the parametric study (natural frequency, amplitude and equivalent static load at mid span to obtain the same amplitude)

Span [m]	Natural frequency first mode [Hz]	Maximum theoretical amplitude [mm]	Equivalent static load [kN]
16	12.6	0.1	1.7
24	5.9	0.5	2.6
26	6.2	0.4	2.5
34	3.7	1.4	4.0
40	2.7	3.0	5.4
44	2.4	3.9	6.6
48	2.0	6.0	7.9
52	1.7	10	11.9
58	1.4	16	13.8

The equivalent static loads for structures with a span larger than 50 m are above the range (2.3 to 9.4 kN) of the static design loads discussed in section 3.2. The equivalent static load based on the parametric study should only be applied at mid span of the structure. This is not mentioned in the design rules on truck induced wind loads from literature. This equivalent static load from the parametric study is not a design load for vehicle induced wind loads, it is only calculated to compare the design loads from section 3.2 with the parametric study. Besides it is based on a pure theoretical load event where more than 30 trucks drive in the exact multiple of the oscillation period. If a more realistic load event occurs, then the static equivalent design load for vehicle induced wind loads will be lower than this maximum load. Also an estimation of the amount of cycles is required to set up a design load for vehicle induced wind load.

6.3 Fatigue

This section describes which theoretical maximum stress ranges are expected from vehicle induced wind loads for the standard sign gantries. The structure used for the measurements is also assessed by calculating the stress ranges from displacements that were observed.

Measurement structure (span 52 m)

An estimation of the stress variation can be made based on the results of the measurements. The global stresses in the structure are determined using MatrixFrame by applying a deformation similar to the measurements (amplitude of 5 mm). The global stresses are linearly related to the displacements of the truss beam. The maximum displacement from the measurements is applied to the structure and the stresses are computed by dividing the member forces through the cross sectional area.

The structure is modelled with bar elements and fixed nodes (figure 6.3). The stiffness of the calculation model in MatrixFrame can be validated with the static analytical solution, which was also used for the dynamic calculation. The displacement at mid span from MatrixFrame is compared with the displacement calculated using the analytical solution shown in Appendix B. A force of 10 kN is applied to compute the displacement at mid span, for the analytical solution this results in 9.9 mm and in MatrixFrame the displacement is equal to 9.8 mm (excluding the 0.3 mm horizontal deformation from the column). This stiffness and mass were already validated with the measurements and the discrete beam model by means of the natural frequency.

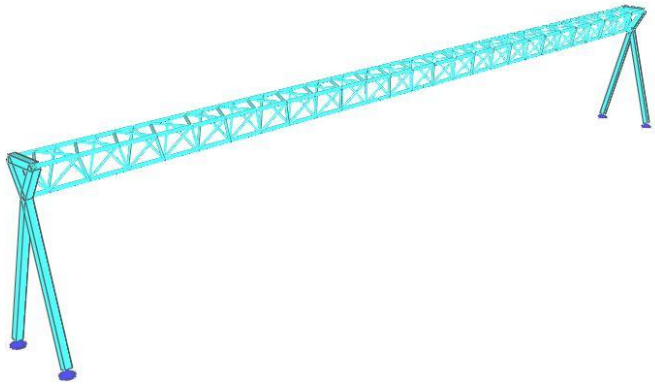

Figure 6.3 MatrixFrame calculation model with only bar elements connected rigidly. The governing location is the K-joint at mid-span in the upper plane of the truss

The horizontal deformation of the beam results in stresses in the two top chords of the triangular shaped truss. When the structure is deformed with 5 mm, then the global force in the chord at mid span is equal to 36.3 kN. The global force in the brace is equal to 1.9 kN. This results in the following stresses: 4 MPa for the chord and 1 MPa for the brace. The structure is vibrating, so the nominal stress ranges are:

$\Delta\sigma_{nominal,chord}$ = 8 MPa and $\Delta\sigma_{nominal,\ brace}$ = 2 MPa.

Full scale measurements on a sign gantry spanning 43.5 m showed similar results (Staalduinen & Dijkstra, 1990). The strains in the chord were measured and a part of the data was observed for vibrations due to vehicle induced loads only. The highest stress that occurred in the chord at mid span was equal to 4 MPa. The vibrations were only in the first horizontal mode shape and the natural frequency was equal to 1.7 Hz.

The K-joint between the chord and the braces does not comply with standard structural detail categories for fatigue from NEN-EN 1993-1-9 table 8.7 because the thickness of the chord is 20 mm (>8 mm). A company commissioned by Rijkswaterstaat, named PT Structural, has performed a study on fatigue for natural wind loads. Their study focussed on two designs, the new design of the structure (2012) and the older design of the structure (2005). In the older design of structure the weld between the brace and the chord consists of a combination of a partial penetration and a fillet weld, see figure 6.4. This connection is changed in the newer version where the weld is a full penetration weld, see figure 6.5. In the old series detail classes of 71 MPa (root of the weld at the chord) and 36 MPa (root of the weld at the brace) were used for the welds. In the newer series detail classes of 114 MPa (toe of the weld) and 71 MPa (root of the weld) were used. These values were derived from several other researches on fatigue. In their study they computed the hot spot stresses and computed the fatigue damage using Miner's rule (PT Structural, 2015). Based on this study the fatigue detail classes of the K-joint are estimated conservative: 2005 series $\Delta\sigma_c$ = 36 MPa and 2012 series $\Delta\sigma_c$ = 71 MPa.

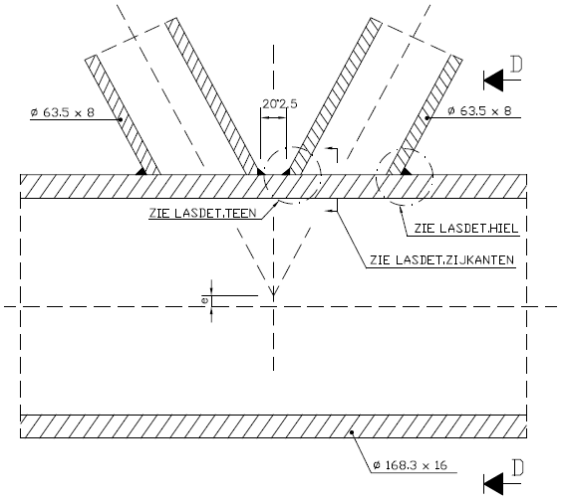

Figure 6.4 Weld detail of the chord-brace connection (2005 series)

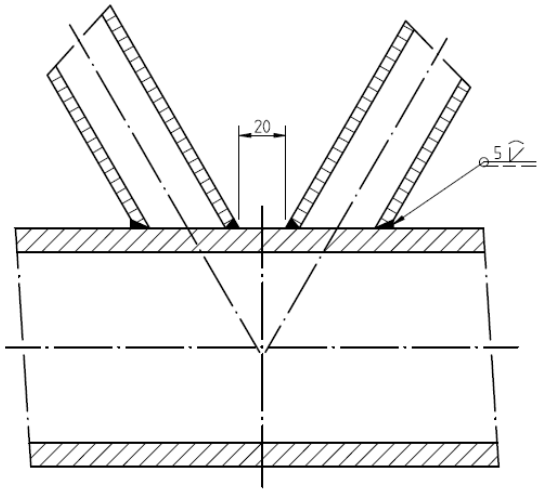

Figure 6.5 Weld detail of the chord-brace connection (2012 series)

Figure 6.6 shows the SN-curve from NEN-EN 1993-1-9, if the stress ranges are below the cut off limit vehicle induced wind loads do not have to be taken into account in the fatigue calculation of sign gantries. The stress ranges below the constant amplitude fatigue limit should be taken into account because the natural wind loads also cause fatigue stress ranges above the constant amplitude fatigue limit. Rijkswaterstaat uses γ_{Mf} = 1.35 and γ_{Ff} = 1.15 as partial factors for fatigue calculations, no structural inspection plan exist for sign gantries. For detail class $\Delta\sigma_c$ = 71 MPa the cut off fatigue limit is equal to: $\Delta\sigma_L = 0.405 \cdot \Delta\sigma_c$ = 29 MPa and taking into account the partial safety factor $\Delta\sigma_L / \gamma_{Mf}$ = 21 MPa, if it is calculated according to NEN-EN 1993-1-9. For detail class $\Delta\sigma_c$ = 36 MPa the cut off fatigue limit, including the partial safety factor, is equal to 11 MPa.

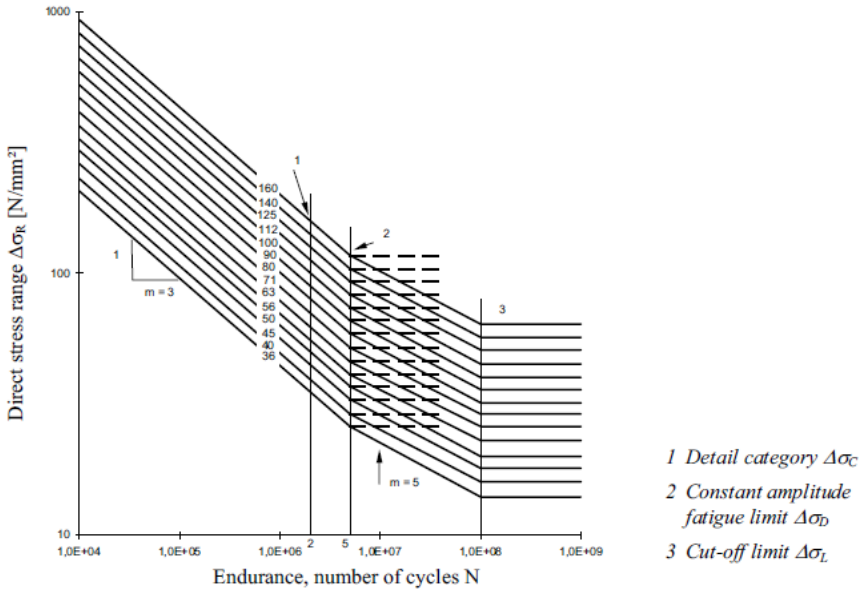

Figure 6.6 S-N curve from NEN-EN 1993-1-9

From the nominal stresses in the chord (which is governing) the modified stress range ($\Delta\sigma_{E,2}$) can be calculated, this is equal to $k_1 \cdot \gamma_{Ff} \cdot \Delta\sigma_{chord}$ = 1.5·1.15·8 = 14 MPa. The factor k_1 is taken from table 4.1 from NEN-EN 1993-1-9 and is equal to 1.5 and assumed to be applicable to this problem (nominal stresses from a truss modelled rigidly with an applied deformation of 5 mm).

The structure used for measurements is built around 1999. The fatigue detail category is observed in a conservative way and a detail class of 36 MPa is used with a cut off limit equal to 11 MPa. The nominal stress ranges are above the cut off limit, therefore vehicle induced wind loads should be taken into account in the fatigue design. Cycles with an amplitude larger than 4 mm cause stress ranges above the cut off limit. During the measurements 12 cycles were above this limit of 4 mm in 8 minutes of measuring. If 8 minutes is a representative time frame, then 90 cycles are above the cut off limit in 1 hour. Assume 4 hours per day with this amount of cycles then the total amount of cycles is equal to $6.57 \cdot 10^6$ in 50 years.

Now an indication of the fatigue damage can be given according to Miner's rule and equation 6.1 from NEN-EN 1993-1-9. $\Delta\sigma_D$ = 20 MPa and $\Delta\sigma_{E,2}$ = 14 MPa, the amount of cycles until fatigue damage occurs is equal to $2.97 \cdot 10^7$. The fatigue damage is then equal to 0.22.

$$\Delta\sigma_R^m N_R = \Delta\sigma_D^m 5 \cdot 10^6 \text{ with } m = 5 \text{ for } 5 \cdot 10^6 \le N_R \le 10^8 \qquad \text{(NEN-EN 1993-1-9)} \qquad (6.1)$$

The parametric study is performed in order to see if the displacement of the structure could be higher and thus result in higher stresses. The maximum displacement was twice as high as the maximum displacement from the measurements. Thus the stresses in the structure would also be twice as high since there is a linear relationship between the deformation and stresses in the structure.

Standard structures

The results from the computations of the standard structures are tabulated in table 6.4. Sign gantries with a small span have a large natural frequency, because of a relative high stiffness and therefore the maximum theoretical amplitude is low compared to the structures with large spans.

Table 6.4 Results of the parametric study (maximum stresses in the chords and braces)

Span [m]	Natural frequency first mode [Hz]	Maximum theoretical amplitude [mm]	$\Delta\sigma_{chord}$ [N/mm^2]	$\Delta\sigma_{brace}$ [N/mm^2]
16	12.6	0.1	<1	<1
24	5.9	0.5	2	1
26	6.2	0.4	2	1
34	3.7	1.4	4	2
40	2.7	3.0	7	3
44	2.4	3.9	8	3
48	2.0	6.0	10	4
52	1.7	10	15	5
58	1.4	16	20	6

All joints in the standard sign support structures are similar and assuming the fatigue detail category and the cut off fatigue limit is the same for all structures of the 2012 series (i.e. 29 MPa), only fatigue damage could occur for sign support structure that spans 58 m. The modified stress range in the chord in this structure is equal to 35 MPa which is higher than the cut off limit. However, the chance of occurrence is very small, trucks have to drive in an exact time configuration and if this would occur the amount of cycles is limited. For the older sign gantries (2005 series) with a fatigue detail category of $\Delta\sigma_c$ = 36 MPa fatigue damage occurs but the amount of stress cycles is still unknown for a period of 50 years. Based on these results fatigue from vehicle induced wind loads does not have to be taken into account for spans smaller than 40 m, for both 2005 and 2012 series.

6.4 Discussion and conclusion

The maximum theoretic amplitude of the truss for different types of sign support structures is computed based on the modified pulse load from the measurements. This pulse load was based on literature and the results of the calculation model compared to the measurements. The exact height difference between the moving trucks and the signboards varies for various sign gantries. If the distance between the vehicles and the signboards is smaller, then the load will be higher, but the

magnitude of the load is not known. Besides the magnitude of a single pulse, it is also not known what the pulse load would be when multiple trucks drive close to each other, in case of platooning. In that situation the pulse load will presumable be lower because the air that has to be displaced by the truck will have a certain velocity or is turbulent. Therefore, the parametric study might give a conservative result because pulse loads were applied very close to each other.

The truck configuration was exactly chosen that the time distances between trucks were n-times the natural oscillation period in order to have resonance. The situation when 39 trucks drive exactly with a time distance of 3.12s (or another time interval) in between is highly uncertain, even for self-driving trucks. In the near future self-driven vehicles will not be rare on the highways and thus platooning trucks would drive on the highway. In general this could result in higher amplitudes of vibration of sign gantries, but the pulse load might also be different (lower for the following trucks).

For the test structure stress ranges from vehicle induced wind loads were calculated based on the measured amplitude of the truss. The fatigue detail class of the governing joint is not provided by the Eurocode therefore estimated detail classes were used. The modified nominal stress method from NEN-EN 1993-1-9 was used despite the use of a model with fixed bar elements. If the problem is observed in a conservative manner, a detail class of 36 MPa (2005 series), and when all partial safety factors are applied, then the cut off limit is exceeded. This means that the structure encounters fatigue damage from vehicle induced wind loads. The amount of cycles is only known from the 8 minutes of measurements and cannot be used for an entire year or reference period of 50 years.

Based on this preliminary study it can be concluded that truck induced wind loads do not cause extra fatigue damage next to natural wind loading for a fatigue detail class of 71 MPa, which applies to newer series of sign structures. The stresses are below the cut off limit in a S-N curve. The parametric study showed that is possible to exceed this limit, but this is based on pure theoretic events of truck passes that would be very unlikely to occur. However, it should be pointed out that this parametric study is based on simple measurements and on only one sign gantry. A more sophisticated measurement method and a more thorough assessment of the fatigue stresses in the structure would be required to conclude if fatigue damage from vehicle induced wind loads can occur.

(this page is intentionally left blank)

7 Energy content

The truck induced wind flow might be of interest for energy harvesting purposes. Many ideas exist on this topic, but minor research has been performed yet. In this chapter the available literature is compared with the energy in the structural vibration.

7.1 Summary of available literature

Mattana, Salvadori, Morbiato & Borri (2014) studied the interaction between passing trucks and objects above a highway using a computational fluid dynamics (CFD) model. It was shown that objects above passing vehicles influence the energy consumption of the vehicle in a negative way. In order to harvest energy from the vehicle induced flow with a positive net value a threshold value of 1.4 kW should be overcome. A resource estimation assessment for wind energy harvesting from transport systems has been performed by Morbiato, Borri & Vitaliani (2014). In this research real time wind speed measurements were carried out to analyse the vehicle induced wind flow under a sign gantry. This is also compared with natural wind speed measurements. They concluded that it is possible to harvest energy from passing vehicles having a positive net value. However, the passing rate of trucks plays an important role on the amount of energy possible to harvest and a suitable energy harvesting device still has to be researched.

A sign support structure would be suitable to support an energy harvesting device if the weight is not too large compared to the weights of signboards, the signboards have a relative large mass, e.g. 700 kg for a signboard of 5x3.9 m. If in the future sign support structures are not used anymore then they could be used for this purpose. However, the amount of energy that can be harvested is still very low and the load from the harvesting device on the structure should be checked. From the research of Morbiato et al. (2014) the amount of net harvestable energy on one weekday is about 6.8 kWh. This is based on 3600 trucks on one day and a power coefficient of 0.1. A wind turbine of 3 MW produces on average 16500 kWh per day from natural wind (European Wind Energy Association, 2018). In order to harvest this amount of energy 2400 devices would be required that are able to harvest the same amount of energy from vehicle induced wind loads. A comparison of the price per kWh could be made after a design is made for the device capable of harvesting energy from vehicle induced wind flows.

7.2 Signboards

From another perspective of harvesting the energy, one could argue that it is more efficient to save energy by not placing the signboards above the road, because the objects have a negative influence on the vehicle's energy consumption. Rectangular and circular objects above a truck have been analysed by Mattana et al. (2014) with a CFD model. The rectangular object was varied in thickness, and the height (2.5 m) and the width (truck width) were constant. The energy loss ratios were calculated according to formula 7.1 for thicknesses of 0.4 m; 0.8 m and 1.6 m, their results are shown in table 7.1.

$$\frac{E - E_0}{E_{ref}} = \frac{\int_{domain} (CD - CD_0) d\tau}{CD_0 \Delta\tau} \tag{7.1}$$

Table 7.1 Energy loss ratios for three thicknesses of a rectangular object from Mattana et al. (2014)

Thickness object	Energy loss ratio
1.6 m	3.47%
0.8 m	1.95%
0.4 m	1.42%

A signboard has a thickness of only 1 cm, so if the results are extrapolated to an object thickness close to zero than the energy loss ratio will be equal to 1.04%. The energy loss ratio is calculated for a non-dimensional time interval of $\Delta\tau$= 3, this corresponds to time of 2.2 s for a vehicle of 16.6 m long and travelling with a speed of 80 km/u. Based on an energy consumption of 382 kW for a heavy truck

with a constant speed of 105 km/h and 25% energy loss due to aerodynamic drag (Morbiato et al., 2014) the extra energy consumption will be 382·0.25·0.0104=0.99 kW. For a truck travelling with a speed of 80 km/h this value will be lower because less power is required to maintain this constant speed. If this is calculated relative to the speed than the energy consumed due to aerodynamic drag will be reduced with $(105^2-80^2)/105^2$ = 0.41. So now the extra energy consumption of a truck will be 382·0.25·0.41·0.0104= 0.41 kW. The extra energy produced for passing the object is then equal to 0.41·2.2 = 896 J. For example, if two million trucks pass one signboard a year than the extra energy consumption is equal to 1.79 GJ. Compared to the yearly electricity consumption of a Dutch household of 4 persons (4700 kWh) this is 10%. The energy loss of 3600 trucks due to a signboard is equal to 0.9 kWh, this 13% of the harvestable energy from an energy harvesting device.

7.3 Structural vibration

In chapter 5 the results from the measurements were modelled with a discrete Euler-Bernoulli model in MATLAB. Based on this computation the amount of energy in the vibration of the beam can be estimated by calculating the kinetic energy. This is performed for a beam discretized with 26 segments, the total energy in the beam is equal to the summation of kinetic energy for each element, see equation 7.2.

$$E_{kin} = \sum E_{kin,i} = \sum \frac{1}{2} m_i v_i^2 \tag{7.2}$$

The result of the kinetic energy in time is plotted in figure 7.1. This figure shows that during the measurements the maximum amount of energy in the beam was equal to 9.6 J.

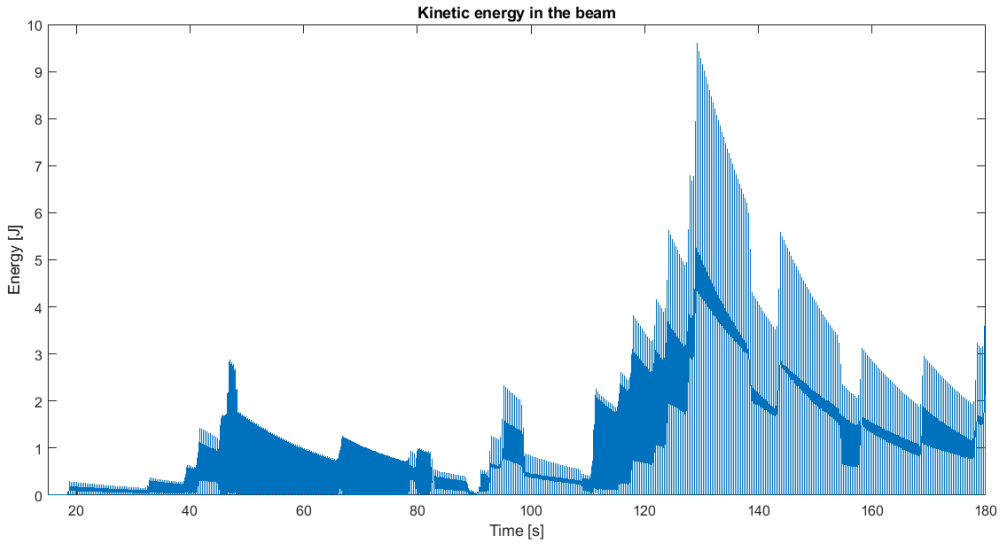

Figure 7.1 Kinetic energy in the beam

The energy in the vibration of the beam due to vehicle induced wind loads is very small for energy harvesting purposes. The amount of energy that can be dissipated from the system depends on the velocity of the nodes. From the parametric study it was found that the response of the beam depends on the damping, because at a certain time the amplitude reached a maximum value. The maximum amplitude will be smaller if the damping is higher, therefore the energy in the system and the possible harvested energy from the vibration will be even lower.

The amount of energy that is brought into the system by the first truck is equal to 0.25 J. If this is compared with the extra amount of energy that a truck has to deliver to pass a signboard, it is noticeable that there is a large difference. From literature (section 7.2) it was estimated that a single truck has to deliver 896 J extra to pass a signboard and from this amount of energy only 0.25 J is brought into the system. A large part of the energy is presumably lost in turbulence.

7.4 Discussion and conclusion

From literature it was shown that it is possible to harvest energy from vehicle induced wind flows. However, the device still has to be designed and the amount of energy that could be harvested is very low compared to regular wind turbines. If the costs of a device are known then a feasibility study can be performed to compare the price per kWh of electricity.

Based on extrapolated results from literature an estimation was made for the energy consumption of a truck that passes a signboard. The extra energy consumption is about 900 J. However, if this is compared with the amount of energy that is stored in the structural vibration of the beam it seems to be very high. The maximum amount of energy in the structural vibration is estimated around 10 J during the measurements, which is not of interest for energy harvesting purposes.

(this page is intentionally left blank)

8 Conclusion and discussion

8.1 Conclusion

Vehicle induced wind loads bring the beam of a sign gantry in motion and the beam vibrates mainly in it its first horizontal mode. Based on a simple and inexpensive measurement method with video cameras it is shown that this can be modelled with a discrete Euler-Bernoulli beam model which is loaded by concentrated pulse loads from passing trucks and trailer-trucks. However, the magnitude of the pulse load, which is found from literature research, had to be factored with 4.5 in order to use a single pulse load for all trucks and trailer trucks on different lanes. It is possible to define a static equivalent load that resembles the deformation of the structure and thus the stresses, but this is different for each span and signboard configuration of a sign gantry. The modified stress ranges in the chord of the K-joint in mid-span are estimated with a simple model with bar elements in MatrixFrame. The stresses are higher than the cut off limit of the fatigue detail category in case of the older sign support gantries. The newer types of sign gantries (2012) have a higher detail category and the modified stress ranges are below the cut off limit and thus do not experience damage from vehicle induced wind loads. Based on this study vehicle induced wind loads should be incorporated into the design of sign gantries with a span larger than 40 m, but no appropriate design rule has been set since the amount of cycles that should be taken into account is still unknown.

8.2 Discussion

After validation of the calculation model with the measurements it was shown that a single modified pulse load could be used for trucks and trailer trucks. However, the original pulse load was estimated based on studies which were not directly applicable for large signboards, so the results were extrapolated and therefore an error was expected. The error was larger than expected; a factor 4.5 in magnitude was used to model all trucks and trailer trucks with the same pulse load. Possible causes of this factor are an error in the extrapolation from small panels (2 m^2) to large panels (20 m^2); also the pressure of the wind flow could be higher due to a more confined area of the flow. Furthermore, smaller errors can also come from other factors such as different types of trucks and different signboards. These factors give information about the distances between the vehicle and the signboard, which is an important parameter of the truck induced wind load. The dimensions of the structure are only based on construction drawings and site visits and could not be measured. Despite the large amount of parameters that influence the problem a single pulse load could be used for trucks and trailer trucks and the main reason of the error is presumably caused by a wrong extrapolation from small signboards to large signboards. It should also be pointed out that the shape and magnitude of the pulse load could be influenced if a vehicle drives very close to another vehicle. In case of platooning trucks a single pulse load cannot be used for all trucks.

The measurement method was simple and inexpensive but it is presumably less accurate than measurements with more sophisticated devices such as accelerometers and strain gauges. Effects of natural wind gusts cannot be registered with video measurements, an anemometer could be used in order to explain effects of natural wind gusts. Ground vibrations from passing trucks resulted in small vibrations of the video camera, which also caused small errors in obtaining the amplitude of vibration. The frame rate of the cameras was too low, therefore for future measurements other cameras should be used in order to obtain accurate times of truck passes.

The parametric study was performed based on the validated calculation model and the damping was an important factor in computing the maximum theoretical amplitude of vibration. This amplitude will be higher if the damping is lower and lower if the damping is higher. Based on the modified stress calculation for fatigue it was concluded that vehicle induced wind loads should be taken into account in the fatigue design of the structure for spans larger than 40 m. Probably a conservative detail category is used, therefore the outcome of design will also be conservative. Furthermore, no exact stress ranges and corresponding cycles are known in order to perform a fatigue calculation for the entire lifetime of the structure.

8.3 Recommendations

To validate the magnitude of the pulse load from this research and to see what the pressure variation is, a similar test as Lichtneger & Ruck (2014) should be performed with a large signboard. These tests could also be implemented with multiple vehicles driving close to each other to see how the pulse load from a second vehicle is influenced by the vehicle driving in front of it. During these tests the vehicles energy consumption can be observed in order to see how much extra energy a vehicle has to deliver to pass a signboard.

More extensive measurements will be performed on the sign gantry that has been observed. Strain gauges and/or accelerometers can be used to measure the strains and accelerations at most relevant locations. Due to vehicle induced wind loads the structure vibrates in its first horizontal mode. An accelerometer at mid span of the structure will give the relevant information of the structural response. These measurements could validate the video measurements. A reference truck should be used to measure the structural vibration caused by one truck without the effects of other vehicles at the highway. Cameras with a high frame rate are still required to obtain the time and location of the truck with respect to the structure. Combining the measurements with an anemometer, the stress in the structure could also be related to the natural wind loads. The force coefficient and the $c_s c_d$ factor from NEN-EN 1991-1-4 can be validated.

The structural response from vehicle induced wind loads is assessed for a sign gantry with so called ‘A-frames’. Another study can be performed on sign support structures with only two columns, these structures are mostly made of aluminium and are much lighter. Other interesting structures are cantilevered sign support structures.

The exact fatigue detail categories are not known for the standard sign support structures. A more extensive study on this will give governing information whether fatigue damage occurs from vehicle induced wind loads.

Traffic models can give information on how many vehicles pass a sign structure. This information can be used to compute possible maximum amplitudes of the vibration. The computational results give the amount of load cycles that can cause fatigue damage in the structure.

References

Blauwendraad, J. (2006). *Plate analysis, theory and application - Volume 2, Numerical Methods.* TU Delft, Structural Mechanics. Delft: TU Delft, Faculty of Civil Engineering and Geosciences.

European Wind Energy Association. (2018, April 15). *Wind energy's frequently asked questions*. Opgehaald van Wind energy basics: http://www.ewea.org/wind-energy-basics/faq/

Fouad, F., & Hosch, I. (2011). *Design of Overhead VMS Structures for Fatigue Loads.* Birmingham: University Transportation Center for Alabama.

Giannoulis, A., Stathopoulos, T., Briassoulis, D., & Mistriotis, A. (2012). Wind loading on vertical panels with differnet permeabilities. *Journal of Wind Engineering and Industrial Aerodynamics*(107-108), 1-16.

Ginal, S. (2003). *Fatigue Performance of Full-Span Sign Support Structures Considering Truck-Induced Gust And Natural Wind Pressures.* Milwaukee, Wisconsin: Marquette University.

Hong, H., Zu, G., & King, J. (2016). Estimating fatigue design load for overhead steel sign support structures under truck-induced wind pressure. *Canadian Journal of Engineering*(43), 279-286.

Hosch, I., & Fouad, F. (2010). Design Fatigue Load of Sign Support Structures Due to Truck-Induced Wind Gusts. *Transportation Research Record*(2172), 30-37.

KNMI. (2018, February 28). *Klimatologie - Uurgegevens van het weer in Nederland*. Retrieved from Website van het KNMI: https://projects.knmi.nl/klimatologie/uurgegevens/selectie.cgi

Leendertz, H. (2016). *Samenvatting en discussie windrapporten.* Rotterdam: Rijkswaterstaat.

Letchford, C. (2001). Wind loads on rectangular signboards and hoardings. *Journal of Wind Engineering*(89), 135-151.

Lichtneger, P., & Ruck, B. (2014). Full scale experiments on vehicle induced transient loads on roadside plates. *Journal of Wind Engineering and Industrial Aerodynamics*(136), 73-81.

Mattana, A., Salvadori, S., Morbiato, T., & Borri, C. (2014). On the ground-vehicle induced flows and obstacle interaction for energy harvesting purposes. *Journal of Wind Engineering and Industrial Aerodynamics*(124), 121-131.

Mijn eigen weer. (2018, February 28). *Weerstation Rotterdam Alexander*. Retrieved from Website of weerhuisje.nl: https://www.mijneigenweer.nl/weerstationrotterdamalexander/graphs.php

Morbiato, T., Borri, C., & Vitaliani, R. (2014). Wind energy harvesting from transport systems: A resource estimation assessment. *Applied Energy*(133), 152-168.

NEN. (2005). *Eurocode 1: Belastingen op constructies - Deel 1-4: Algemene belastingen - Windbelasting.* Delft: NEN.

NEN. (2012). *Eurocode 3: Ontwerp en berekening van staalconstructies - Deel 1-9: Vermoeiing.* Delft: NEN.

NLR. (1976). *Trillingsmeting aan de regel van een verkeersportaal.* Amsterdam: Nationaal Lucht- en Ruimtevaartlaboratorium.

PT Structural. (2015). *Verkeerskundige Draag Constructies (VDC) versie 2005 en 2012.* Rotterdam: PT Structural.

PT Structural. (2016). *Standaard RWS Verkeerskundige Draagconstructies.* Ridderkerk: PT Structural.

Rijkswaterstaat. (1981). *Berkening standaard - portaal tot 30 m.* Rijkswaterstaat Directie Bruggen.

Rijkswaterstaat. (2012). *Componentspecificatie Verkeerskundige Draagconstructies (VDC).* Utrecht: Rijkswaterstaat.

Rijkswaterstaat. (2017, November 13). *Kaders, portalen en uithouders*. Opgehaald van Rijkswaterstaat: https://www.rijkswaterstaat.nl/zakelijk/werken-aan-infrastructuur/bouwrichtlijnen-infrastructuur/portalen-en-uithouders.aspx

Rijkswaterstaat. (2017). *Richtlijnen Ontwerp Kunstwerken v1.4.* Utrecht: Rijkswaterstaat GPO.

Rijkswaterstaat Dienst Infrastructuur. (2012). *Verkeerskundige DraagConstructies.* Utrecht: Rijkswaterstaat Dienst Infrastructuur.

Rijkswaterstaat, D. V. (2012). *Functionele productspecificatie, Tijdelijke en Mobiele Signaleringsystemen.* Delft: Rijkswaterstaat.

Spijkers, J., Vrouwenvelder, A., & Klaver, E. (2005). *Lecture Nodes on Structural Dynamics.* Delft: TU Delft, Faculty of Civil Engineering and Geosciences.

Staalduinen, P., & Dijkstra, O. (1990). *Metingen aan het combiportaal aan de A20 bij belasting door wind en verkeer.* Delft: TNO IBBC.

Transport Infrastructure Ireland. (2014). *Design of Support Structures for Roadside Furniture.* Dublin: National Roads Authority.

(this page is intentionally left blank)

Appendices

Appendix A **Construction drawings**

This appendix contains the construction drawings of the sign gantry used for full scale measurements the structure is numbered as no. 5962 according to a numbering system from Rijkswaterstaat.

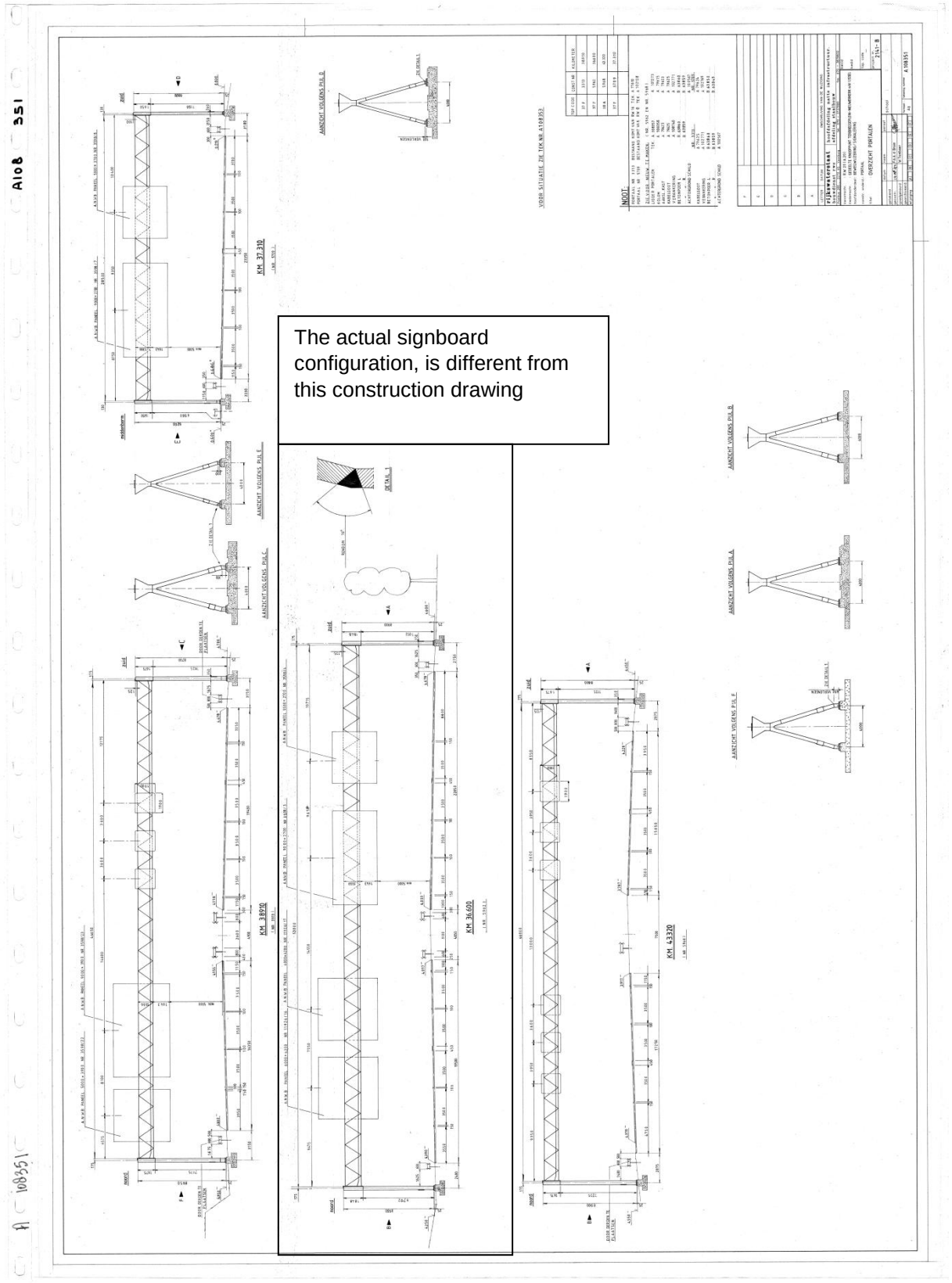

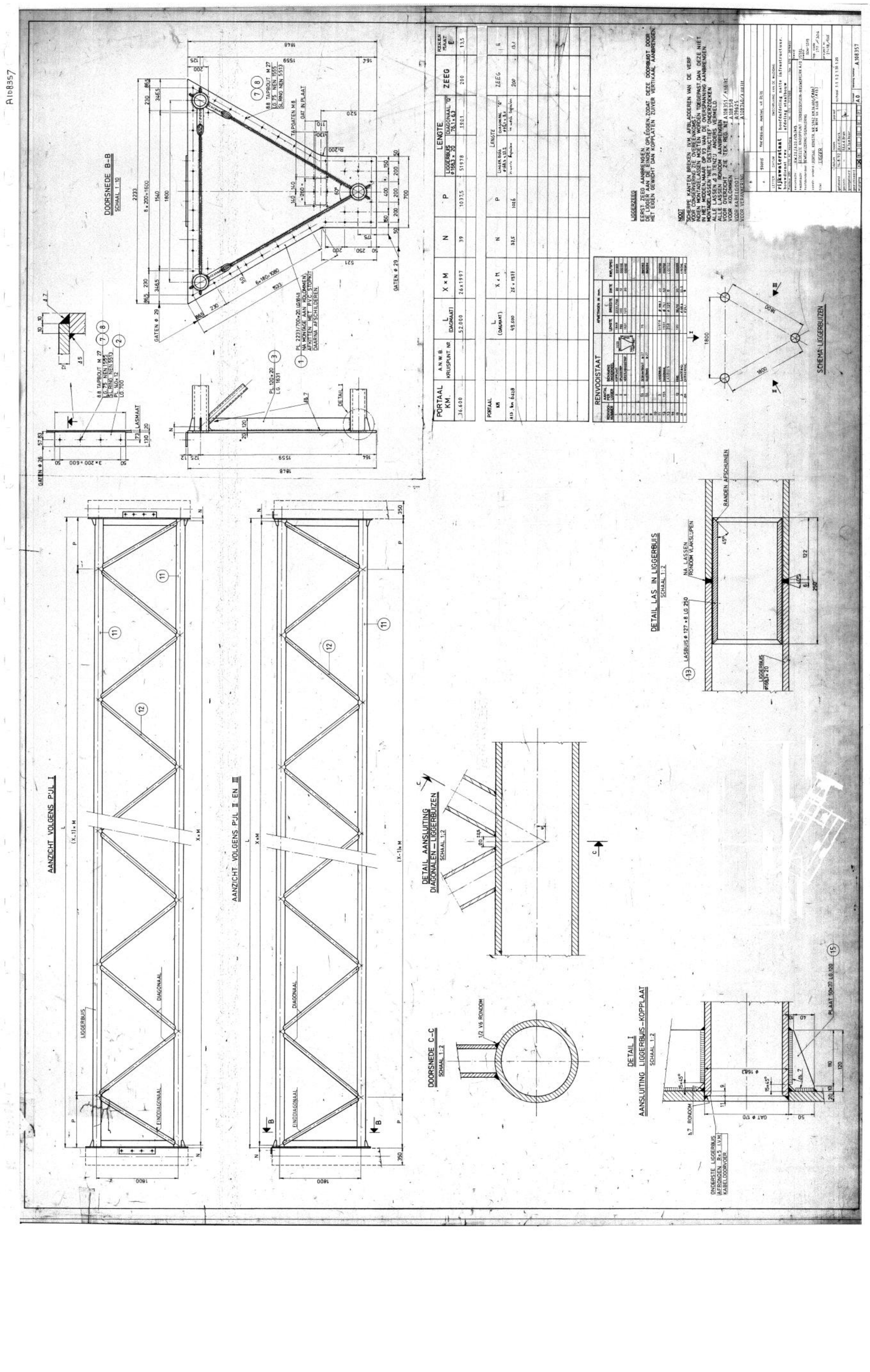
DOORSNEDE B-B
AANZICHT VOLGENS PIJL I
AANZICHT VOLGENS PIJL II EN III
DETAIL AANSLUITING DIAGONALEN-LIGGERBUIZEN
DOORSNEDE C-C
DETAIL I
AANSLUITING LIGGERBUIS-KOPPLAAT
DETAIL LAS IN LIGGERBUIS
SCHEMA LIGGERBUIZEN
RENVOOISTAAT

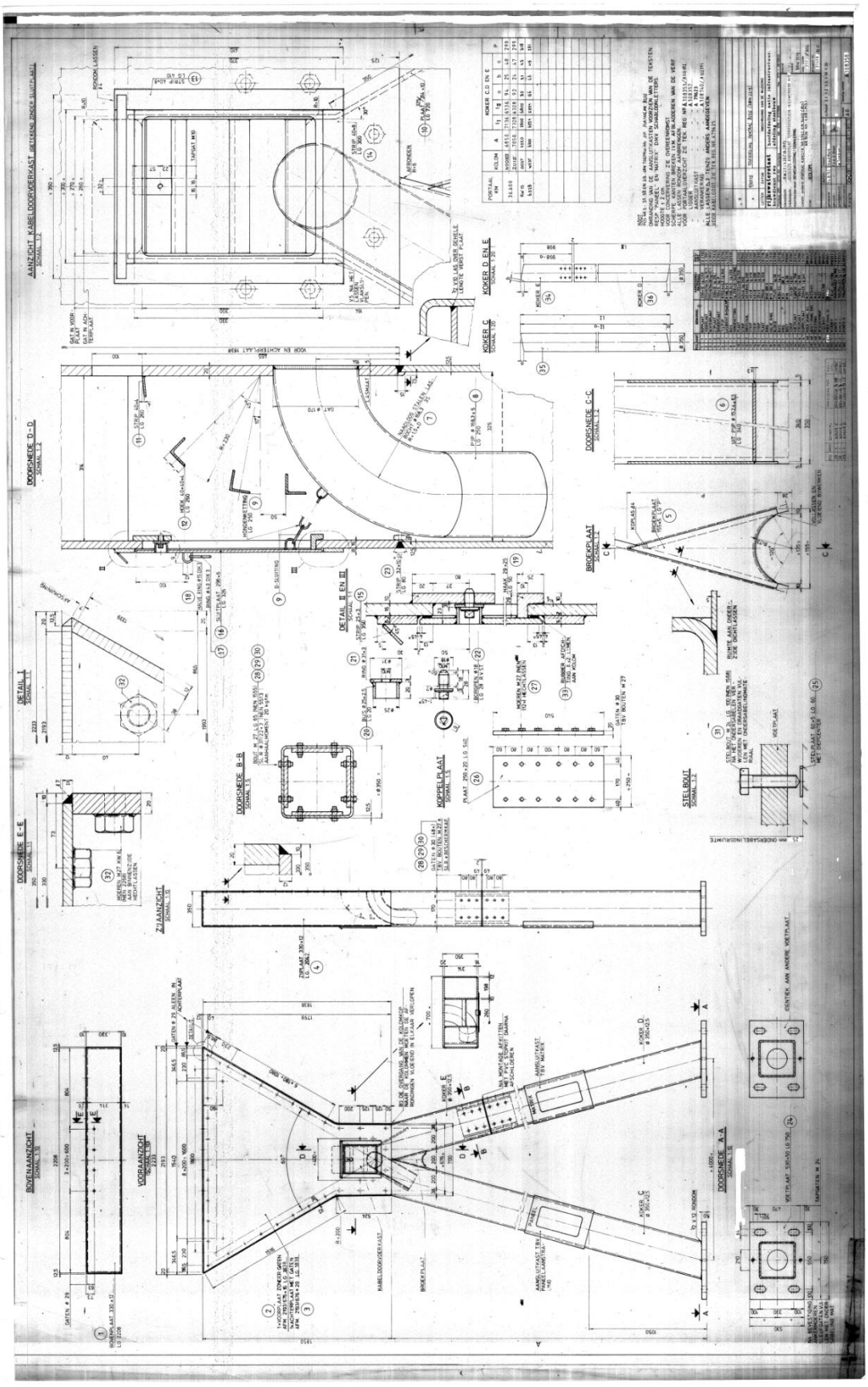

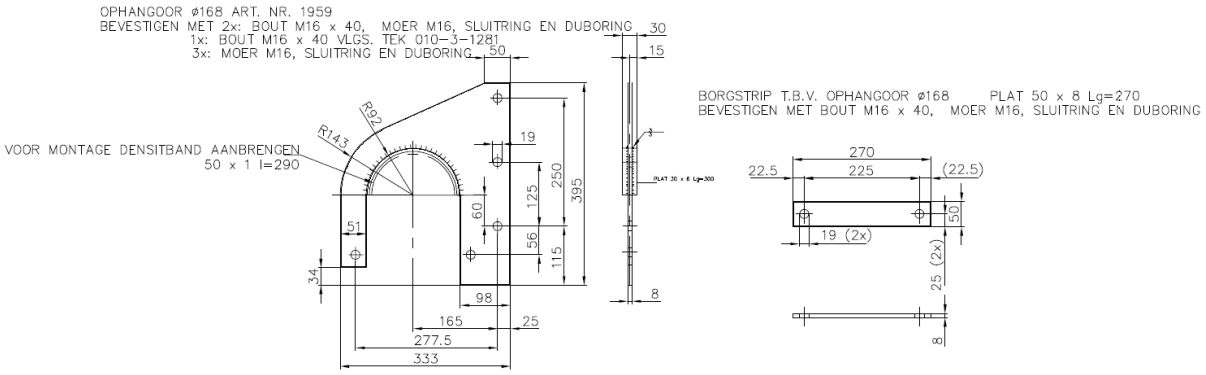

Actual signboard configuration, different from the construction drawing

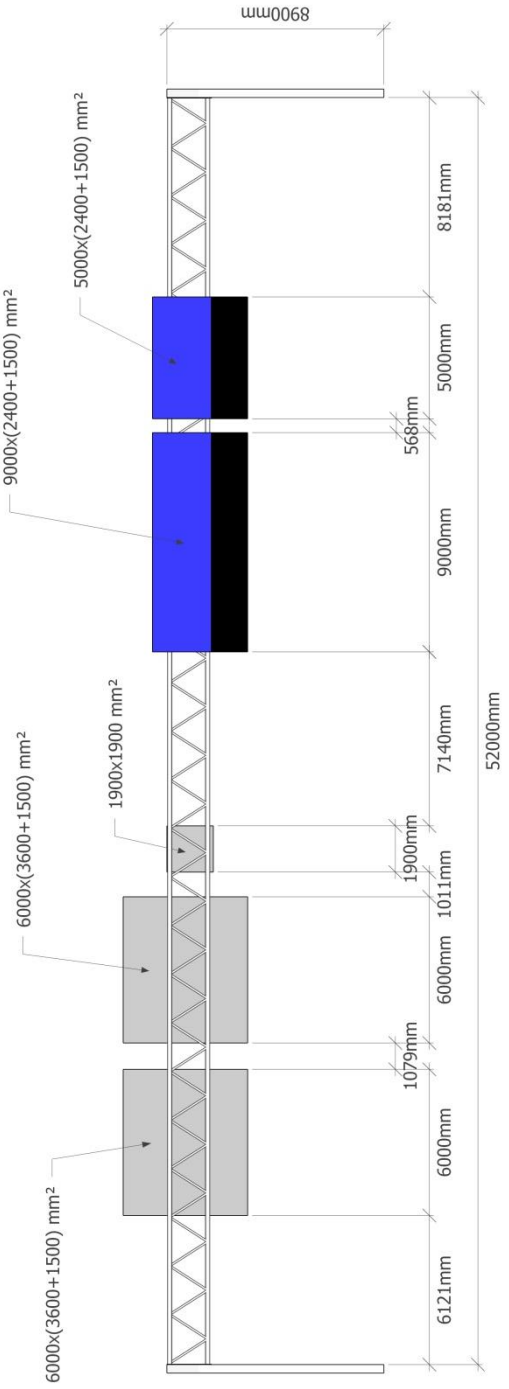

Appendix B **Structural properties and static response**

B1 General properties of the structure

The static horizontal deformation of beam due to wind load is computed with a hand calculation. This analytical calculation serves as a verification of the computational model used further in this report. For calculation of the horizontal displacements the contribution of the deformation of the columns is negligible, so only the deformation of the beam can be calculated by assuming a simply supported Euler Bernoulli beam (Rijkswaterstaat, Berkening standaard - portaal tot 30 m, 1981). This assumption is checked by calculating both cases.

Properties of the structure

Location	Rotterdam A20
Span length	52 m
Height (gantry)	8.9 m
Steel grade	S235
Chords	ø168.3x20 mm
Braces	ø76.1x6.3 mm
Columns	RHS 350x350x12.5 mm
Number of signboards	5
Total signboard area	30.6+30.6+3.6+35.1+19.5=119.4 m^2

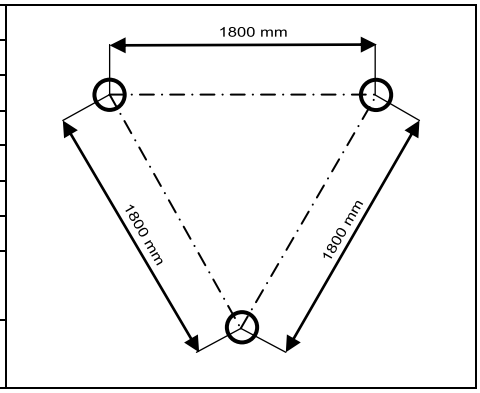

The stiffness of the truss beam is calculated using Steiner's rule multiplied with a factor of 0.85 to take into account shear deformation in a truss beam. The second moment of area for one chord, I_0 = $2.608 \cdot 10^7$ mm^4. The centroidal axis of the beam is at a height of 520 mm from the centre of the top two chords. This results in a stiffness of $3 \cdot I_0 + 2 \cdot 9318 \cdot 520^2 + 9318 \cdot 1039^2 = 1.5176 \cdot 10^{10}$ mm^4; multiplied with 0.85, I = $1.29 \cdot 10^{10}$ mm^4. The E-modulus of steel is 210000 N/mm^2. This results in a stiffness of the truss beam, EI = $2.71 \cdot 10^{15}$ Nmm^2 = $2.71 \cdot 10^9$ Nm^2.

B2 SCIA Output rotational stiffness column

The rotational stiffness of the column is estimated using the software of SCIA Engineer. Plate elements are used for the two oblique columns and the head connecting the two columns, see the figures on the next page. The dimensions of the construction drawings are used.

Figure Column in SCIA Engineer

Material

Steel grade S235 is used with a Young's modulus of 210000 N/m^2 and a shear modulus of 80769 N/mm^2.

Supports

The column is supported in y-direction in the top and rotations are allowed. The columns are supported with line supports at the bottom; these are fixed for translations, but allow rotations.

Forces

Two different load configurations are applied to the column. The first configuration is force couple (-10 and 10 kN) that is applied at the top of the structure in the xy-plane, this results in a torsion moment which is used to compute the torsion stiffness of the column. The second load configuration (2X 10 kN) is applied in x-direction to compute the equivalent stiffness of the column in x-direction.

The first configuration leads to a torsion moment of 22.33 kNm.

Deformed structure

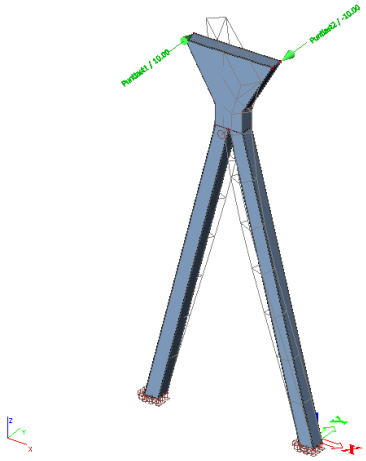

Figure Deformed structure due to the first load configuration (torsion moment)

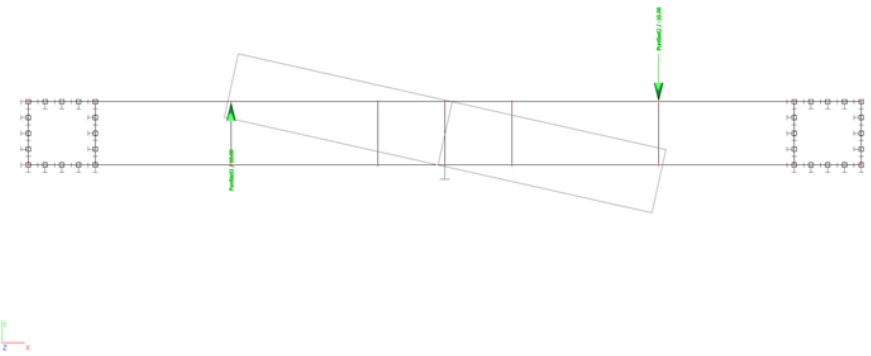

Figure Top view of the deformed structure due to the first load configuration (torsion moment)

The rotation of the top plate is equal to -1.8 mrad. The equivalent torsion stiffness k_r is then:

$$k_r = \frac{T}{\theta} = \frac{2.233 \cdot 10^4}{1.8 \cdot 10^{-3}} = 1.24 \cdot 10^7 Nm/rad$$

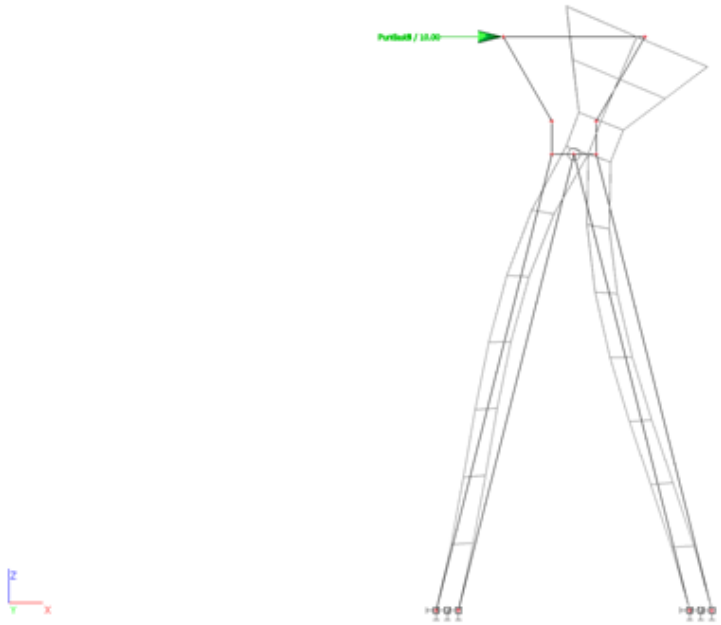

Figure Deformed structure due to the second load configuration (bending moment)

The horizontal displacement in x-direction of the top plate of the column is equal to 0.9 mm. The equivalent horizontal stiffness k_{hor} is then:

$$k_{hor} = \frac{F}{u} = \frac{20 \cdot 10^3}{0.9 \cdot 10^{-3}} = 2.22 \cdot 10^4 N/m$$

B3 Static deformation of the structure due to wind load

Wind load on the structure

The wind loads acting on the sign support structure are calculated according to NEN-EN 1991-1-4. Design pressure of q = 0.85 kN/m^2 according to the national annex (reference height is 10 m). The force coefficient of the signboards is 1.6 (based on literature).

The $c_s c_d$-factor is calculated according to NEN-EN 1991-1-4 and the Dutch national annex. A length of 52 m and an equivalent height of 2.3 m is assumed in order to take into account the signboard area on the structure. The reference height is equal to z_s = 10 m; $v_{b,0}$ =27 m/s; c_0 = 1; z_{min} = 2 m; z_0 = 0.05 m; k_l = 1; the first natural frequency is 1.56 Hz (see chapter 4) and the logarithmic decrement is equal to 0.048 based on the given method from NEN-EN 1991-1-4. This results in a $c_s c_d$-factor of 0.91. A lower value than 1.0 was also expected based on the literature research. PT Structural (2016) has calculated the $c_s c_d$-factor for multiple sign gantries, and concluded that for all structures the $c_s c_d$-factor is lower than 1.0.

Now all input parameters for the characteristic load are known and the following formula is used:

$$F_w = c_s c_d \cdot c_f \cdot q_p(z_e) \cdot A_{ref}$$

A_{ref} = 30.6; 30.6; 3.6; 35.1; 19.5 m^2

The characteristic loads on the 5 signboards are respectively, 37.9; 37.9; 4.46; 43.4 and 24.1 kN. The loads are concentrated in the centre of the signboard. In the construction drawing the 3th signboard is missing. The wind load on the chords and braces are not taken into account in this preliminary calculation.

Horizontal deformation

The horizontal deformation is calculated using the principle of superposition. The horizontal deflection in mid span of the beam is calculated for wind loads on the 5 signboards.

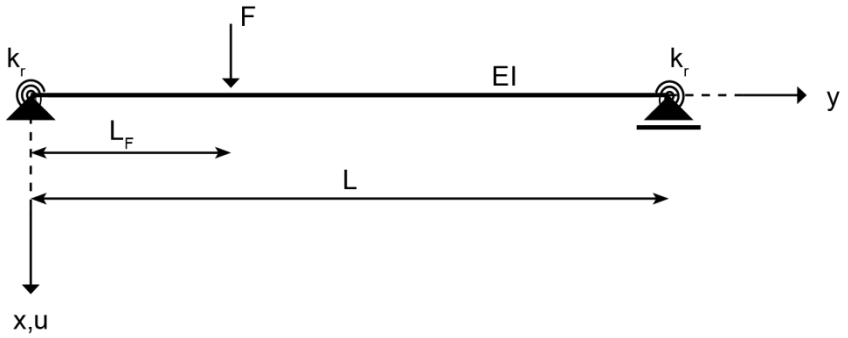

Figure Mechanical scheme for calculation of the horizontal deflection of the beam. The principal of superposition is used to calculate the deflection at mid span

The horizontal displacement is calculated using the analytical solution for a simply supported beam with and without rotational springs, for a beam without rotational stiffness at the supports k_r is equal to zero. The beam is loaded at a distance L_F by a concentrated load. The differential equation for an Euler Bernoulli beam is used to solve the problem on an analytical basis. Maple software is used to solve the differential equation. If k_r is equal to zero the problem is the same as a hinged-hinged beam, if k_r goes to infinity the problem is same as a clamped-clamped beam.

$$\mathrm{EIu_1}'''' = 0\,;\ \mathrm{EIu_2}'''' = 0$$

The following boundary conditions are applied:

y = 0: $u_1 = 0$
$M = k_r \cdot \theta_1$ ($EIu_1'' = k_r \cdot u_1'$)
y = L_F: $u_1 = u_2$
$\theta_1 = \theta_2$
$M_1 = M_2$
$V_1 - V_2 - F = 0$
y = L: $u_2 = 0$
$M_2 = - k_r.\theta_2$ ($EIu_2'' = - k_r \cdot u_2'$)

For y = 0.5L and $L_F = L_{i,F}$:

F_1 = 37.9; F_2 = 37.9; F_3 = 4.46; F_4 = 43.4; F_5 = 24.1 kN

L_{1F} = 9.12 m; L_{2F} = 16.2 m; L_{3F} = 21.16 m; L_{4F} = 33.75 m; L_{5F} = 41.32 m;

Without rotational spring:
$u_{0.5L,1}$ = 21 mm; $u_{0.5L,2}$ = 33 mm; $u_{0.5L,3}$ = 4.6 mm; $u_{0.5L,4}$ = 41 mm; $u_{0.5L,5}$ = 15 mm;

$u_{tot,\ mid}$ = 115 mm

With rotational spring:
$u_{0.5L,1}$ = 19 mm; $u_{0.5L,2}$ = 31 mm; $u_{0.5L,3}$ = 4.2 mm; $u_{0.5L,4}$ = 38 mm; $u_{0.5L,5}$ = 14 mm;

$u_{tot,\ mid}$ = 106 mm

Appendix C **Maple script mass-spring-damper system**

This Maple script shows the analytical solution of the response of a SDOF due to one load pulse of a passing truck.

```
> restart;
> v := 22.22 : L := 16.6 : m := 9625 : E := 2.1·10^11 : II := 1.289·10^-2 : Lb := 52 : k :=
      48·E·II / Lb^3 ; ω0 := evalf(sqrt(k/m)); zeta := 0.005; ω1 := ω0·sqrt(1 - zeta^2); T := L/v;
  q := 1.0 :
```

$$k := 924066.9096$$

$$\omega_0 := 9.798313715$$

$$\zeta := 0.005$$

$$\omega_1 := 9.798191235$$

$$T := 0.7470747075 \qquad (1)$$

```
> P1 := q·0.17·143 : P2 := q·(-143) : P3 := q·0.25·30 :
> tau1 := 0.50·T : tau2 := 0.98·T : tau3 := 1.02·T : tau4 := 1.70·T : tau5 := 1.85·T : tau6 := 2.20
      ·T :
> F1 := P1/tau1 ·tau :
> F2 := P1 - (P1 - P2)/(tau2 - tau1) ·(tau - tau1) :
> F3 := P2 - P2/(tau3 - tau2) ·(tau - tau2) :
> F4 := 0 :
> F5 := P3/(tau5 - tau4) ·(tau - tau4) :
> F6 := P3 - P3/(tau6 - tau5) ·(tau - tau5) :
> F7 := 0 :
>
>
> x(t)1 := 1/(m·ω0) ·int(F1·exp(-zeta·ω0·(t - tau))·sin(ω1·(t - tau)), tau = 0..t) :
> x(t)2 := 1/(m·ω0) ·int(F1·exp(-zeta·ω0·(t - tau))·sin(ω1·(t - tau)), tau = 0..tau1) + 1/(m·ω0)
      ·int(F2·exp(-zeta·ω0·(t - tau))·sin(ω1·(t - tau)), tau = tau1..t) :
> x(t)3 := 1/(m·ω0) ·int(F1·exp(-zeta·ω0·(t - tau))·sin(ω1·(t - tau)), tau = 0..tau1) + 1/(m·ω0)
      ·int(F2·exp(-zeta·ω0·(t - tau))·sin(ω1·(t - tau)), tau = tau1..tau2) + 1/(m·ω0) ·int(F3
      ·exp(-zeta·ω0·(t - tau))·sin(ω1·(t - tau)), tau = tau2..t) :
```

$$> x(t)_4 := \frac{1}{m\cdot\omega_0}\cdot int\left(F_1\cdot\exp\left(-\text{zeta}\cdot\omega_0\cdot(t-\text{tau})\right)\cdot\sin\left(\omega_1\cdot(t-\text{tau})\right),\ \text{tau}=0\,..\text{tau}_1\right)+\frac{1}{m\cdot\omega_0}\cdot int\left(F_2\cdot\exp\left(-\text{zeta}\cdot\omega_0\cdot(t-\text{tau})\right)\cdot\sin\left(\omega_1\cdot(t-\text{tau})\right),\ \text{tau}=\text{tau}_1\,..\text{tau}_2\right)+\frac{1}{m\cdot\omega_0}\cdot int\left(F_3\cdot\exp\left(-\text{zeta}\cdot\omega_0\cdot(t-\text{tau})\right)\cdot\sin\left(\omega_1\cdot(t-\text{tau})\right),\ \text{tau}=\text{tau}_2\,..\text{tau}_3\right)+\frac{1}{m\cdot\omega_0}\cdot int\left(F_4\cdot\exp\left(-\text{zeta}\cdot\omega_0\cdot(t-\text{tau})\right)\cdot\sin\left(\omega_1\cdot(t-\text{tau})\right),\ \text{tau}=\text{tau}_3\,..\text{t}\right):$$

$$> x(t)_5 := \frac{1}{m\cdot\omega_0}\cdot int\left(F_1\cdot\exp\left(-\text{zeta}\cdot\omega_0\cdot(t-\text{tau})\right)\cdot\sin\left(\omega_1\cdot(t-\text{tau})\right),\ \text{tau}=0\,..\text{tau}_1\right)+\frac{1}{m\cdot\omega_0}\cdot int\left(F_2\cdot\exp\left(-\text{zeta}\cdot\omega_0\cdot(t-\text{tau})\right)\cdot\sin\left(\omega_1\cdot(t-\text{tau})\right),\ \text{tau}=\text{tau}_1\,..\text{tau}_2\right)+\frac{1}{m\cdot\omega_0}\cdot int\left(F_3\cdot\exp\left(-\text{zeta}\cdot\omega_0\cdot(t-\text{tau})\right)\cdot\sin\left(\omega_1\cdot(t-\text{tau})\right),\ \text{tau}=\text{tau}_2\,..\text{tau}_3\right)+\frac{1}{m\cdot\omega_0}\cdot int\left(F_4\cdot\exp\left(-\text{zeta}\cdot\omega_0\cdot(t-\text{tau})\right)\cdot\sin\left(\omega_1\cdot(t-\text{tau})\right),\ \text{tau}=\text{tau}_3\,..\text{tau}_4\right)+\frac{1}{m\cdot\omega_0}\cdot int\left(F_5\cdot\exp\left(-\text{zeta}\cdot\omega_0\cdot(t-\text{tau})\right)\cdot\sin\left(\omega_1\cdot(t-\text{tau})\right),\ \text{tau}=\text{tau}_4\,..t\right):$$

$$> x(t)_6 := \frac{1}{m\cdot\omega_0}\cdot int\left(F_1\cdot\exp\left(-\text{zeta}\cdot\omega_0\cdot(t-\text{tau})\right)\cdot\sin\left(\omega_1\cdot(t-\text{tau})\right),\ \text{tau}=0\,..\text{tau}_1\right)+\frac{1}{m\cdot\omega_0}\cdot int\left(F_2\cdot\exp\left(-\text{zeta}\cdot\omega_0\cdot(t-\text{tau})\right)\cdot\sin\left(\omega_1\cdot(t-\text{tau})\right),\ \text{tau}=\text{tau}_1\,..\text{tau}_2\right)+\frac{1}{m\cdot\omega_0}\cdot int\left(F_3\cdot\exp\left(-\text{zeta}\cdot\omega_0\cdot(t-\text{tau})\right)\cdot\sin\left(\omega_1\cdot(t-\text{tau})\right),\ \text{tau}=\text{tau}_2\,..\text{tau}_3\right)+\frac{1}{m\cdot\omega_0}\cdot int\left(F_4\cdot\exp\left(-\text{zeta}\cdot\omega_0\cdot(t-\text{tau})\right)\cdot\sin\left(\omega_1\cdot(t-\text{tau})\right),\ \text{tau}=\text{tau}_3\,..\text{tau}_4\right)+\frac{1}{m\cdot\omega_0}\cdot int\left(F_5\cdot\exp\left(-\text{zeta}\cdot\omega_0\cdot(t-\text{tau})\right)\cdot\sin\left(\omega_1\cdot(t-\text{tau})\right),\ \text{tau}=\text{tau}_4\,..\text{tau}_5\right)+\frac{1}{m\cdot\omega_0}\cdot int\left(F_6\cdot\exp\left(-\text{zeta}\cdot\omega_0\cdot(t-\text{tau})\right)\cdot\sin\left(\omega_1\cdot(t-\text{tau})\right),\ \text{tau}=\text{tau}_5\,..t\right):$$

$$> x(t)_7 := \frac{1}{m\cdot\omega_0}\cdot int\left(F_1\cdot\exp\left(-\text{zeta}\cdot\omega_0\cdot(t-\text{tau})\right)\cdot\sin\left(\omega_1\cdot(t-\text{tau})\right),\ \text{tau}=0\,..\text{tau}_1\right)+\frac{1}{m\cdot\omega_0}\cdot int\left(F_2\cdot\exp\left(-\text{zeta}\cdot\omega_0\cdot(t-\text{tau})\right)\cdot\sin\left(\omega_1\cdot(t-\text{tau})\right),\ \text{tau}=\text{tau}_1\,..\text{tau}_2\right)+\frac{1}{m\cdot\omega_0}\cdot int\left(F_3\cdot\exp\left(-\text{zeta}\cdot\omega_0\cdot(t-\text{tau})\right)\cdot\sin\left(\omega_1\cdot(t-\text{tau})\right),\ \text{tau}=\text{tau}_2\,..\text{tau}_3\right)+\frac{1}{m\cdot\omega_0}\cdot int\left(F_4\cdot\exp\left(-\text{zeta}\cdot\omega_0\cdot(t-\text{tau})\right)\cdot\sin\left(\omega_1\cdot(t-\text{tau})\right),\ \text{tau}=\text{tau}_3\,..\text{tau}_4\right)+\frac{1}{m\cdot\omega_0}\cdot int\left(F_5\cdot\exp\left(-\text{zeta}\cdot\omega_0\cdot(t-\text{tau})\right)\cdot\sin\left(\omega_1\cdot(t-\text{tau})\right),\ \text{tau}=\text{tau}_4\,..\text{tau}_5\right)+\frac{1}{m\cdot\omega_0}\cdot int\left(F_6\cdot\exp\left(-\text{zeta}\cdot\omega_0\cdot(t-\text{tau})\right)\right.$$

```
        ·sin(ω1·(t − tau)), tau = tau5..tau6) + 1/(m·ω0) ·int(F7·exp(−zeta·ω0·(t − tau))·sin(ω1·(t
        − tau)), tau = tau6..t) :
>
> with(plots) :
> f1 := plot(F1, tau = 0..tau1, color = red) :
> f2 := plot(F2, tau = tau1..tau2, color = red) :
> f3 := plot(F3, tau = tau2..tau3, color = red) :
> f4 := plot(F4, tau = tau3..tau4, color = red) :
> f5 := plot(F5, tau = tau4..tau5, color = red) :
> f6 := plot(F6, tau = tau5..tau6, color = red) :
> f7 := plot(F7, tau = tau6..3, color = red) :
> display({f1, f2, f3, f4, f5, f6, f7});
```

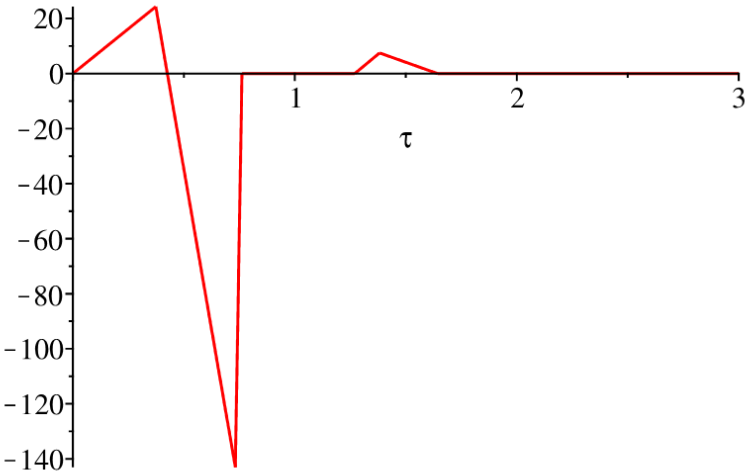


```
>
>
> with(plots) :
> x1 := plot(1000·x(t)1, t = 0..tau1, color = red) :
> x2 := plot(1000·x(t)2, t = tau1..tau2, color = red) :
> x3 := plot(1000·x(t)3, t = tau2..tau3, color = red) :
> x4 := plot(1000·x(t)4, t = tau3..tau4, color = red) :
> x5 := plot(1000·x(t)5, t = tau4..tau5, color = red) :
> x6 := plot(1000·x(t)6, t = tau5..tau6, color = red) :
> x7 := plot(1000·x(t)7, t = tau6..10, y = −0.4..0.4, color = red) :
> display({x1, x2, x3, x4, x5, x6, x7}, thickness = 0, labelfont = ["Arial"], labels = ["time [s]",
        "Displacement [mm]"], labeldirections = [horizontal, vertical], size = [0.6, 0.4]);
```

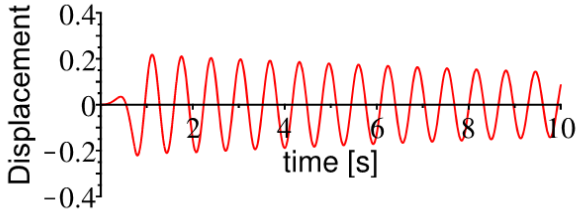


```
>
```

Appendix D **MATLAB script discrete Euler-Bernoulli beam model**

Background information to the model in MATLAB

The functions ode45 or ode 23 in MATLAB are able to solve coupled first order ordinary differential equations, ode 45 is more accurate than ode23. The differential equation to be solved consists of the equation of motion for damped mass spring system for a SDOF. In case of a beam model with n degrees of freedom the equation of motion is similar as for a SDOF but set up in matrix notation. The equation of motion for a damped mass spring system is a second order differential equation. In order to numerically solve this second order ODE in MATLAB the equation has to be rewritten into a system of two coupled first order ODEs.

The equation of motion for a SDOF:

$$\ddot{u} + 2\zeta\omega_0\dot{u} + 2\omega_0^2 u = f(t)/m$$

Rewrite this second order ODE into two coupled first order ODEs

$$x_1 = u$$

$$\dot{x}_2 = \dot{u} = \dot{x}_1$$

$$\dot{x}_2 = \ddot{u} = -2\zeta\omega_0\dot{u} - 2\omega_0^2 u + \frac{f(t)}{m}$$

Now that we have a coupled system of first order ODEs it can be given as input for the ode45 function in MATLAB. The input is given in a vector q, called the state vector.

$$\dot{q} = [\dot{x}_1\ \dot{x}_2]$$

Other input parameters for the ode45 function are the initial conditions and the time span over which the system of ODEs has to be integrated numerically. The initial conditions consist of the initial displacement and the initial velocity of the system (x_1 and x_2).

In case of a system with NDOF the equation of motion is given in matrix notation:

$$M\ddot{u} + C\dot{u} + Ku = F(t)$$

Rewrite this system of second order ODEs into a system of two coupled first order ODEs

$$x_1 = u$$

$$\dot{x}_2 = \dot{u} = \dot{x}_1$$

$$\dot{x}_2 = \ddot{u} = -M^{-1}C\dot{u} - M^{-1}Ku + M^{-1}F(t)$$

The state vector q̇ will be similar as for a SDOF only the size of the vector is different, it will be a 2 times n vector. The first n entries give the displacement and the last n entries give the velocity. This is also the case for the initial conditions.

Validation stiffness and mass matrix

Stiffness

The stiffness matrix is checked with the analytical solution for a simply supported beam with rotational springs and for a beam without rotational stiffness at the supports, then k_r is equal to zero. The beam is loaded at a distance L_F by a concentrated load.

$$EIu_1'''' = 0\ ;\ EIu_2'''' = 0$$

The boundary conditions:

y = 0: $u_1 = 0$
$M = k_r \cdot \theta_1$ ($EIu_1'' = k_r \cdot u_1'$)
y = L_F: $u_1 = u_2$
$\theta_1 = \theta_2$
$M_1 = M_2$
$V_1 - V_2 - F = 0$
y = L: $u_2 = 0$
$M_2 = - k_r \cdot \theta_2$ ($EIu_2'' = - k_r \cdot u_2'$)

The differential equation for an Euler Bernoulli beam is used to solve the problem on an analytical basis. Maple software is used to solve the differential equation with the above boundary conditions taken into account. If k_r is equal to zero the problem is the same as a hinged-hinged beam, if k_r goes to infinity the problem is same as a clamped-clamped beam.

The stiffness matrix is checked for the case with k_r is zero (hinged-hinged beam) and k_r is equal to the rotational stiffness of the column (i.e. $1.241 \cdot 10^7$ Nm/rad).

	Analytical	Computational N=26	Error	Computational N=52	Error
Displacement at mid span (10 kN) $k_r = 0$	10.8217 mm	10.8537	0.30%	10.8297 mm	0.07%
Displacement at mid span (10 kN) $k_r = 1.241 \cdot 10^7$ Nm/rad	9.95731 mm	9.98577 mm	0.29%	9.96354 mm	0.06%

The error becomes smaller when the amount of segments of the beam is increased, but the error for the case with 26 elements is still acceptable.

Mass
The mass matrix is checked in combination with the stiffness matrix by calculating the natural frequencies of the beam, in this case the beam has a uniformly distributed mass over the length and zero spring stiffness. The frequencies are calculated as follows:

$$\det(-\omega^2 M + K) = 0$$

In MATLAB the natural frequencies of the beam can easily be calculated using the eigenvalue function: eig(K,M). This function returns the squared natural frequencies. The analytical natural frequencies of the beam can be found using the following formula (Spijkers, Vrouwenvelder, & Klaver, 2005):

$$\omega_i = C_w \sqrt{\frac{EI}{mL^3}}$$

C_w is a coefficient for the mode shape and is equal to [9.87; 39.5; 88.9; 158; 247] for the first 5 mode shapes.

As expected the error becomes smaller when the amount of segments of the beam is increased. For 52 and 26 segments the error in the first 5 natural frequencies of the computational model versus the analytical solution is:

Mode	ω [rad/s] (analytical)	ω [rad/s] (computational 52 segments)	Error [%] (52 seg.)	ω [rad/s] (computational 26 segments)	Error [%] (26 seg.)
1:	9.7818	9.7785	0.03	9.7695	0.13
2:	39.1472	39.0782	0.18	38.9357	0.54
3:	88.1059	87.7922	0.36	87.0732	1.17
4:	156.5886	155.7429	0.54	153.4801	1.99
5:	244.7636	242.6822	0.86	237.1879	3.11

The following parameters were used:

Number of segments	26 and 52
Young's modulus	$2.1 \cdot 10^{11}$ N/m^2
Moment of area	$1.289 \cdot 10^{-2}$ m^4
Total mass beam	19600 kg
Length beam	52 m

The same conclusion as for the stiffness holds for the check of natural frequencies, the error in natural frequency for the first two modes is smaller than 0.6%. Therefore, the computation with 26 segments is preferable because the computational time is reduced with a factor 20 compared to the computation with 52 segments.

The natural frequencies of the beam with rotational stiffness included and a non-uniformly distributed mass over the length are also computed for 26 and 52 segments. $\omega_{1;26}$ = 9.9723 rad/s and $\omega_{1;52}$ = 10.001 rad/s. These natural frequencies are close to natural frequency of the structure with a hinged-hinged and uniformly distributed mass over the length of the beam.

```
clc;close;clear;
tic
% Parameters NDOF
P.N = 26;N = P.N;%amount of beam segments
L = 52; % Length [m]
E = 2.1*10^11; % Young's Modulus of steel [N/m^2]
I = 1.289*10^-2; % Second moment of area [m^4]
a = L/N; % Segment length [m]
m = 14749; %14749 mass of the beam without signboards; % 19249 Total mass of the beam [kg]

% Parameters load
lanes = 6; %number of lanes loaded with truck pulses
N_trucks = [4 11 2 8 1 9]; %amount of trucks on lane i
t_truck = [66.15 32.09 110.11 17.89 46.04 38.54; ...
90.29 40.80 137.97 44.69 0 47.60; ...
92.05 65.78 0 78.00 0 81.79; ...
128.29 79.29 0 94.35 0 88.24; ...
0 82.15 0 110.45 0 89.42; ...
0 98.08 0 142.96 0 108.45; ...
0 117.07 0 153.96 0 114.86; ...
0 123.32 0 157.37 0 121.13; ...
0 127.07 0 0 0 179.09; ...
0 168.14 0 0 0 0;
0 177.61 0 0 0 0];%time of truck pass [s] at:
%[(east)lane 2 lane 3 lane 4 (west) lane 3 lane 4 lane 5]


pulse = 2; %Ginal=1 or Lichtneger&Ruck=2
q = 4.5; % 4.5 load factor

% Parameters time
t_step = 0.01;%[s]
t_start = 15;
t_end = 180; % [s]
tspan = t_start:t_step:t_end; % [s]

%% Stiffness matrix
kr = 1.241*10^7; %Rotational spring [Nm/rad] kr=2*E*I/a (clamped)
K = zeros(N-1);
K(1,1:3) = [5+kr*a/(E*I),-4,1];%First row (rotational spring)
K(2,1:4) = [-4,6,-4,1];%Second row (simply supported)
for i=3:N-3
    K(i,i-2:i+2) = [1,-4,6,-4,1];%In-between rows (beam molecule)
end
K(N-2,N-4:N-1) = [1,-4,6,-4];%Second-last row(simply supported)
K(N-1,N-3:N-1) = [1,-4,5+kr*a/(E*I)];%Last row (rotational spring)
P.K = K*E*I/a^3;

%%Mass matrix
Mv=ones(N-1,1)*m/N;
%52 segments
%Mv(7:12)=Mv(7:12)+1113/6; %signboard 1 [kg]
%Mv(14:20)=Mv(14:20)+1113/7; %signboard 2 [kg]
%Mv(21:22)=Mv(21:22)+260/2; %signboard 3 [kg]
%Mv(29:38)=Mv(29:38)+1346/10; %signboard 4 [kg]
%Mv(39:44)=Mv(39:44)+668/6; %signboard 5 [kg]

%26 segments
Mv(4:6) = Mv(4:6)+1113/3; %signboard 1 [kg]
```

```
Mv(8:10) = Mv(8:10)+1113/3; %signboard 2 [kg]
Mv(11) = Mv(11)+260; %signboard 3 [kg]
Mv(15:19) = Mv(15:19)+1346/5; %signboard 4 [kg]
Mv(20:22) = Mv(20:22)+668/3; %signboard 5 [kg]
M = diag(Mv);

P.M = inv(M);

%diag(v)
%%Damping matrix Proportional damping (Rayleigh damping)
omg_1=10.10; %Frequency first mode [rad/s]
omg_2=38.08; %Frequency second mode [rad/s]
zeta_1=0.005; %Damping ratio first mode
zeta_2=0.01; %Damping ratio second mode
a_0=2*omg_1*omg_2*(zeta_1*omg_2-zeta_2*omg_1)/(omg_2^2-omg_1^2);
a_1=2*(zeta_2*omg_2-zeta_1*omg_1)/(omg_2^2-omg_1^2);
P.C=a_0*P.M+a_1*P.K;
P.C(13)=P.C(13)+0;
%P.C=zeros(N-1);

%Undampded natural frequencies
nf=(eig(P.K,M)).^0.5; %gives natural frequencies of the beam in [rad/s]
nf1=nf(1)/(2*pi)

%% Truck induced wind - pulse load
% paramters peaks and length/speed
if pulse==1

%Pulse Gin ------------------------------------------------------------
   P1 = 534; % [N]
   P2 = -534; % [N]
   P3 = 0; % [N]
   Tt = 1; % [s]

   % parameters time of pulse
   tau1 = 0.375*Tt;
   tau2 = 0.75*Tt;
   tau3 = 1.125*Tt;
   tau4 = 1.1250001*Tt;
   tau5 = 1.1250002*Tt;
   tau6 = 1.1250003*Tt;
else
%---------------------------------------------------------------------

%Pulse L&R ------------------------------------------------------------
   P1 = 0.17*143*q; % [N]
   P2 = -143*q; % [N]
   P3 = 0.25*143*q*0; % [N]
   Tt = 16.6/22.22; % [s]

   % parameters time of pulse
   tau1 = 0.50*Tt;  % [s] 0.50
   tau2 = 0.98*Tt;  % [s] 0.98
   tau3 = 1.02*Tt;  % [s] 1.02
   tau4 = 1.03*Tt;  % [s] 1.70
   tau5 = 1.04*Tt;  % [s] 1.85
   tau6 = 1.05*Tt;  % [s] 2.20
end
%---------------------------------------------------------------------
```

```
tp = [0 tau1 tau2 tau3 tau4 tau5 tau6]; %Time coordinates of pulse

% defining pulse into array
fp = [0 P1 P2 0 0 P3 0];
% time and load matrices for all lanes
load_M=zeros(lanes,max(N_trucks)*7+2);
time_M=zeros(lanes,max(N_trucks*7+2));

for n=1:lanes

   for i=1:N_trucks(n)
            load_M(n,2+7*(i-1):8+7*(i-1)) = fp;
      time_M(n,2+7*(i-1):8+7*(i-1)) = tp+t_truck(i,n);
      time_M(n,7*i+2)=t_end;
   end

end

%plot loads in time
figure;

for n=1:lanes
   for j=1:N_trucks(n)
      subplot(lanes/2,2,n)
      plot(time_M(n,1:7*j+2),load_M(n,1:7*j+2),'-k')
      title(['Load event on lane ' num2str(n) ' with ' num2str(N_trucks(n)) ' truck(s)'])
      xlabel('Time [s]')
      ylabel('Force [N]')
      xlim([0 180])
      %Loads defined for func_eqm_N
      P.load{n}=load_M(n,1:7*j+2);
      P.time{n}=time_M(n,1:7*j+2);

   end
end


%%
%initial conditions are trivial
%load bound.mat
q_0=zeros(2*N-2,1);%bound;
q_0(1:25)=0.0000001; %small initial displacements is used for computational reasons

% make anonymous function
AF = @(t,q) func_eqm_N(t,q,P);
[T,Y] = ode45(AF,tspan,q_0);

bound=Y((t_end-t_start)/t_step+1,:)'; % Conditions at t_end if boundary is used
%% plot response of NDOF
tpp=zeros(11,6);
%load('N52_6_lanes.mat')
load('meetgegevens.mat');
figure;
hold on
pc=plot(T,1000*Y(:,15),'k');
pm1=plot(meetgegevensS1(:,3),meetgegevensS1(:,1),'g--','LineWidth',2);
pm2=plot(meetgegevensS1(:,3),meetgegevensS1(:,2),'g--','LineWidth',2);
pt=plot(t_truck,tpp,'r.','MarkerSize',10);
set(gca,'Fontsize',12);
```

```
title('Dynamic response of the beam')
xlabel('Time [s]')
ylabel('Displacement [mm]')
legend([pc pm1 pt(1)],{'Computation','Measurement','Truck pass'})
xlim([15 180])
ylim([-5 5])
hold off
toc

load chirp
sound(y, Fs)

%
   %%Energy
   vel=Y(:,N:2*N-2); % Velocity nodes [m/s]
   Ekin=0.5*Mv'.*vel.^2; % Kintec energy [J]
   Ekinb=zeros((t_end-t_start)/t_step+1,1);
   Ekinb(:,1)=sum(Ekin,2); % Total kinetic energy in the beam [J]
   figure;
   plot(T,Ekinb)
   set(gca,'Fontsize',12);
   title('Kinetic energy in the beam')
   xlabel('Time [s]')
   ylabel('Energy [J]')
   xlim([15 180])
%}
%{
   %% Static check stiffness
   Fst=zeros(N-1,1);
   Fst(round(N/2))=5000;
   disp=zeros(N+1,1);
   disp(2:N)=P.K\Fst;
   disp(1)=0;disp(N+1)=0;
   Len=linspace(0,52,N+1);
   data1=load('Maple_solution\analytical1.dat');
   data2=load('Maple_solution\analytical2.dat');
   figure;
   hold on
   plot(Len,disp)
   plot(data1(:,1),data1(:,2),'g--')
   plot(data2(:,1),data2(:,2),'g--')
   hold off
   legend('Computational','Analytical')
   xlabel('x [m]')
   ylabel('Displacement [m]')
   set(gca,'Fontsize',12);
   xlim([0 52])
%}
```



```
function [ q_dot ] = func_eqm_N(t,q,P)

u(:)=q(1:P.N-1);
u_dot(:)=q(P.N:2*P.N-2);

f=zeros(P.N-1,1);

f(17)=interp1(P.time{1},P.load{1},t); %f(34) if 52 segments
f(19)=interp1(P.time{2},P.load{2},t); %f(37)
f(21)=interp1(P.time{3},P.load{3},t); %f(41)
f(8)=interp1(P.time{4},-P.load{4},t); %f(15)
f(6)=interp1(P.time{5},-P.load{5},t); %f(11)
f(4)=interp1(P.time{6},-P.load{6},t); %f(8)

%f(P.N/2)=interp1(P.time1,P.load1,t);

q_dot(1:P.N-1)=u_dot;
q_dot(P.N:2*P.N-2)=P.M*(f-P.K*u'-P.C*u_dot');
q_dot=q_dot';
end
```